

Founded 1925

Incorporated
by Royal Charter 1961*To promote the advancement
of radio, electronics and kindred
subjects by the exchange of
information in these branches
of engineering*

The Radio and Electronic Engineer

The Journal of the Institution of Electronic and Radio Engineers

The Present Status of Surround Sound Reproduction

THE first public recognition of stereophonic directional effects seems to have been at the Paris Electrical Exposition of 1881. Some eighty carbon microphones were placed on the stage of the Opéra, each connected by landline to its own earpiece; this being necessary for multiple listening before the days of amplifiers. An enhanced sense of space was noticed when a listener held one earpiece to each of his ears.¹

Systematic developments which laid the foundations of modern stereo were carried out by A. D. Blumlein in the early 1930s, and incorporated in his famous 1931 patent.² Another historic landmark was the relay in 1933 from the Academy of Music in Philadelphia to Constitution Hall, Washington DC, which used spaced-microphone techniques.³ It was not however until the mid-1950s that stereo records began to be issued commercially in any numbers, and for a decade after this many record retailers maintained a separate section of their shop for stereo.

Thus commercial exploitation of stereo had been preceded by several decades of theoretical and experimental development. Even so some of the early releases were little more than dual-mono, and earned for themselves the description 'ping-pong stereo'.

The directional illusion given by stereo is confined to a front sector. It was an obvious idea to extend this to all directions, and by the 1970s a number of systems for surround reproduction had been launched commercially. These mainly aimed at achieving or imitating the transmission of four separate signals to corresponding loudspeakers, thus giving what has been called 'ping-pang-pung-pong quadraphonics'. These proposals were not preceded by the long period of development and assimilation that stereo had enjoyed, and in retrospect may be thought to have been based on inadequate concepts, aims and methods. For whatever reason, 'quadraphonics' did not succeed in the market-place.

Meanwhile understanding has been accumulating of the basic problems of surround reproduction and their solution under realistic constraints. Contributions to this knowledge were not all of the same kind, nor did they all come from the same source. It was necessary to understand which signal formats could convey valid directional information, how such signals could be generated either from natural soundfields or by a 360° extension of stereo pan-pot methods, how such signals could be conveyed to the listener by records or broadcasting, and how they could be decoded so as to present to the ears of the consumer, via his loudspeakers, a good illusion of the intended direction of arrival. Contributors have included B. Bauer, D. Cooper, P. Craven, J. Eargle, P. Fellgett, M. Gerzon, D. Hafler, P. Scheiber and T. Shiga; corporate contributions have come from Sony and JVC. The BBC, according to its generous practice, published the findings of its Research Laboratories as the work proceeded, so that its results could contribute to the pool at the first opportunity. It was also found that physicists

and mathematicians of the last century had developed techniques that could contribute, notably Helmholtz, Poincaré, Lord Rayleigh and Stokes.

There comes a time when knowledge of this kind reaches a 'critical mass' at which a mature technology can emerge. The vehicle for this development may prove to have been the NRDC-sponsored Ambisonic technology.

Unlike earlier quadrasonic proposals, in which the system and the signal formats could scarcely be separated, the Ambisonic technology allows formats to be chosen suited to different purposes, and to different methods of transmission or recording. As the result of a series of consultations over several years, the NRDC Ambisonic team have recommended for consumer distribution a hierarchy of compatible specifications, designated UHJ, applicable to media having different numbers of channels.⁴ The IBA, while proposing a non-hierarchical specification of its own, has stated that UHJ is the best of the hierarchical proposals.⁵ The recent paper by Gaskell indicates BBC acceptance of UHJ.⁶ At least two record companies are using UHJ. We may be seeing an end to the incompatibilities of standards that haunted the quadrasonic era of surround reproduction.

P. B. FELLGETT

References

- 1 Clément Ader's 'Théâtrephone'. Quoted by Barton, G. J., in 'On perception and technology in the reproduction of sound'. Doctoral Thesis, University of Reading, 1979.
- 2 Blumlein, A. D., British Patent 394325 (1931).
- 3 Steinberg, J. C. and Snow, W. B., 'Symposium on Wire Transmission of Symphonic Music and its Reproduction in Auditory Perspective'. *Bell Syst. Tech. J.*, 13, pp. 245-58, 1934.
- 4 National Research Development Corporation Response to Federal Communications Commission Notice of Inquiry Docket No. 21310, December 1977 and Reply Comments August 1979.
- 5 Independent Broadcasting Authority Comments on FCC Notice of Inquiry, Docket 21310, January 1979.
- 6 Gaskell, P. S., 'System UHJ: a hierarchy of surround sound transmission systems', *The Radio and Electronic Engineer*, 49, pp. 449-59, 1979.

INSTITUTION OF ELECTRONIC AND RADIO ENGINEERS BENEVOLENT FUND

Notice of Annual General Meeting of Subscribers

NOTICE IS HEREBY GIVEN that, in accordance with the Trust Deed approved at the Special General Meeting on 22nd May 1980, the Annual General Meeting of subscribers to the IERE Benevolent Fund will be held on Thursday, 23rd October 1980, at the London School of Hygiene and Tropical Medicine, Keppel Street, London, W.C.1. The meeting will commence at 6.30 p.m. approximately (immediately after the Annual General Meeting of the Institution).

AGENDA

1. To receive the Annual Report of the Trustees
(To be published in the October 1980 issue of the Journal).
2. To receive the Income and Expenditure Account and Balance Sheet for the year ended 31st March 1980
(To be published in the October 1980 issue of the Journal).
3. To note the appointment of members of the Management Committee
(Clause 4 of the Trust Deed states that: 'The Management Committee shall consist of three *ex-officio* members namely the President, the Honorary Treasurer and the Secretary for the time being of the Institution and such additional members as the *ex-officio* members shall in their absolute discretion co-opt and the *ex-officio* members shall have power from time to time to remove and if thought fit replace any co-opted member as they may think proper'.')
4. To appoint Solicitors
The Trustees recommend the appointment of Bax, Gibb and Gellatlys (incorporating Braund and Hill), 14 Gray's Inn Square, London, W.C.1.
5. To appoint Accountants
The Trustees recommend the appointment of Gladstone, Jenkins and Company, 50 Bloomsbury Street, London W.C.1.
6. Any other business

4th September 1980

By Order of the Trustees
(Signed) S. M. DAVIDSON
Honorary Secretary

INSTITUTION OF ELECTRONIC AND RADIO ENGINEERS

Notice of Annual General Meeting

NOTICE IS HEREBY GIVEN that the nineteenth ANNUAL GENERAL MEETING of the Institution since Incorporation by Royal Charter will be held on THURSDAY, 23rd OCTOBER 1980, at 6.00 p.m. in the Goldsmith's Hall at the London School of Hygiene and Tropical Medicine, Keppel Street, Gower Street, London W.C.1.

A G E N D A

1. To receive the Minutes of the eighteenth Annual General Meeting of the Institution since Incorporation by Royal Charter held on 25th October 1979. (Reported on pages 593-596 of the December 1979 issue of *The Radio and Electronic Engineer*.)
2. To receive the Annual Report of the Council for the year ended 31st March 1980. (To be published in the October 1980 issue of *The Radio and Electronic Engineer*.)
3. To receive the Auditor's Report, Accounts and Balance Sheet for the year ended 31st March 1980. (To be published in the October 1980 issue of *The Radio and Electronic Engineer*.)
4. To confirm election of the Council for 1980-81.
In accordance with Bye-Law 49 the Council's nominations were sent to Corporate members by a Notice dated 5th June 1980 in the June 1980 issue of *The Radio and Electronic Engineer*. As no other nominations have been received under Bye-Law 50 for the following offices, a ballot will not be necessary and the following members will be elected:

The President

J. Powell, T.D., B.Sc., M.Sc.

The Vice-President

Under Bye-Law 46, all Vice-Presidents retire each year but may be re-elected provided they do not thereby serve for more than three years in succession.

For Re-election: H. E. Drew, C.B.; Professor J. R. James, B.Sc., Ph.D.; Brigadier R. W. A. Lonsdale, B.Sc.; P. K. Patwardhan, M.Sc., Ph.D.; S. J. H. Stevens, B.Sc.(Eng.)

The Honorary Treasurer

For Re-election:

S. R. Wilkins

Ordinary Members of Council

Under Bye-Law 48, ordinary Members of Council are elected for three years and may not hold that office for more than three years in succession.

MEMBERS

For Election:

J. J. Jarrett

The remaining members of Council will continue to serve in accordance with periods of office laid down in Bye-Law 48.

5. To appoint Auditors and to determine their remuneration. (Council recommends the re-appointment of Gladstone, Jenkins & Co., 50 Bloomsbury Street, London W.C.1.)
6. To appoint Solicitors. (Council recommends the appointment of Bax, Gibb and Gellatlys (incorporating Braund and Hill), 14 Gray's Inn Square, London W.C.1.)
7. Awards to Premium Winners.
8. Any other business. (*Notice of any other business must have reached the Secretary not less than forty-two days prior to the meeting.*)

By Order of the Council,

S. M. DAVIDSON, *Secretary.*

1st September 1980.

*After the conclusion of the formal business of the Annual General Meeting,
Mr John Powell will give his Presidential Address.*

Some Features of a New Colour Television Receiver

Following on the launch last year of its TX9 single circuit board colour television receiver chassis for 90° picture tubes up to 20 in, Ferguson has now developed the TX10 factory-made single board chassis for colour receivers with 22 in and 24 in 110° tubes.

In the production process the TX10 chassis starts as a single p.c.b. and during manufacture this is parted into two sections—the larger, horizontal board carrying the heavy components, and the smaller section, which folds and locks vertically, containing the signal circuitry. The advantage of this approach is that it enables the slimmest possible receiver design to be achieved and gives total service accessibility when the smaller section is pulled back and locks in the horizontal position. This constructional feature can be seen in the accompanying photograph.

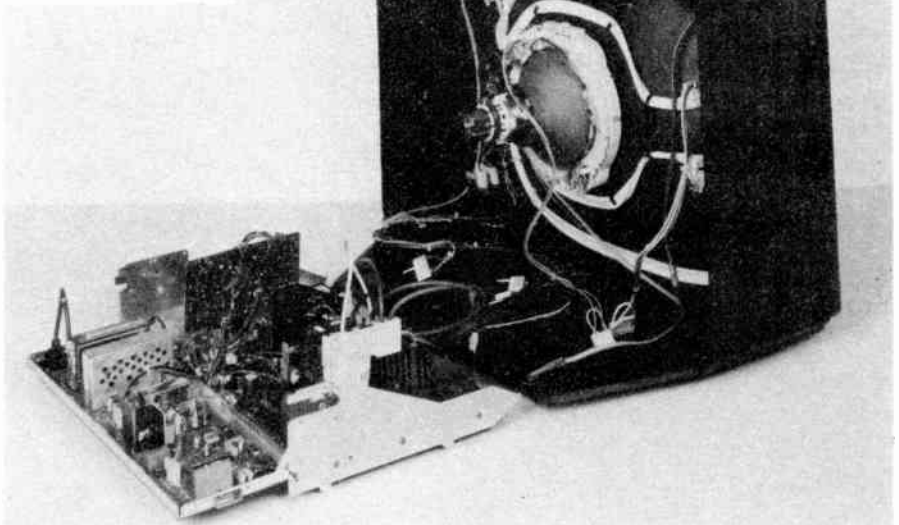


Fig. 1. The TX10 receiver with the large and small chassis boards latched into the horizontal position for servicing and drawn out from the cabinet to expose all components.

Circuit Engineering

Power consumption on the TX10 chassis has been reduced to less than 70 watts at black level—hitherto it has been around 150 watts for 110° chassis. The TX10 chassis is therefore economical in operation and, since it uses less power, less heat is generated than in conventional 110° tube receivers, resulting in longer component life and improved reliability. From the safety viewpoint the chassis is electrically isolated, enabling servicing to be carried out more safely whilst the mains power is on.

Picture performance and data display on TX10 receivers is claimed to be dramatically improved compared with other 110° receivers. This is due to the inclusion of a luma-chroma processor developed specifically for the TX10 which works in tandem with an improved video amplifier.

The Luma-Chroma Processor I.C.

The luma-chroma processor is a single integrated circuit and its special capability is said to be in the mixed mode of programme picture/data display where the brilliance and registration of both data and picture is retained simultaneously. Additionally, the video circuit was designed to give a greatly increased bandwidth for improved fine detail definition in connection with data display reproduction, as well as normal viewing. A third of the pre-set adjustments normally required have been eliminated on the TX10—another important contributing factor towards improved reliability since there are fewer opportunities for human error.

This specially developed integrated circuit (TDA 3560) effectively replaces three i.c.s in previous designs and contains the following main circuit functions.

Luminance Amplifier. A black level clamp for the input signal followed by a 20 dB range contrast control circuit. Contrast adjustment is simply achieved by applying a variable d.c. voltage to pin 7. The controlled video voltage is then fed to the R, G and B matrix.

Chroma Amplifier. The chroma signal first passes through an a.c.c. circuit which has a control range of about 26 dB. The now constant amplitude signal is passed through contrast and saturation control circuits, the latter having a 40 dB control range controlled by a variable d.c. voltage applied to pin 6. The contrast controlled stage is necessary in order that the saturation level tracks with adjustment of the contrast control. The chroma output signal, on pin 28, which includes fixed amplitude burst is then fed to the delay line and after matrixing is then applied to the burst phase detector input and the modulator input (pins 21 and 22).

Oscillator and Identification Circuit. The oscillator operates at 8.8 MHz and is then divided by 2 to obtain a 4.4 MHz signal. By using two ÷ 2 circuits, one operating on positive-going edges

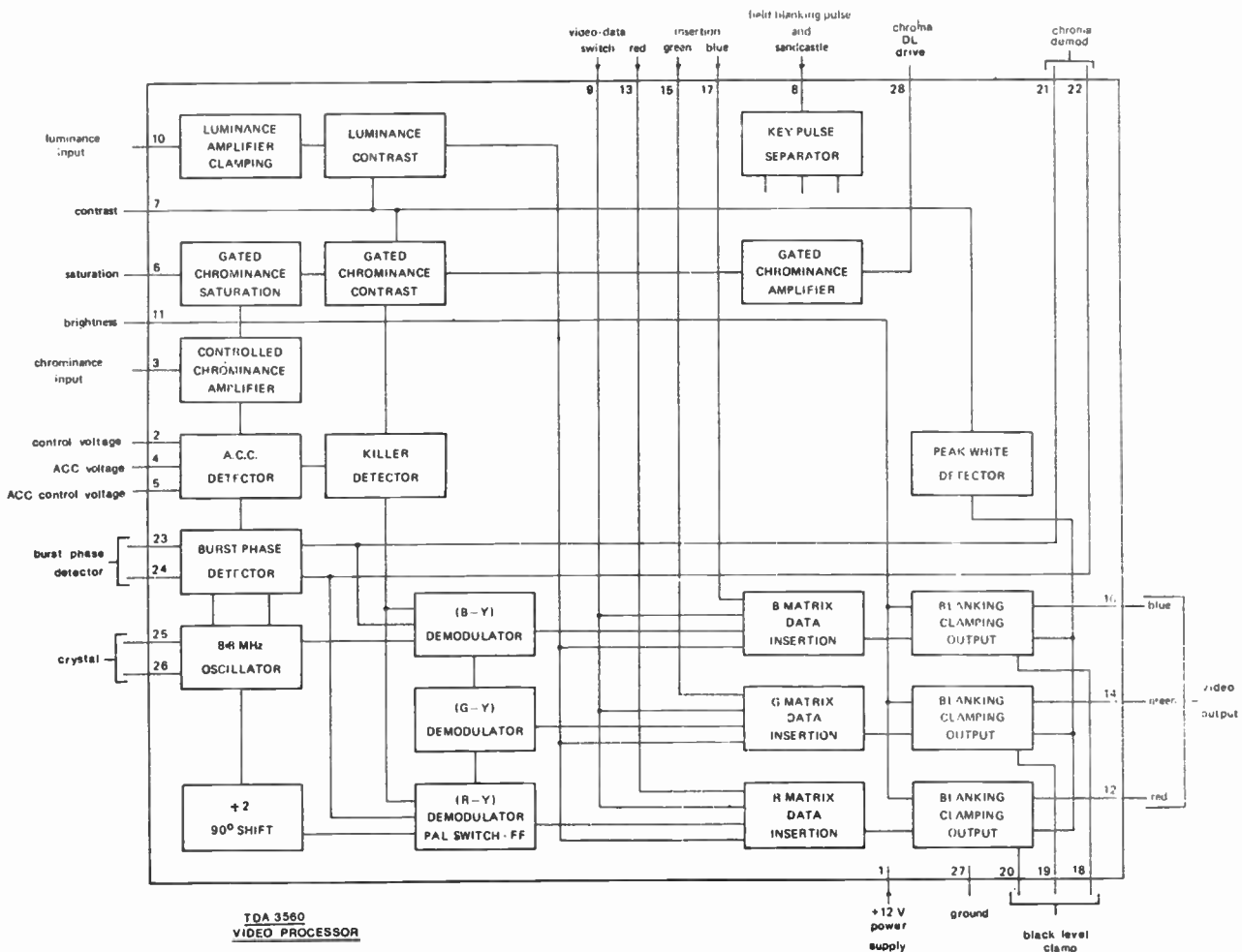


Fig. 2. The TDA 3560 Luma Chroma Videoprocessor.

of the 8.8 MHz signal, and the other operating on negative-going edges, a 90° phase shift is automatically obtained thus eliminating a 90° phase adjustment.

Chroma Demodulators. The 4.4 MHz quadrature signals driving the chrominance demodulators are derived within the TDA 3560 from an 8.8 MHz crystal controlled oscillator which is frequency and phase locked to the chroma signal.

Pulses. Three pulse functions are required within the i.c. They are:

- Chroma and burst separation
- Line flyback blanking
- Frame blanking

By the use of amplitude multiplexing techniques ('sandcastle pulse') only one i.c. pin in the TDA 3560 is used for all three functions.

RGB Matrix and Video Output. The demodulated colour difference signals are combined with the luminance signal yielding the RGB primary signals, which are then clamped to a d.c. level variable by adjustment of the viewer brilliance control. These signals are then blanked by the line flyback and frame blanking components of the sandcastle pulse and are then applied to the video output stages.

Data Insertion. Ceefax, Oracle or Prestel information is applied to all three output signals prior to clamping and brilliance control. When text is shown together with picture all picture information is blanked wherever text occurs, ensuring maximum clarity of the data.

Other Circuit Innovations

A surface acoustic wave filter replaces most of the conventional i.f. amplifier coils together with some other components and eliminates adjustment following assembly since its characteristics are determined during the initial engineering design.

The inclusion of a new, all-integrated field time-base generator i.c. has enabled a drastic component reduction eliminating the need for 8 transistors, 7 capacitors, 6 diodes and 17 resistors. In fact, in the basic TX10 chassis there are only 448 components and only four cable forms (including the tube base assembly and tuning controls) which is 35% fewer than in comparable 110° receivers.

The TX10 range will use the Philips 30AX 110° tube which has soft flash protection, and is self aligning and self converging.

Production Features

To ensure the highest degree of measurement accuracy followed through from design, tooling and production, the TX10's p.c.b. was drawn by computer, the data then being translated to punched tape for programming the jig-boring machines which punch the holes in the p.c.b.s. Automatic insertion machinery is also set up using the same program information, and quality control tests also use the same punched tape.

The TX10 chassis is being manufactured at the Enfield plant of Thorn Consumer Electronics.

Knife Cleaning Machines to Computer Systems

PETER CULLEY*

The development and present day capability of the Kent organization are traced from the early days of a Victorian entrepreneur who had the vision to realize the potential of flow measurement in industrial and domestic fields, to the present international network of companies with a product range extending from inexpensive mechanical water meters to computerized process control systems using the latest technologies.

When George Kent ceased manufacturing blinds and started making domestic machinery in the Strand in London in 1838, industrial measurement and control as we understand it today was virtually unknown. But from what we know of George, he would not be unduly surprised if he could see the present-day activities of the business he founded.

From these early beginnings George quickly extended his range of domestic aids and the business flourished, supported by a hard-sell approach that was the Victorian equivalent of much of today's consumer-goods promotion. The turning point came in 1885 when George obtained the rights to manufacture and sell a German mechanical water meter, anticipating a statutory requirement for the metering of water supplies in London. This has never happened, but the metering business was established, and markets were found elsewhere; now over 80% of meter sales are outside the UK.

Mechanical meters led to the rights to sell the 'new' Venturi differential-pressure flow-meter outside the United States; other developments followed – the successful application of differential pressure flow-measuring techniques to air and steam measurements, and other innovations with associated recorders and indicators. Meanwhile, the early days of other present-day members of the Kent organization saw the development, for example, of galvanometric chart recorders for electrical measurements and temperature. Indeed, the history of Kent is marked with technological 'firsts', such as the first automatic control system for a central power generation boiler in the early 1930s, using the now accepted boundless control technique – in those days an electro-mechanical system.

Kent continued as an independent company and increased its range of products and capability by internal development and growth, a policy that continued until the early 1960s when it was realized that internal growth alone would not enable the company to achieve its capability goals within a reasonable period of time. A programme of external acquisitions was embarked upon

*Publicity Manager, Brown Boveri Kent Ltd, Biscot Road, Luton, Bedfordshire LU3 1AL

which brought together a number of companies who were significant specialists in their own fields of industrial measurement and control, and gave to Kent a unique overall capability.

In late 1974 a scheme of arrangement was concluded between Kent and BBC Brown Boveri, the Swiss-based electrical engineering group. This gave Kent assured financial stability, the opportunity to avail itself of formidable research facilities, and an entry to market sectors not previously readily accessible. BBC Brown Boveri now hold 54.5% of the Kent equity.

What is unique about Kent? Its history has demonstrated how deeply the organization is rooted in industrial measurement, and it has developed a reputation as an organization dedicated to solving customers' instrumentation and control problems. To become and remain successful in this field it is necessary for an organization to demonstrate its total capability by producing an across-the-board range of products (Fig. 2) which can be marketed separately, or linked together as a complete system for process control. Few organizations can claim this total capability, and there are probably no more than ten companies throughout the world who can—Kent is one of them. Other companies have tried to break into the process control systems market without success, and eventually have had to achieve their objective by buying an established instrument manufacturer.

The reasons for this are quite simple. The systems buyer is essentially cautious. He has to be absolutely certain about his instrument supplier, that the products and technologies being offered are reliable, and that his process plant can be used to optimum efficiency and safety throughout its life. The international nature of most major process plant projects places additional demands on the instrument supplier who must provide comprehensive back-up facilities in terms of local assembly, workshop facilities and engineers, plus a guaranteed supply of components and assemblies for periods of up to 20 years.

But total capability means much more than this; in Kent terms it means three basic requirements – product range, organizational capability to provide services in

the right place at the right time, and applicational capability to understand and solve the customer's problems.

Product Range

This is best explained by examining the basic closed-loop control system (Fig. 3). Each measurement, control and regulating element involves a vast choice conditioned by the parameters to be measured, accuracy, price, performance limits and so on.

Take recorders as an example: the requirement may be for a 6 in × 3 in (152 mm × 76 mm) panel front recorder as part of a pneumatic system or a 250 mm (10 in) chart width 12-point electronic recorder to monitor temperatures throughout a process; or it may be for a simple 100 mm (4 in) chart recorder linked to a pipeline flow sensor. Add to each of these the need to provide pneumatic or electronic three-term control, on/off control, high or low level alarms, programme control, and the list of standard options grows enormously.

Pipeline flow measuring devices are another example where the choice must depend on size, characteristics of the fluid, temperature, pressure, cost, accuracy, acceptable head loss and so on, and this is one of the reasons why the Kent range extends from giant pressure-difference devices and electromagnetic flow meters up to 2 metres in diameter to mechanical oil meters, capable of measuring the flow of oil to a small boiler at an accuracy of $\pm 0.5\%$.

Figure 4 gives a list of the basic measurements—flow, pressure, level, temperature, liquid and gas analysis, etc, and the instruments and sensors available from Kent for each of these measurements.

Organizational Capability

Today Kent is organized in three main manufacturing activities, each of which provides a special type of service or products to meet particular customer or market requirements. In addition there are two geographic groupings of companies outside the UK—one for Europe and one for the rest of the world—which are mainly for selling purposes but with some local manufacture and assembly.

Kent Process Control is the largest company in the group and manufactures and markets a wide range of instruments for the measurement and control of process variables, including pneumatic and electronic transmitters and panel-mounted instruments, orientated towards the needs of the capital intensive industries. It specializes in the supply of complete systems for process control applications world-wide, including responsibility for engineering, commissioning and installation. These systems often include products manufactured by other Kent companies. A fast growing sector of this business is concerned with the design and manufacture of advanced computer-based systems for process control in the chemical and petrochemical industries, as well as in steel and public utilities.

Introl process control valves are important products from this company; they have particular application in the chemical and petrochemical industries and in power generation. Their products are applied to virtually any fluid, ranging from crude oil on off-shore oil production platforms, to highly inflammable fluids in chemical plants. Introl have secured an important technological lead in meeting low noise specifications which are vital in meeting environmental and safety standards.

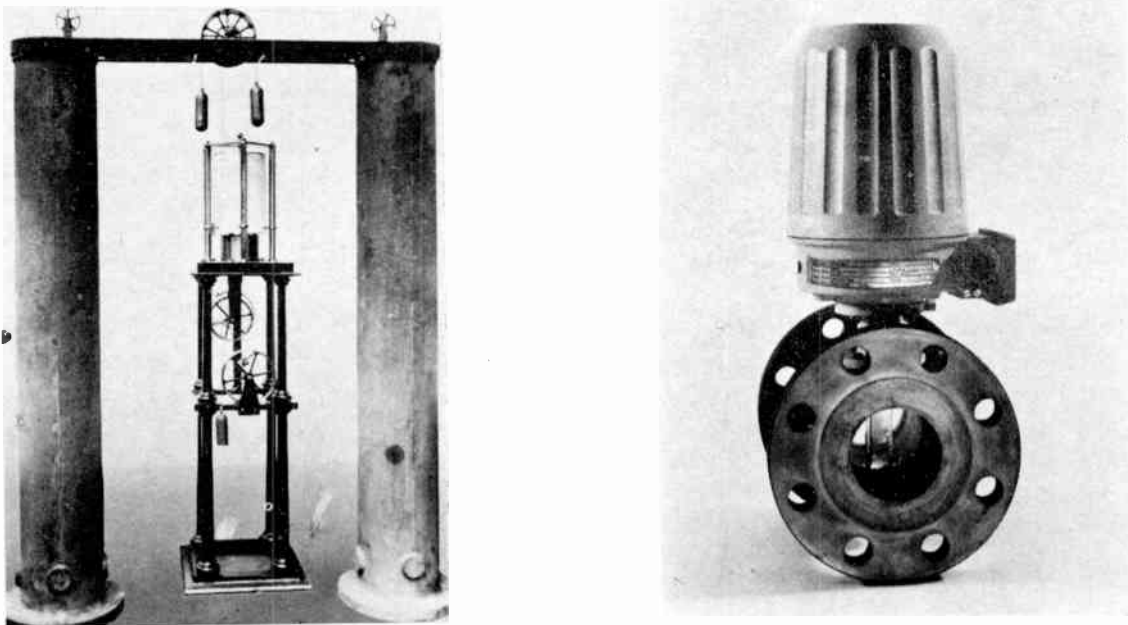


Fig. 1. A 1920 vintage mechanical water meter and its present day equivalent.

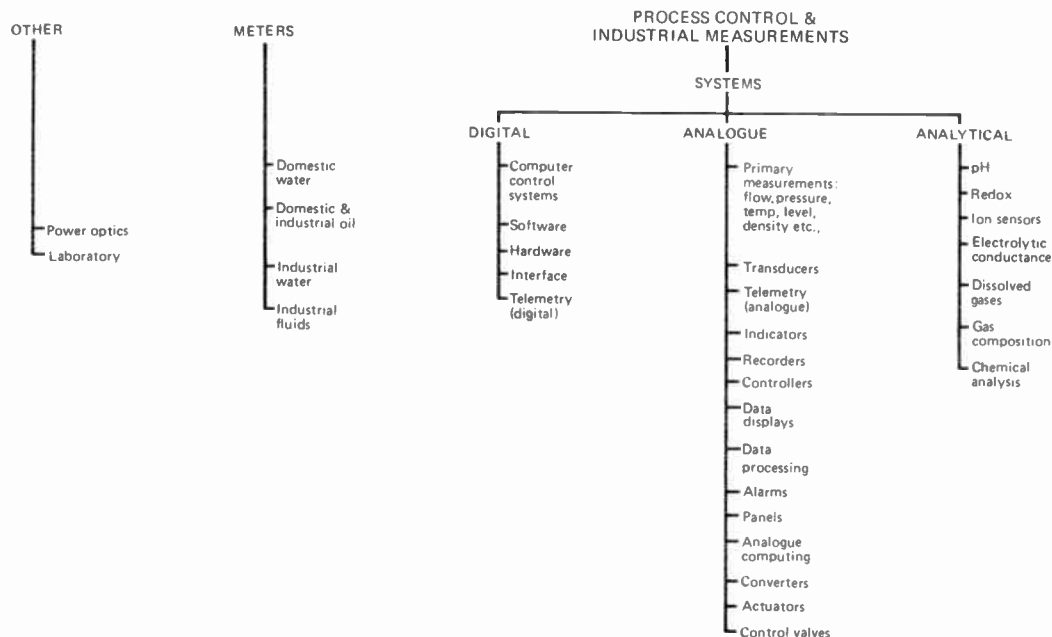


Fig. 2. This diagram shows the broad product types in the Kent range. Within each category there is a wide choice of product ranges produced in a variety of models, sizes, operating limits, etc., to suit particular application requirements. Each broad product type is often related to one or more others, e.g. an indicator/recorder/controller with alarms, or can be combined as simple or complex measurement and control systems.

Kent Process Control also has separate organizations in the USA and Singapore to meet the special needs of the markets in those areas.

Kent-Tieghi which is based in Italy, is an important part of the Kent process control business with extensive manufacturing facilities and wide involvement in the petrochemical and other industries.

Kent Industrial Measurements comprises manufacturing and marketing units providing instrumentation and control products which are sold for individual applications or which are integrated into process control systems. The Foster Cambridge range is predominantly for temperature, pressure, humidity and level measurement and control across a variety of industries; EIL Analytical Instruments hold a leading market position in analytical 'wet chemistry' instrumentation particularly in the power and environmental areas. GKEP Analytical Instruments manufacture a wide range of gas analysis equipment with applications as diverse as monitoring the atmosphere in road tunnels to the monitoring of CO₂ in breweries.

Kent Meters is involved with the manufacture of meters for the measurement of water, oil and other liquids for domestic and industrial applications. Manufacture and assembly are carried out in a number of important markets outside the UK, including Belgium, South Africa, Australia, Malaysia, Singapore, Thailand and Puerto Rico.

Evershed Power-Optics has a highly specialized business concerned with products and systems for the television and other industries. A recent development is the production of servo-controlled heads for incorporation

in surveillance systems being supplied to a number of countries.

European Division comprises seven companies which are primarily concerned with selling, although in some markets local assembly facilities have been set up for particular product ranges. These companies are located in Austria, Belgium, Federal Republic of Germany, France, Holland and Spain.

International Division employs over 1000 people in countries throughout the world, and in the main acts as a sales outlet for the manufacturing companies within the Kent organization. The companies, which are located in Australia, Malaysia, New Zealand, Singapore, South Africa, Thailand, Zambia and Zimbabwe have, apart from their primary sales function, some substantial local assembly and manufacturing facilities, including the construction of instrument panels and complete installation and commissioning facilities.

Applicational Capability

The deployment of personnel and resources into a number of specialized market areas (although in practice each of them has very close associations with the others), make Kent's technical and field experience readily available to the customer. Close customer relationships are an essential part of the operation, and with their accumulated experience Kent engineers are able to find a solution to most control or instrumentation problems, advise on the best approach, and develop an appropriate system.

The range of applications is virtually limitless, but there are certain key industries with which Kent have

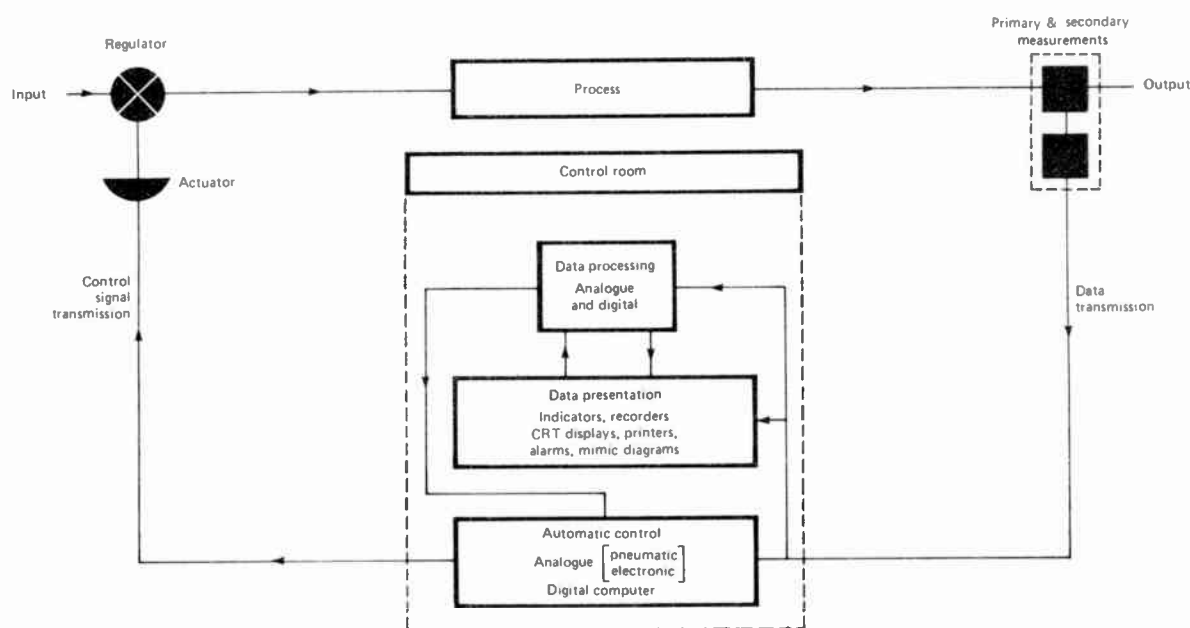


Fig. 3. Total capability in process control can only be claimed when all the elements of the basic closed-loop control system shown here—measurement, transmission, presentation/control, regulation—can be met. The products necessary to fulfil such a system vary considerably and depend on the applicational requirements. Each Kent product type required to complete the loop is shown in Fig. 4.

developed a particularly close association extending over a long period of time.

Power

An early example was the power industry in which Kent have consistently been innovators, not only in conventional central power generation, but in nuclear power, industrial power plant, district heating and associated activities such as desalination plants. Recent contracts, some of which have included complete boiler control systems, have been for power plants in India, Libya, Hong Kong, Switzerland and USA.

In addition, specialist instrumentation such as EIL boiler feed water analysis equipment has been installed in plants throughout the world, recent examples being boiler water sampling and analysis for 16 power stations in New South Wales and 400 analysis loops for thermal and nuclear power plant in Spain. Desalination plant applications have grown at a high rate over the past few years, particularly in those areas where conventional water supplies are scarce. Kent have been involved in supplying complete control packages for desalination plants throughout the Middle East area and in other countries such as southern Italy and Spain

Oil, petrochemicals and chemicals

In oil, petrochemicals and chemicals Kent equipment has long become an accepted part of these multi-national industries. With the development of North Sea oil and gas resources in both the British and Danish sectors, Kent has been in the forefront in supplying entire packaged metering systems, complete with meter provers

and associated control instrumentation, including computers; similar systems have been shipped to installations in the Middle East. Many hundreds of Inrol valves have been provided for production platforms, plus complete process control systems, a typical example being the control room with more than 100 control loops for Mobil's platform on the Beryl field in the North Sea.

Chemicals

In the chemical industry Kent has supplied large numbers of separate instruments but there has been an ever-increasing demand for computer systems for many types of chemical process to achieve optimum plant performance. Kent computer systems are being successfully applied to processes such as film coating machines in the Federal Republic of Germany, a synthetic fibres plant in the USSR, a plastics plant in the USA, pharmaceuticals in Switzerland and many more.

Metals

The metal industries, both ferrous and non-ferrous, are long-standing users of Kent equipment of all types. Computer-based control systems are in use on annealing furnaces, soaking pits and L/D converters; other systems are in continuous operation on sintering and pelletizing plants, coke ovens, arc furnaces, continuous casting machines and re-heat furnaces. Again the geographic spread is world wide and includes a sinter plant in South Korea, blast furnaces in Mexico, L/D converters in Austria and many applications for British Steel.

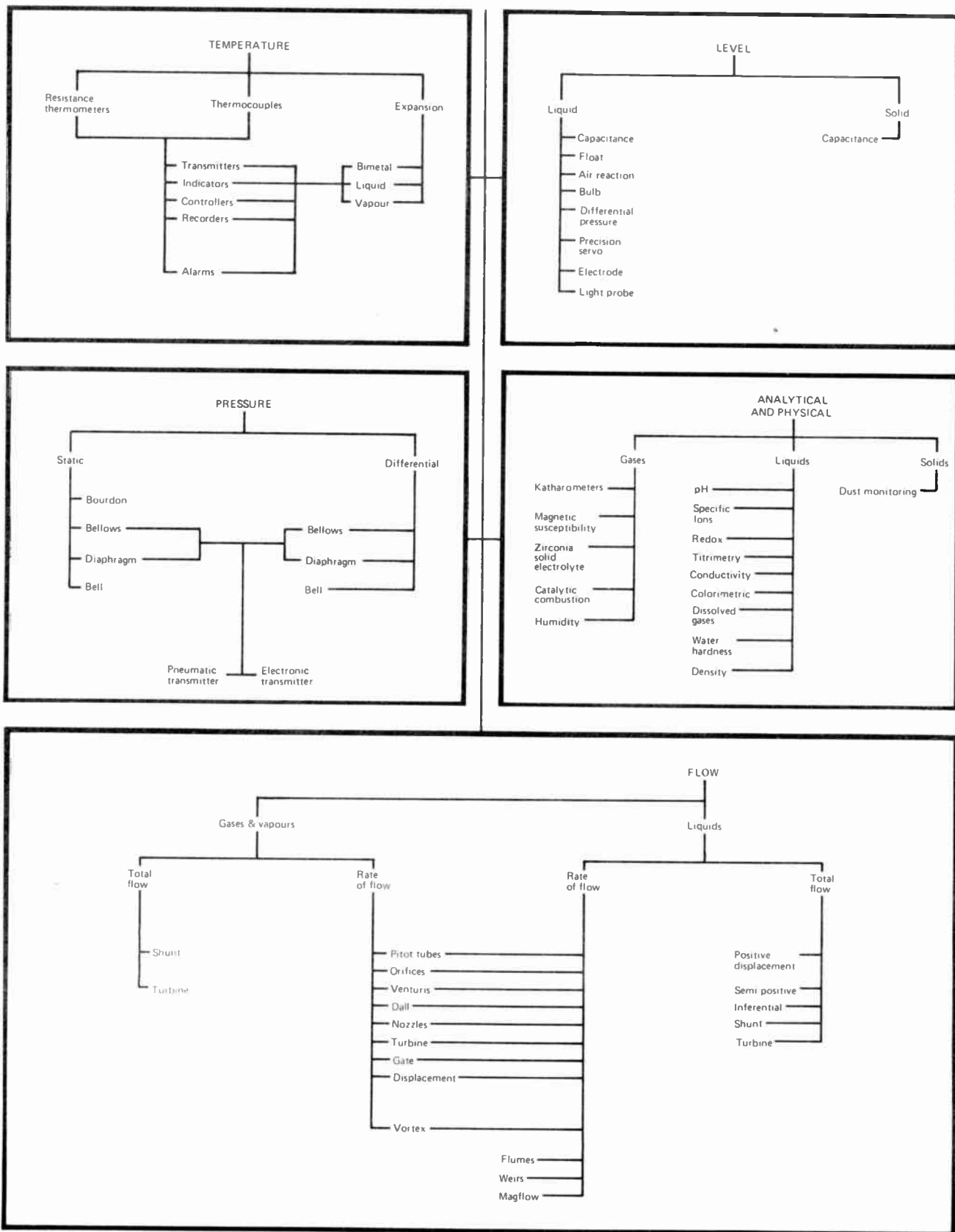


Fig. 4. The satisfactory measurement of every process plant parameter depends on the operating conditions, the degree of accuracy required, initial costs, maintenance and reliability. Within each of the main measurement areas indicated in the five sections of this diagram is a wide choice of detecting elements in the Kent range.



Fig. 5. The control room of the energy-saving refuse incinerator plant at Ulu Pandan, Singapore. The plant will produce low-cost electricity while providing an effective way of disposing of rubbish. Kent were responsible for the instrumentation: BBC Brown Boveri of Mannheim were responsible for the electrical generating equipment and the engineering, supplying, installation and commissioning of both the electrical control and instrumentation packages.

Water supply and sewage treatment

Kent have had long associations with public utilities such as water supply and sewage treatment. In both areas Kent have been pioneers – during the early years in flow measurement, but more recently in the introduction of computer control. Kent have been main suppliers of

many of the world's first computer controlled water distribution systems, and supplied and installed the first major computer controlled sewage plant in Australia. Equipment for many kinds of effluent control and water quality monitoring is in wide use in water management schemes, and projects recently completed include the continuous monitoring of the water in the rivers Rhine and Maas in Holland.

Food

Food manufacture, though characteristically a batch process, offers increasing opportunities for large scale automated flow production, including computer control. Processes involve the accurate measurement of temperatures, level and other parameters as well as on-line analysis and have ranged from the grading of potatoes and storage of apples to the control of cooking and the quality of wine.

These industrial examples are just a few demonstrating Kent involvement in different industries where complete instrumentation and control systems are helping to achieve optimum performance from a wide variety of industrial plants and processes.

Hertz and the 'Golden Age' of Science

In the final paragraph of his widely acclaimed Inaugural Address, 'Electronics—a Profession in its Golden Age', the Institution's President, Professor William Gosling spoke of the 'excitement and challenge' presented in this 'great time, the very greatest time, in which to be an electronic engineer'. We were reminded of this tribute to man's continuing striving to push forward the frontiers of knowledge by a surely uncharacteristic statement by Heinrich Hertz. In a volume of memoirs of the German scientist,* his fellow countryman, the late Dr Max von Laue, concludes his assessment of an all too short life (less than 38 years) by quoting a letter from Hertz to his family in which he refers to a book published in Leipzig in 1684—'Acta Eruditorum'. Hertz wrote appreciatively about the

* See 'New Books Received', *The Radio and Electronic Engineer*, 50, no. 4, p. 141, April 1980.

advances in mathematics and natural sciences made in that period and continued:

'Sometimes I really regret that I did not live in those times, when there was still so much that was new: to be sure enough is yet unknown, but I do not think that it will be possible to discover anything easily nowadays that would lead us to revise our entire outlook as radically as was possible in the days when the telescope and the microscope were still new'.

von Laue commented that Hertz himself most fundamentally controverted this opinion: indeed he surely would have changed his mind quite considerably in the light of the advances in electronics and radio. Arguably Hertz was the first radio and electronic engineer who, with his experimental verification of Clerk Maxwell's electromagnetic equations, laid important foundations for the 'Golden Age'.

European Conference on Solid State Circuits

In response to the growing interest in semiconductors and integrated circuits a European conference, of special significance to industry, was organized and took place in Great Britain for the first time six years ago. Since then this conference has been held each year in a different European country. By its very nature it is a conference which has attracted an audience of some hundreds of interested people, as it provides a unique opportunity to keep pace with the latest technical advances in both European and world industry.

In 1980 the sixth such ESSCIRC conference (European Solid State Circuits Conference) will be held this time in France in the town of Grenoble from 22nd to 25th September within the university confines itself and is being organized under the auspices of the following scientific bodies: EUREL, European Physical Society, Societe Française de Physique, Societe des

Electriciens et Electroniciens.

In addition to the scientific papers which have been selected by an International Programme Selection Committee, Invited Papers will be delivered by European, American and Japanese authorities in the different specialist branches of the semiconductor industry. The Invited Papers will be on subjects of general interest such as the impact of semiconductors on different industries (e.g. telecommunications, computer, automobile), the choice of solutions (either analogue or numeric), the exact nature of the collaboration between manufacturer and customer (e.g. custom-designed circuits, customizable circuits and standard circuits).

Registration forms and further programme details from CNET, Locazirst 4, Chemin des Pres, BP42, 38240 Meylan, France.

Contributors to this issue

Dick French (Fellow 1980, Member 1964, Graduate 1959) who is with the Systems Division at Philips Research Laboratories, Redhill, studied telecommunications at Norwood Technical College. He received the Ph.D. degree in 1973 from the CNAA for work on speech scrambling and synchronization techniques undertaken at PRL and Brighton Polytechnic. After two years of national service in the RAF he joined Muirhead and Co. and worked on facsimile equipment. In 1960 he moved to the then Mullard Research Laboratories, Redhill, where he has worked on communications and signal processing projects in the Communications Group. His current work is on data transmission in mobile radio networks. The paper in this issue is the fourth he has contributed to the Journal and he has given several other papers at IERE Conferences.



Professor Dennis Towill (Fellow 1970) has occupied the Chair of Engineering Production in the Department of Mechanical Engineering and Engineering Production in the University of Wales Institute of Science and Technology, Cardiff, since 1970 and he is founder and leader of the Dynamic Analysis Group at UWIST. He has held a number of industrial consultancies and was for some years with the then Bristol Aircraft Company as a dynamic analyst. Professor Towill is the author of numerous papers and books, and six of his papers have gained Institution Premiums. He is a member and past chairman of the IERE Automation and Control Systems Group Committee.



Michael Granieri is at present Assistant Executive Director of ManTech International Corporation. A 1965 graduate of the University of New Hampshire (B.S.E.E.), Mr Granieri did postgraduate work at Long Island University and the Polytechnic Institute of New York. Prior to joining ManTech in 1976, he served as Senior Electrical Engineer for Harris Corporation where he performed both hardware and software system design for three major a.t.e. systems—IHAS, VAST, and MIDGET II. Mike also was associated with Grumman Aerospace Corporation from 1965–67 where he performed Ground Support Equipment design. He is author or co-author of numerous published papers on a.t.e.



William Schmitt is technical Director for ATE Applications in ManTech International Corporation's Advanced Support Technology Division. He is responsible for all technical support activities for Test Program Set development and ATE/UUT selection program. Mr Schmitt graduated from the Polytechnic Institute of New York in 1961 with a BEE degree, and received a MSEE from New York University in 1969. Prior to joining ManTech in 1977, he was a Project Engineer for Harris Corporation where he did a.t.e. application software and a.t.e. hardware design for the following major projects: IHAS, VAST, and F-18. Bill Schmitt was also associated with Sander's Associates and Western Electric as an electrical engineer.



Tom Brown spent four years with the British Post Office and then went for a year on Voluntary Service Overseas at Kaduna Polytechnic, Nigeria. On returning to England he read for a B.Sc. honours degree in electrical engineering at Loughborough University which he was awarded in 1972. For the next three years he lectured in Telecommunications at Openshaw Technical College in Manchester and in 1975 he went as a Research Assistant to Manchester Polytechnic to study the recording of high density digital data on magnetic tape. Since 1977 he has been Experimental Officer at Manchester Medical School working on medical applications of electronics.



Barry Critchley graduated from the University of Surrey in 1973 and gained an M.Phil. degree five years later. The programme of work for his thesis formed the basis of the present paper. In 1978 he joined Standard Telecommunication Laboratories where he is currently involved in radio subsystems research and development.



Quin Davis is a Reader in Telecommunications at the University of Surrey. A note on his career was given in the July issue when a previous paper was published.

Barry Middleton is a Senior Lecturer in the Department of Electrical and Electronic Engineering at Manchester Polytechnic. Please see the August Journal for a biographical note.

Common channel multi-transmitter data systems

R. C. FRENCH, Ph.D., C.Eng., F.I.E.R.E.*

Based on a paper presented at the IERE Conference on Land Mobile Radio in Lancaster in September 1979

SUMMARY

The error performance of multi-transmitter data systems is described for mobile and stationary users in overlap areas, as a function of carrier frequency and modulation timing difference. Plots of bit error rate and error distribution are given, and the conclusion is reached that performance is comparable to single transmitter systems at the same signal level. The constraints on the choice of data modulation are discussed

1 Introduction

In a multi-transmitter mobile radio system several base station sites are set up, either to cover a large service area beyond the range of a single transmitter, or to provide intensive coverage of a smaller area. Transmissions are made from these sites to the mobiles, with the same message being sent simultaneously on the same channel. These systems are also called 'quasi-synchronous' and 'simulcast'. In some parts of the service area a mobile receives one strong signal, probably from a nearby base station, and a number of weak signals from the other sites. With data transmission the weak signals have a negligible effect and the error performance is the same as for data received from a single transmitter, as described in References 1-7. There will also be places in the service area where the coverage of two transmitters overlap and the mobile hears approximately equal signals from them. A number of measurements have been made to find the error rate and error distribution in these overlap areas, as a function of carrier frequency difference and modulation timing difference, for both moving and stationary users.

The error performance measurements have been made so that multi-transmitter systems using data transmission of predictable performance can be designed. The error statistics are analysed so that coding schemes for error control can be chosen which provide an acceptable performance whether the user is mobile or stationary, and whether one, two or more transmitters are heard.

2 Overlap Areas

Consider a typical multi-transmitter system with two transmitters spaced 20 km apart. The size and position of the overlap areas is determined by the nature of the radio propagation from the base stations to the mobile; there are three aspects to this. First, the area mean signal level depends on the range from the transmitter according to an inverse fourth-power law, so that each decade increase in range reduces the mean level by 40 dB. By itself this law would result in a single overlap area (shaped like a convex lens) lying half way between equal power transmitters. Inside this area the signals from the two transmitters would be equal within a certain margin, and the error performance could be found by driving through the overlap and recording the error pattern. However in practice the situation is complicated by the other two aspects of mobile radio propagation, which are fading and shadowing.

The fading is a rapid fluctuation in the signal envelope caused by multipath propagation, which results in sharp peaks and nulls in the received signal envelope as the waves add and cancel. The shadowing is a slower change caused by variation in topography such as street width, building height, hills, etc. The fading causes the received signal envelope to vary relative to the local mean signal

* Philips Research Laboratories, Redhill, Surrey RH1 5HA.

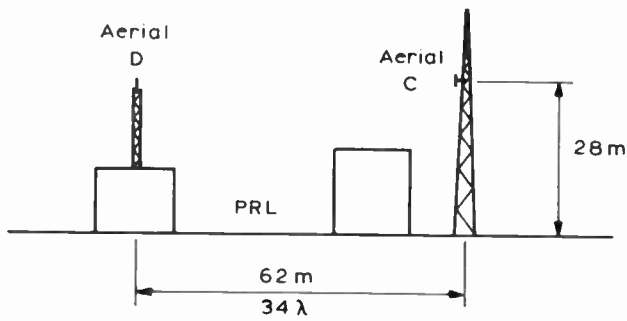


Fig. 1. Base station transmitter aerials.

level (averaged over about 50 m) and the shadowing results in the local mean varying about the area mean. This propagation model is more fully described in References 1 and 8.

The shadowing has the effect of breaking up the single overlap area into many small areas where the local means of the signals from the two transmitters are nearly equal, with areas in between where they are quite different. The small overlap areas are certainly large enough for a complete data exchange to take place, with the result that reliable statistics of error performance in these areas are needed. However the areas are too small for enough bits to be transmitted to a moving vehicle for

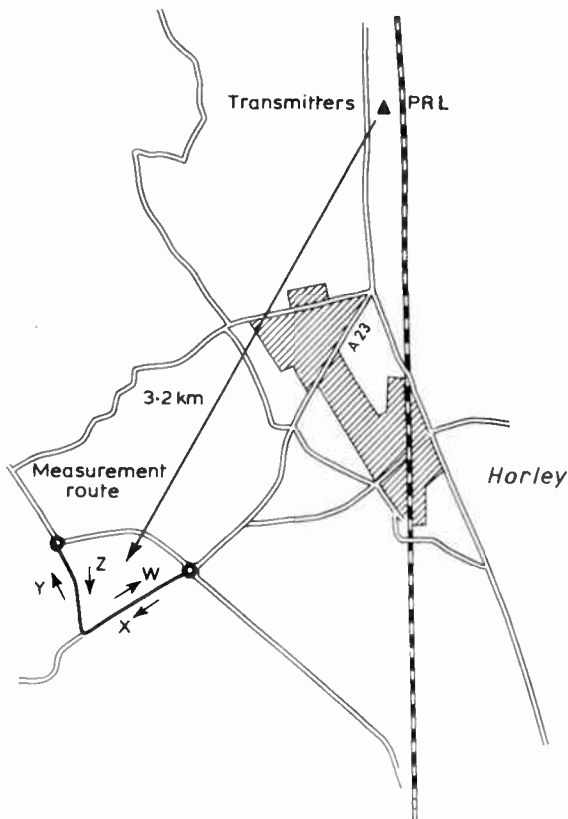


Fig. 2. Measurement location.

a statistically significant measurement of the error performance to be made. If a long measurement is made it will include transmission in areas of very different local mean level, where the performance may be quite different, which would give a false view of the overlap area.

3 The Measurement System

The problem was overcome by setting up two transmitters close together, with their aerials only 62 m (34λ) apart, as shown in Fig. 1. With such close spacing the local mean signal levels from the two transmitters are generally well correlated in the service area, and suitable measurement routes were found where the local means were sufficiently equal for the whole route to be considered a continuous overlap. Continuous data transmissions were made to the measurement vehicle as it was driven around the route. (Fig. 2).

We must now consider the final aspect of the radio propagation, the fading. With widely-spaced transmitters the fading in the two signals received at the vehicle would be uncorrelated in normal situations. In the measurement system, with its closely-spaced transmitters, there is a danger that the fading in the two signals may be correlated if the spacing is too small; however if it is too large the correlation in the local mean levels will be lost. The propagation measurements

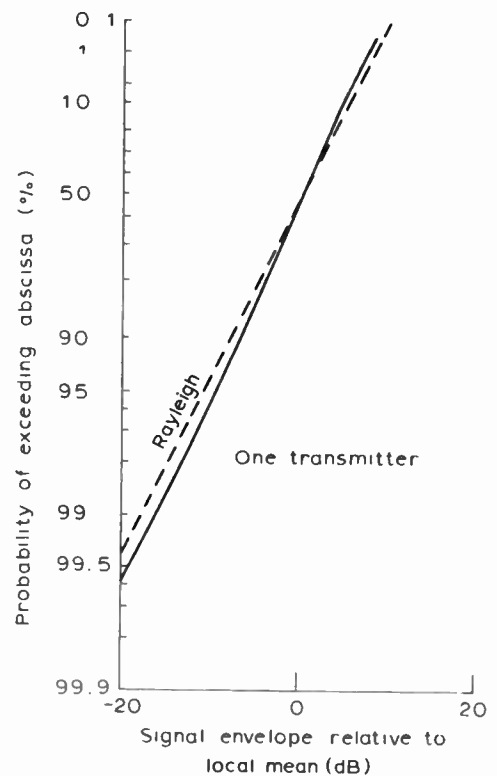


Fig. 3. Received signal envelope distribution with one transmitter.

described below show that the route used for the measurements had a satisfactorily low correlation in the fading, and a high correlation in the shadowing giving a large overlap area in which meaningful measurements can be made.

4 Propagation Measurements

Careful measurements were made to determine the propagation conditions over the measurement route and the correlation between the signals from the two transmitters. Initially the signal envelope from only one transmitter was recorded and analysed as described in Reference 8. With a 20W transmitter the measurement route has an overall mean signal level of 40 dB relative to 1 μ V p.d. This high signal level made it possible to use a 20 dB attenuator in the aerial lead of the receiver to exclude ignition noise from the measurements, and this was done in the field measurements.

The local mean signal level was found by averaging the received signal envelope over distances of about 50 m. Due to shadowing the local mean was found to vary relative to the overall mean of the route, showing an average difference of 3 dB and a maximum difference of 7 dB. The signal envelope was also normalized to the local mean levels to remove the variation due to shadowing, and the remaining fading was found to be substantially Rayleigh-distributed, as shown in Fig. 3.

The correlation between unmodulated envelopes from the two transmitters was measured by shifting the carrier frequencies 5 kHz apart and using two receivers with narrow band i.f. filters, fed from a common aerial. Initially both transmitters also fed a common aerial and it was established that identical recordings were made from the two receivers (the correlation of their outputs was 0.99), showing that the propagation path is the same for signals with a 5 kHz difference in carrier frequency. Simultaneous signal recordings were then made, one from each receiver, whilst the two transmitters fed their own aeriels, still with a 5 kHz carrier difference, and the signal recordings were processed to find the correlation in the signal fading. For this purpose the recordings were normalized to the local mean signal level in order to eliminate the shadowing and leave only the variation due to fading. The route was divided into four sections, W X Y Z, and the correlation coefficients for these sections were 0.08, 0.23, 0.36 and 0.41, which are low enough for the signals to be considered uncorrelated.

Next the degree of correlation in the local mean levels was measured. To do this the two signal level recordings were smoothed to remove the rapid fading and the remaining variations, the changing local means due to shadowing, were correlated. Over the four sections of the route the correlation coefficients were 0.88, 0.65, 0.95 and 0.88 showing a fairly good correlation. With a coefficient of 0.88 the average difference between the local mean levels was 1.7 dB, the standard deviation of

the difference was 1.3 dB, and the maximum difference was 4.8 dB. The transmitters were then returned to the same channel.

5 Error Performance when Mobile

The two transmitters were tuned to a nominal 164.975 MHz and a carrier frequency difference of 1 Hz with two Pye Telecommunications HS400 high stability drive units, and were directly frequency-modulated by baseband data to a deviation of 2.4 kHz. Initially the modulation timing difference was set to zero. The bit error rate for both single and multi-transmitter operation is shown in Fig. 4 as a function of mean received signal level. Each measured point results from about 3×10^5 bits transmitted to the vehicle as it makes one lap around the measurement route. As can be seen from Fig. 4 there is no significant difference between the bit error rates (b.e.r.) whether the signal is received from a single transmitter or from two half-power transmitters, particularly at the higher signal levels. This is a very convenient result since the b.e.r. in multi-transmitter data systems can be predicted using the techniques developed for the single transmitter case.¹ At first sight it is perhaps surprising that multi-transmitter operation has not significantly altered the b.e.r., but the following explains why.

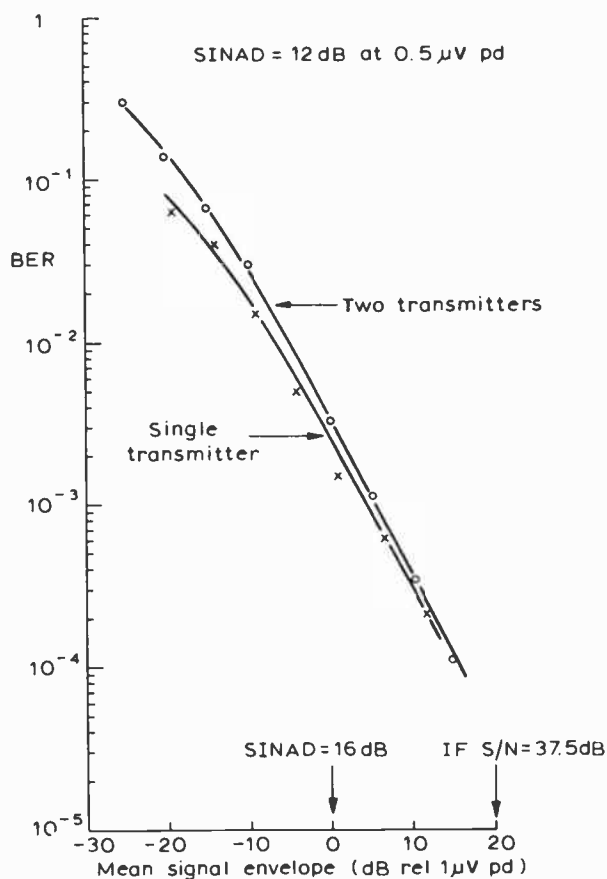


Fig. 4. Error performance—mobile, 1200 b/s d.f.m.

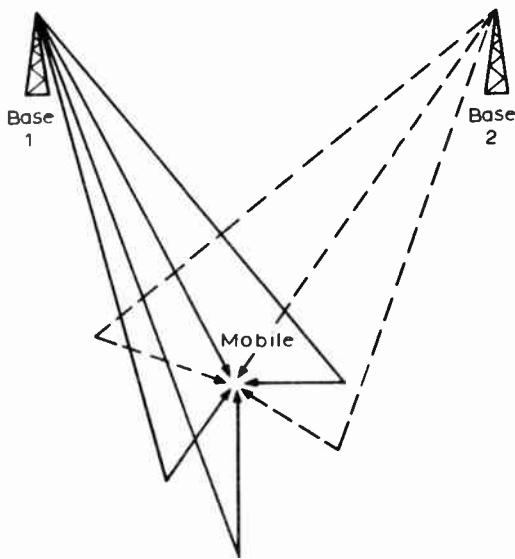


Fig. 5. Multipath from two base stations.

Figure 5 illustrates multi-path propagation from two base stations to a mobile. The mobile receives many multi-path signals from the first transmitter, each with an arbitrary phase and a small Doppler frequency shift, which depends on where the multi-path reflector is relative to the moving vehicle. The mobile also receives multi-path signals from the second transmitter which also have an arbitrary phase and a small Doppler frequency shift. Clearly a phase difference between the carriers at the two transmitting sites will have no effect,

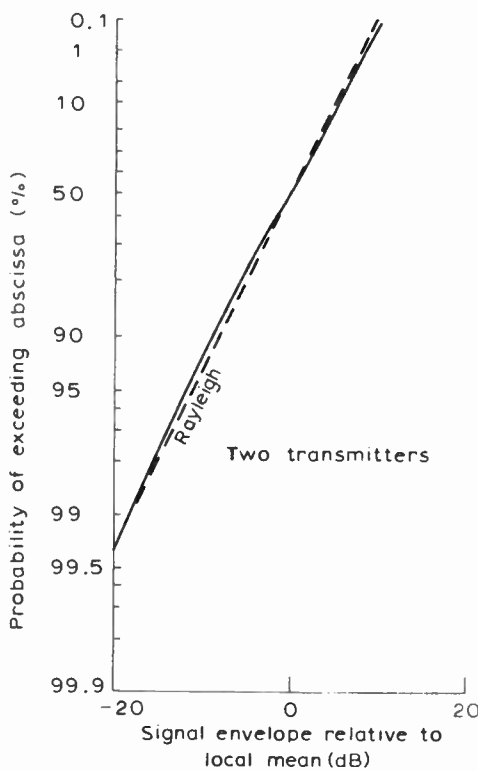


Fig. 6. Received signal envelope distribution with two transmitters.

since all the multi-path components have an arbitrary phase anyway; also the difference in carrier frequency at the sites would not be expected to have much effect so long as it is less than the Doppler shifts. Since a large number of multi-path signals leads to a Rayleigh-distributed signal, having about twice as many in the overlap area with two transmitters will only tend to make the distribution more closely Rayleigh. This is indeed borne out by the distribution shown in Fig. 6 for two transmitters. Consequently much the same b.e.r. would be expected with multi-transmitter operation, as with a single transmitter. It might be thought that when the second transmitter is switched on it will fill in some of the fades in the field of the first transmitter. This is true, but it will also interfere with the first transmitter to produce new fades, resulting in much the same number of fades overall.

5.1 Modulation Timing

Multi-path signals from a single transmitter will have a small difference in time of arrival of a few microseconds, but this has negligible effect at low bit rates like 1200 b/s. In multi-transmitter systems the time-of-flight delay difference is unlikely to be more than a few tens of microseconds in the overlap areas, which is still too small to matter at 1200 b/s. The main problem is the delay in signals passed over leased lines between the control room and the base station sites. These delays must be equalized to give a differential delay of less than about 0.3 of the bit period, as indicated by the plot of b.e.r. against modulation timing difference given in Fig. 7. Fortunately the error rate is not very dependent on timing difference until the difference reaches about 0.3 of the bit period, when the error rate rises to b.e.r.=0.25.

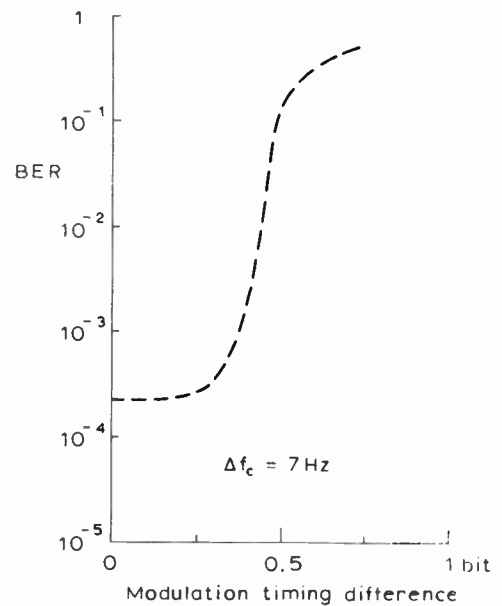


Fig. 7. Bit error rate against modulation timing.

(Note that the b.e.r. becomes equal to 0.25 rather than 0.5, because with one-bit delay difference, half of the bits reinforce by chance and half the remainder are correct by chance). An alternative to padding out the delay in the land lines to the transmitters, and readjusting them should the lines be rerouted, would be to use radio links or 'reverse frequency' working in place of the lines, in which case the delays could be small and constant. Another possibility would be to use an off-air standard as a reference clock to restandardize the data to a common timing at each base station.

5.2 Carrier Frequency Difference

The dependence of b.e.r. on carrier frequency difference, Δf_c is shown in Fig. 8, for the case of zero timing difference. A bit rate of 300 b/s (2.4 kHz deviation) was used so that carrier frequency differences equal to the bit rate frequency could be obtained within the channel bandwidth. The b.e.r. drops with increasing carrier frequency difference and is reduced by about two orders of magnitude with a difference near to the bit rate frequency. This is a significant drop in b.e.r. and could prove useful in intensive coverage systems where a mobile hears two transmitters at a useful signal level over a large proportion of the service area. However the channel bandwidth available would only permit operation at 300 b/s with a carrier frequency difference equal to the bit rate. Where multiple transmitters are used to cover a wide area a mobile is only in an overlap occasionally, and in this case the overall system performance would be higher with 1200 b/s operation. The error rate in the overlap area would be greater than at 300 b/s but this would be more than offset by the

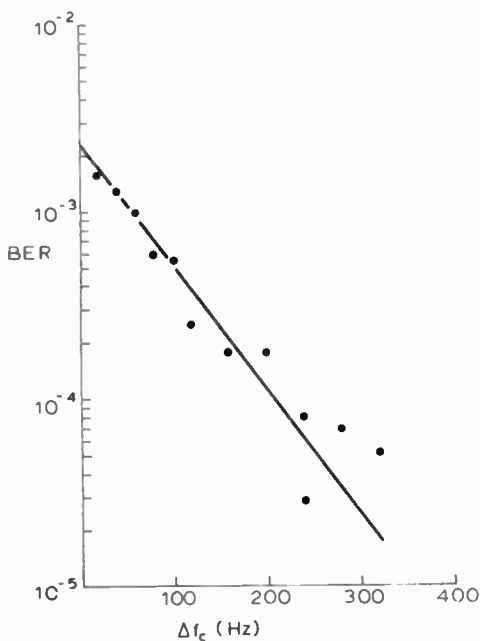


Fig. 8. Bit error rate against carrier frequency difference (300 b/s).

higher throughput and better code performance at 1200 b/s, where more redundancy can be used in the coding than at 300 b/s.

The results show that the b.e.r. in multi-transmitter systems can be predicted using single transmitter methods¹ even when the carrier frequency difference is greater than the Doppler shift, but much less than the bit rate frequency. They also show that the Doppler shift itself is not a limitation to data error performance, in fact driving at a furious speed to produce greater received carrier frequency shifts in the multi-path signals will slightly reduce the number of errors (in the received data message).

Similar measurements were made of b.e.r. as a function of carrier frequency difference at 1200 b/s, and much the same drop in b.e.r. with frequency difference was found, with half the b.e.r. for a frequency difference of a quarter of the bit rate frequency.

5.3 The Error Distribution

It is not enough to know how many errors occur when data is transmitted, we must also know how they are distributed. One useful method of analysing the distribution of errors in the recorded error patterns is to divide the error record into blocks of say, 32 bits and to plot the probability of finding m or more errors in a block, as a function of m , as described in reference 9. A typical result is shown in Fig. 9, where the distribution for the single transmitter case is compared with multi-transmitter results for carrier frequency differences of 1,

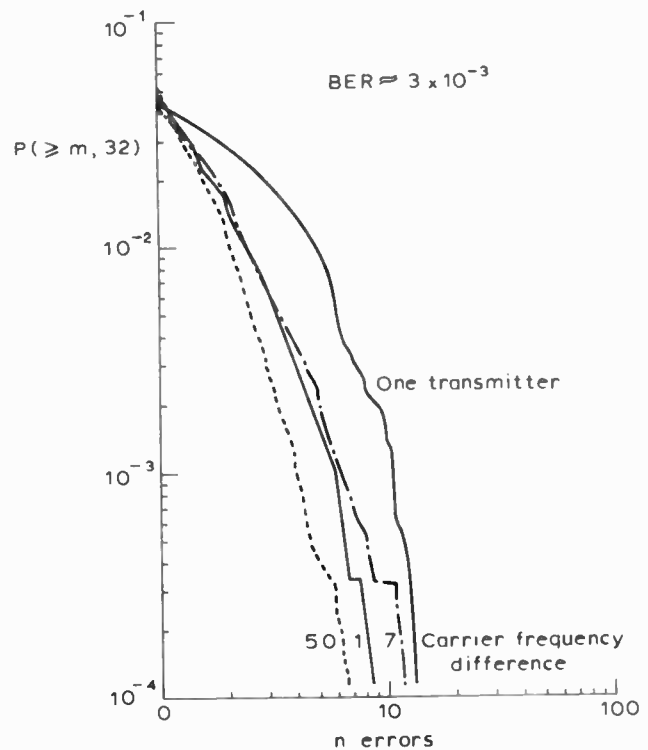


Fig. 9. Error distributions—mobile, 1200b/s d.f.m.

7 and 50 Hz. The curves show the number of errors that a coding scheme must cope with for a given performance. The wider the curve the greater is the number of errors in a block. The y axis intercept in Fig. 9 gives the probability of a block containing errors, and therefore the success rate for an error detecting code, which is much the same for single and multi-transmitter operation. The width of the plot is a measure of the number of errors in a block and an indicator of the false rate in codes and the success rate in an error-correcting code. Multi-transmitter systems are between two and ten times better than single transmitter systems with the best results obtained at a larger carrier frequency difference. Further insight into the use of curves like Fig. 9 is contained in reference 9.

6 Multi-transmitter Modulation Schemes

Multi-transmitter operation imposes a number of constraints on the choice of modulation scheme. The measurements described here used direct frequency modulation of the r.f. carrier with base-band data, which has been used in a number of paging schemes. The approach is simple and offers the maximum tolerance to modulation timing difference; also the data demodulator in the mobile is cheap and has a high performance, within 1 dB of the theoretical optimum.

In multi-transmitter systems the data must be passed from the control room to the base station sites, which will be many kilometres away. The most common method is to lease telephone lines from the Post Office, in which case sub-carrier data modulation must be used, due to the bandpass nature of the lines. It would be convenient and economic to use the same sub-carrier modulation in the base to mobile path so that through signalling could be employed between control room and mobile. Unfortunately there is the problem that the Post Office line may be a derived line (or may become so), in which case there will be a small frequency offset and an arbitrary phase in the data signal received at the base station, which would prevent reception of the data signals at a mobile in an overlap area if simple through-signalling were used. For successful demodulation at the mobile in an overlap area, the data modulation on the carriers from the two transmitters must reinforce.

6.1 Base Station Regeneration

One solution to the derived line problem is to demodulate the sub-carrier data signal at the base station and to modulate the base transmitter with a new data signal, using either direct modulation of the r.f. carrier, or sub-carrier modulation. With direct frequency modulation all that is then needed for the signals to reinforce is to agree the sense of the modulation, e.g. that a logical one reduces the carrier frequency (CCITT recommendation V1). With sub-carrier data modulation the situation is more complicated.

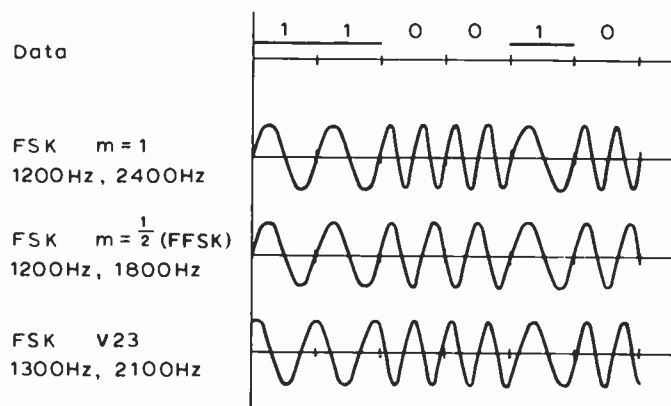


Fig. 10. Subcarrier data modulation schemes.

With f.s.k. $m=1$ modulation there is no problem in the radio path because a logical one is always represented by a cycle of sinewave at 1200 Hz and a logical zero by two cycles at 2400 Hz, as shown in Fig. 10. Symbols from the two transmitters will therefore reinforce at the receiver, although the modulation timing difference is now more critical than with direct modulation. Unfortunately, the low-frequency components in the signal make its transmission on telephone circuits uncertain. FSK V23, which represents a logical one by 1300 Hz and logical zero by 2100 Hz is often used on telephone circuits but is unsuitable for quasi-synchronous systems. Although the symbols from the two transmitters would have the same frequency, they would generally have different phases, since the starting phase in V23 is arbitrary. Even a special version of V23 with a defined starting phase would have the difficulty that a single error in the regeneration at one base station would shift the phase of all the following symbols from that station, compared with the other.

FFSK $m=\frac{1}{2}$ is emerging as a standard for mobile radio data transmission; it represents a logical one by a cycle of 1200 Hz and a logical zero by one and a half cycles of 1800 Hz. To keep the spectrum narrow the phase of the data signal is made continuous so that two logical one symbols are needed (normal and inverted) and two logical zero symbols, as can be seen in Figure 10. Like V23, this leads to the problem that an error in the regenerator at one base station will invert all of the following symbols, resulting in a high error rate for a receiver in an overlap region.

An alternative to regeneration would be to remove the frequency offset introduced by the telephone circuit by a mixing process with a reference tone passed through the same circuit.

6.2 Radio Links

Where radio links or reverse frequency working is used to connect the control room to the base station sites, there need be no frequency offset, and any of the sub-carrier data modulation schemes shown in Fig. 10 can be

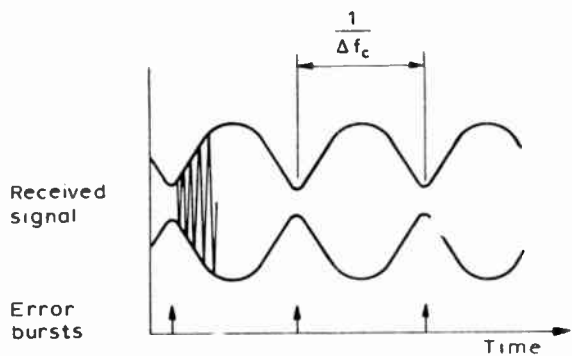


Fig. 11. Received signal envelope—stationary.

used. However with FFSK $m = \frac{1}{2}$ or with V23 it is essential that the signals are not regenerated at the base stations, and that a single data modulator is used at the control room which drives all the base stations with the same modulated data signal.

7 Stationary Users

Stationary users who listen to a multi-transmitter system with a small carrier frequency difference, Δf_c , will hear a signal whose envelope varies as shown in Fig. 11. If the signals from the two transmitters are nearly equal, as in the Figure, the carrier envelope drops to near the noise

level of the receiver, and bursts of errors occur at intervals of $1/\Delta f_c$.

Bench measurements were made in which two data-modulated carriers at 164.975 MHz were combined via attenuators and passed to a receiver, and the error pattern in the demodulated data was recorded. Figure 12 shows a plot of b.e.r. against the level of one of the signals, with the other signal at relative levels between 2 and 10 dB. A substantial number of errors occurs when the two signals are nearly equal, even at high signal levels, and a loss of between 10 and 20 dB in error performance relative to single transmitter working is found. However the b.e.r. is similar to the mobile situation; e.g. both give a b.e.r. = 2.5×10^{-3} at a signal level of 0 dB, and a 2 dB difference in signal level in the stationary case.

With a single transmitter there is a small chance ($\sim 1\%$) that a user will be in a fade and therefore out of touch. With multi-transmitter operation it is far less likely ($\sim 0.01\%$) that the user will be completely without a signal, since this only happens when both signals fade at the same point. However this is offset by the loss of data where the two signals are very closely equal and the b.e.r. is probably too high for successful message reception. Further work is needed to establish exactly what proportion of places will have an unacceptable performance.

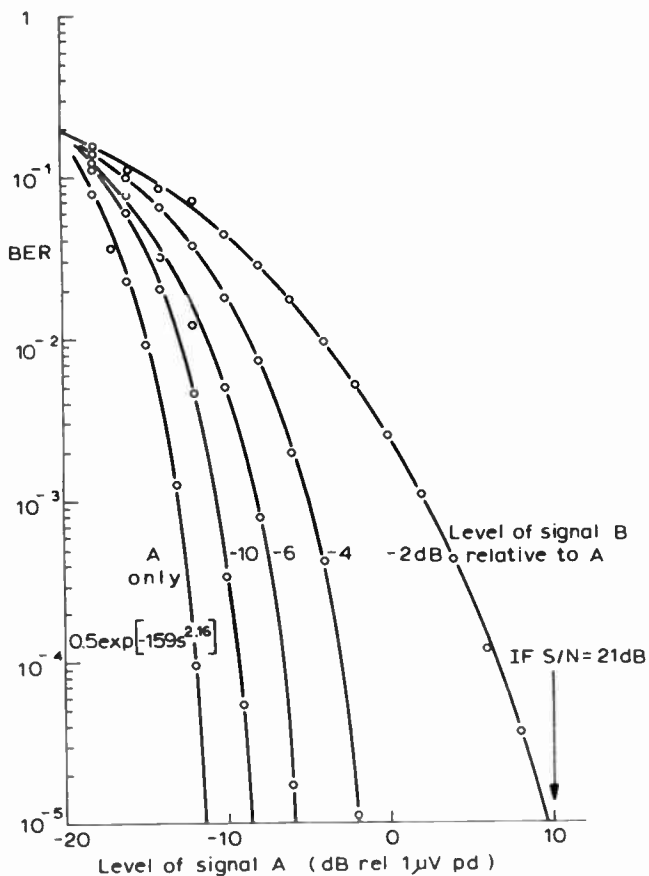


Fig. 12. Error performance—stationary, 1200b/s d.f.m.

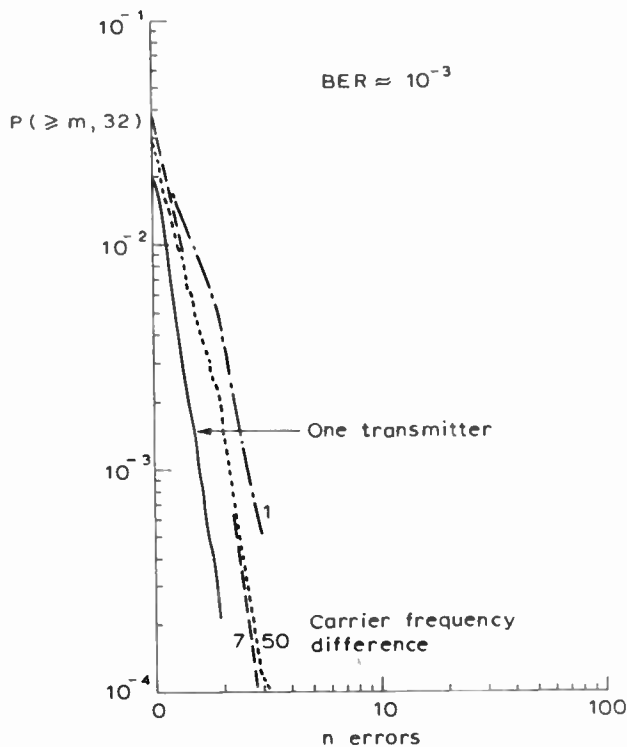


Fig. 13. Error distributions—stationary, 1200b/s d.f.m.

7.1 Error Distribution

Figure 13 shows the error distribution for the stationary case with nearly equal signals, for carrier frequency differences of 1, 7 and 50 Hz, and for only one signal. The distribution shows more errors in a 32-bit block with multi-transmitter signals than with a single signal, particularly when the carrier difference is 1 Hz. However comparison with Fig. 9 shows that there are fewer errors in a block when stationary than mobile, so that a coding scheme which gives acceptable results with mobile operation would have comparable performance when stationary.

One way of dealing with the severe bursts of errors that occur with equal signals relies on the regular spacing of the error bursts. With a carrier frequency difference of 1 Hz, for example, short messages of much less than one second duration are sent. Some messages are lost due to the error bursts at one-second intervals, but this could be controlled by using error-detecting coding and arranging to repeat messages after 1.5 seconds. If the first transmission is lost the repeat will be received.

8 Conclusions

Error performance measurements have been made in a multi-transmitter data transmission system at v.h.f, for both mobile and stationary users. Plots of bit error rate and error distribution have been given, and the dependence of bit error rate on carrier frequency difference and modulation timing difference has been investigated.

The mobile measurements were made in a vehicle moving over a route in a continuous overlap area where the received signals suffered Rayleigh fading and there was a high correlation between the local mean levels in the two signals.

For mobile users the b.e.r. is virtually the same with two half-power transmitters as with a single full-power transmitter. The error distribution is similar to the single transmitter case so that a single coding scheme can be used which will have much the same performance in the overlap areas as where only one transmitter is heard. An explanation for the similarity in performance of multi- and single-transmitter systems is given.

The error performance for stationary users has also been investigated. The situation here is more complicated, and the b.e.r. is shown to depend very strongly on the relative size of the signals from the two

transmitters. In most cases the performance is worse than for a single-transmitter system, but better than for mobile operation. However there are some places where the signals are very closely equal where the performance may be rather worse. The exact proportion of users in these areas remains to be calculated.

Some of the limitations on the choice of modulation scheme imposed by multi-transmitter operation are discussed.

The b.e.r. with multi-transmitter working is not sensitive to the carrier frequency difference, so this parameter can be chosen to suit speech, in mixed speech and data systems.

9 Acknowledgment

I should like to acknowledge the contribution made to this work by my colleagues, P. J. Mabey, R. Wells, T. W. F. Whiter and K. J. Wheatley.

10 References

- 1 French, R. C., 'Error rate predictions and measurements in the mobile radio data channel', *IEEE Trans. on Vehicular Technology*, VT-27, No. 3, pp. 110-6, August 1978.
- 2 French, R. C., 'Error performance in mobile radio data transmission in the urban environment', *NachrTechn Z.*, 31, pp. 200-3, March 1978.
- 3 French, R. C., 'Mobile radio data transmission in the urban environment', *IEEE Intl. Conf. on Communications*, 1976, pp. 27-15 to 27-20.
- 4 Hansen, F. and Meno, F. I., 'Mobile fading-Rayleigh and lognormal super-imposed', *IEEE Trans. on Vehicular Technology*, VT-26, pp. 332-5, November 1977.
- 5 Hansen, F., 'Error rates in mobile signalling systems', *Communications '74 Conference*, Brighton, England, June 1974.
- 6 Kelly, T. C. and Ward, J. E., 'Investigation of digital mobile radio communications'. US Dept of Justice, Law Enforcement Assistance Administration, National Institute of Law Enforcement and Criminal Justice, October 1973.
- 7 Brucket, E. J. and Sangster, J. H., 'The effects of fading and impulse noise on digital transmission over a land mobile radio channel', *IEEE Vehicular Technology Conference*, pp. 14-16, December 1969.
- 8 French, R. C., 'Radio propagation in London at 462 MHz', *The Radio and Electronic Engineer*, 46, pp. 333-6, July 1976.
- 9 Mabey, P. J., 'Mobile radio data transmission—coding for error control'. *IEEE Trans. on Vehicular Technology*, VT-27, pp. 99-109, August 1978.
- 10 Arredondo, G. A., 'Analysis of radio paging errors in multi-transmitter mobile systems'. *IEEE Trans. on Communications*, COM-21, No. 11, pp. 1310-8, November 1975.

Manuscript first received by the Institution in June 1979 and in final form on 15th May 1980.

(Paper No. 1952/Comm 204)

Man-machine interaction in aerospace control systems

Professor D. R. TOWILL,
D.Sc., C.Eng., F.I.E.R.E., M.I. Prod. E.*

Based on a paper presented at an IERE Colloquium on Design of Control Systems for Advanced Aircraft having Relaxed or Negative Stability held in London on 16th October 1979.

SUMMARY

The Multi-Role Combat Aircraft *Tornado* is probably the most spectacular example to date of a complex man-machine system in which design and manufacture are widely dispersed. Even sub-assemblies of this system are extremely complex relative to the technology of just a few years ago. This makes life extremely difficult for an engineer involved in the procurement of the sub-assembly, especially as the overall objective can soon be submerged in a mass of detail.

Starting with a review of desirable dynamic properties of the machine, as seen by the man, typical human operator transfer functions which have found use in closed-loop control system design are presented. Some ways in which microelectronics can reduce pilot work load are then discussed with the object of conveying to the design engineer some of the reasoning behind the performance specification he is trying to meet. Examples include helicopter stability augmentation systems and spacecraft terminal phase control.

1 Introduction

Optimizing the performance of man-machine systems is an inter-disciplinary activity requiring contributions from behavioural scientists, plant designers ('plant' is the generic term used to describe the object being controlled), servomechanism experts, electronic engineers, and systems specialists. Thus the development of a complex man-machine system, such as are met in aerospace applications, requires a large team of engineers and scientists in split locations and separate companies. The *Tornado* aircraft is the most obvious example.

Each group within the team will work towards an itemized performance specification appropriate to the individual hardware or software product being manufactured. Every such product will, in general, be well engineered through the customary evolutionary process which is the hallmark of good practice, and which represents the commercial expertise of industrial companies.

However, the bringing together of all these products and skills to optimize the performance of the man-machine system, i.e. the 'systems engineering' aspect is less well understood. Thus it is not difficult in times of galloping technological obsolescence for designers of individual products to lose sight of the overall system objectives. This in turn will render less effective the highly desirable interchange of ideas between design groups within the team especially with regard to performance specification where the human operator is acting within a closed loop system.

Even worse would be a situation in which a potential hazard went unrecognized. This is particularly true with the increasing use of digital microelectronics, where it is now being recognized that software reliability must be improved.¹ Until we are satisfied in this respect, we should make haste slowly in replacing operationally satisfactory analogue equipment.

2 Contribution of the Present Paper

The purpose of this paper is to bring together the constituent components of man-machine systems in such a way as to provide a firm foundation for the 'systems engineering' aspect of design. As a consequence, the meaning of performance specifications commonly used for each sub-system will become apparent.

In particular, it is intended to highlight the increasing contribution of microelectronics to man-machine system design. For example, Table 1 illustrates the volumetric compression in commercially-developed aircraft flight control system (a.f.c.s.) electronics achieved over a fifteen-year span. It can be seen that volume needed is reduced by approximately 50% every two years. Additionally, of course, it may be argued that the improvement is even more spectacular, because present

* Dynamic Analysis Group, University of Wales Institute of Science and Technology, King Edward VII Avenue, Cardiff CF1 3NU.

Table 1

Microminiaturization of the automatic flight control system (a.f.c.s.) due to advances in electronic technology²

Year	Vehicle	Approximate volume (cm ³)
1958	U.S. Navy A6 aircraft autopilot	950
1962	Missile autopilot	290
1968	Boeing 747 autopilot	40
1973	U.S.A.F. B1 aircraft autopilot	10

day a.f.c.s. are capable of performing a wider range of functions than earlier models.

Wherever possible, the usual systems engineering tools such as block diagrams, flow diagrams, and transfer function techniques will be used. Although most of the readily available published literature on man-machine systems deals with aerospace applications, the subject is of much wider relevance. So we find the same principles applied to skill development,³ shipsteering,⁴⁻⁶ land vehicle steering,^{7,8} and 'bumpless' train shunting.⁹ The opportunity will also be taken to show how micro-electronics can be used to reduce human operator workload, via such techniques as plant augmentation, display quickening, providing a model reference describing the current plant dynamics, 'observers' for state estimation, and fast models for prediction in terminal-phase docking operations.

3 Man-Machine System Concepts

Much of early work on the development of the 'servomechanism' approach to modelling human operator performance in man-machine systems was undertaken during, and shortly after World War II.¹⁰⁻¹⁴

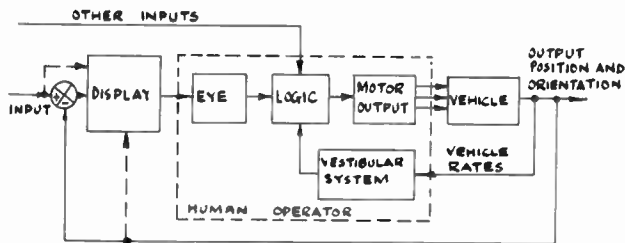
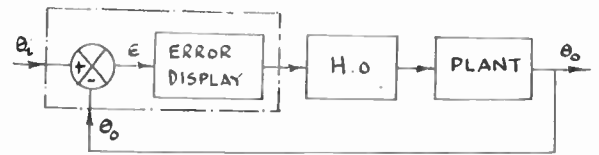


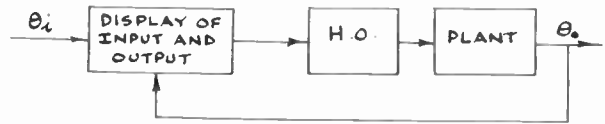
Fig. 1. Basic man-machine control system.

The result is the block diagram shown in Fig. 1 in which the human operator is embedded into a closed-loop system, and reacting to visual, vestibular (perceived motions, such as via the 'seat-of-pants' feeling), and other inputs.¹⁵

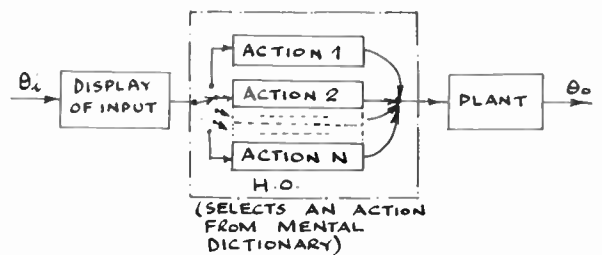
One example of a vestibular sensor transfer function is the horizontal pair of semi-circular canals located in the ear which permit the human operator to perceive



(a) 'Compensatory behaviour'.



(b) 'Pursuit' behaviour.



(c) 'Pre-cognitive' behaviour, i.e. 'no feedback'.

Fig. 2. Stimulus organization and display in human operator skill development. (After Ref. 3.)

angular velocity in a blind situation. A suitable model is

$$\left[\frac{\text{sensor output}}{\text{input angular velocity}} \right] = \frac{10s}{(1 + 10s)(1 + s/10)} \quad (1)$$

From this sensor output it is clear that the human operator has an essentially flat response in sensing angular motions in the range 0.10 to 10 rad/s.¹⁵

4 Display Configurations

The display shown in Fig. 1 can be the perceived visual field, or a 'blind' display. In the former case, the choice of display is made by the operator, whereas in the latter case it is at the discretion of the system designer. As we shall see later, it is possible to relate the display chosen by the human operator to skill development in task performance.

We may describe the operation of the systems shown in Fig. 2 in the following ways:³

'Compensation'

In compensatory tracking the visually displayed effects of the human operator are not distinguishable from the system output. So the operator can only determine the effect of control motion if the input conditions are zero.

'Pursuit'

Past experience provides the operator with information about what to expect in a future input, but he must operate in a closed loop fashion with feedback about his responses. The operator can distinguish the effect of his

actions from changes in input stimuli.

'Pre-Cognitive'

The operator has effectively complete information about the input's future. A stimulus can then trigger off a 'dictionary' of practised, properly sequenced responses on the part of the operator. It is essentially 'open-loop' control, i.e. no feedback.

5 Skill Development Viewed as a Choice of Display

For the well-known example of learning to drive an automobile, skill development may be explained via the sequencing of perceived displays in the following way:³

Phase 1. Novice starts by relating fixed object on car to a guideline on the road, so may aim to keep a constant angle between a point on the body and the curb. This is *compensatory* as the operator attends to error only.

Phase 2. Operator becomes aware of the separate characteristics of the curb and the car. He achieves a *pursuit* display organization of his visual field and hence makes use of the regularities and predictable features of the road.

Phase 3. On achieving complete familiarity with the 'plant', the operator samples entire visual field, and steers vehicle with deft, discrete, movements. This is 'open-loop', or *pre-cognitive* behaviour in which the operator has thoroughly learned his inputs, and by experience seems to provide exactly the right output. Examples are a helmsman meeting a turning ship, and a driver recovering from a skid. The time interval between these short-term bursts of 'open-loop' control depends on environmental conditions.

In apparent contradiction, we note that most published research into man-machine system performance utilizing the servomechanism approach is based on compensatory control. This has been found to be the most relevant configuration for the control of complex multi-loop systems, especially as met in aerospace applications. Examples are instrument-aided landing systems, and terrain following via head-up displays.

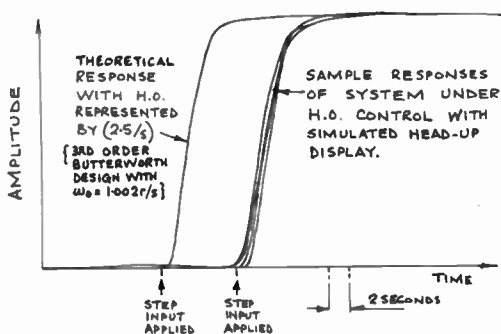


Fig. 3. Step response of 'optimized' vertical rate loop. (After Ref. 16.)

6 Human Operator Variability

Unlike a servomechanism, in which the response to a given stimulus is generally repeatable, human operator response will not always be the same, although in a well-designed system the skilled operator will perform with reasonable consistency. Figure 3 shows a set of step responses obtained during simulator studies with the human operator as part of an eighth-order closed-loop system. Although there is some variability in response, it does not depart significantly from the idealized third-order Butterworth response. This was chosen by the system designer so that little or no overshoot would result, which is thought to be a highly desirable characteristic in terrain-following systems.¹⁶

The design concept used is of interest. Using a simple model (2.5/s) to represent the human operator inside a closed-loop control system, there are then five system zeros and eight system poles, so that we may write

$$\left[\frac{\dot{h}_0}{h_D} (s) \right] = \frac{\left[1 + \sum_{i=1}^{i=5} b_i s^i \right]}{\left[1 + \sum_{i=1}^{i=8} a_i s^i \right]} \quad (2)$$

If the system is now compensated such that the denominator can be factorized into

$$\left[1 + \sum_{i=1}^{i=8} a_i s^i \right] = \left[1 + \sum_{i=1}^{i=5} b_i s^i \right] \times \left[(1 + 2(s/\omega_0) + 2(s/\omega_0)^2 + (s/\omega_0)^3) \right] \quad (3)$$

then five system poles will cancel out the five system zeros, leaving the desired third-order Butterworth design to describe the system response to command signals. The ω₀ parameter is set by the designer, based on the desired speed of response. For 'optimum' performance to be achieved in practice, ω₀ must be compatible with human operator capability. From the results shown in Fig. 3, the value of ω₀ chosen is clearly satisfactory.

7 'Quickening' the Display

The cancellation design is also of interest from two further points of view. Firstly, the design is mechanized by a technique known as 'quickening', as shown in Fig. 4.¹⁷ Here the sensor and synthesized data which are fed back are mixed prior to the display. The human operator therefore reacts to a single stimulus, just as he would in an unquickened system, except that the signal displayed is the 'optimum' needed to achieve the desired closed-loop performance. In contrast, where plant augmentation is used, as will be described later, similar signals are feedback, not to the operator display, but are coupled to the operator output to form one or more minor loops around the plant.

The second point of interest is that to achieve the desired denominator in equation (3), eight independent signals must be available within the system so as to

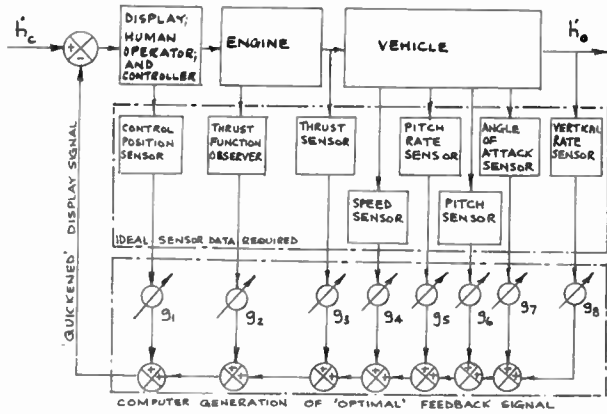


Fig. 4. Block diagram of vertical rate loop with 'quickened' compensatory display. (After Ref. 16.)

shape the a_i coefficients to the requisite values. In practice, the designer has to cope with the situation in which it is unlikely that sufficient sensor generated signals are available, nor are they guaranteed to be independent of each other. To overcome this difficulty, the displayed feedback signal is synthesized from those signals which are available. For reasons of noise filtering, integration techniques are to be preferred to those requiring explicit differentiation.

The particular design technique used to achieve the desired feedback shaping has since become known as the 'H-equivalent' method.¹⁸ It implies the design and implementation of 'observers' to estimate inaccessible signals. This is an important application of electronics within man-machine systems, since either analogue or digital hardware may be used to generate the estimates. A simple example will be detailed in the section on stability augmentation systems (s.a.s.). The effective damping ratio of the s.a.s. will be increased by estimating

pitch angular velocity from pitch angle, rather than incorporating a rate gyroscope to measure velocity directly.

8 Desirable Plant Transfer Functions

A standard method of improving man-machine system performance is to 'shape' the plant transfer function under control so that the human operator is better able to cope. In order to achieve this aim, we must have available 'preferred' transfer functions to which the plant should be tailored. Quite apart from the improved performance to be expected when parameters are at nominal value, correct feedback of sensor signals will reduce the effects of parameter changes,¹⁹ thus leading to improvement throughout the operating envelope.

The best-known set of target transfer functions are probably those derived for the short-period pitch motion of fixed wing aircraft, and reproduced in closed contour form in Fig. 5.^{20,21} The axes are respectively ω_{ns} (undamped natural pulsation) and ζ_s (damping ratio) for the quadratic lag due to the aircraft which appears in the transfer function relating stick deflection to pitch rate.²² These contours are based on pilot opinion, which in turn is related to the Cooper rating scale of Table 2.

The Cooper scale was derived in 1957⁸ in order that pilot ratings might attempt to define quality relative to mission and intended use. In practice it is found that using this scale pilots are able to discriminate adequately enough and repeatably for the system designer to have confidence in these opinions guiding him to an optimum solution.

9 Plant Augmentation via Instrumentation

Historically, plant augmentation has been achieved wherever possible by directly sensing 'states', such as

Table 2
Original Cooper pilot rating scale⁸

	Adjective rating	Numerical rating	Description	Primary mission accomplished	Can be landed
Normal operation	Satisfactory	1	Excellent, includes optimum	Yes	Yes
		2	Good, pleasant to fly	Yes	Yes
		3	Satisfactory, but with some mildly unpleasant characteristics	Yes	Yes
Emergency operation	Unsatisfactory	4	Acceptable, but with unpleasant characteristics	Yes	Yes
		5	Unacceptable for normal operation	Doubtful	Yes
		6	Acceptable for emergency condition only†	Doubtful	Yes
No operation	Unacceptable	7	Unacceptable even for emergency condition†	No	Doubtful
		8	Unacceptable—dangerous	No	No
		9	Unacceptable—uncontrollable	No	No
		10	'Motions possibly violent enough to prevent pilot escape'		

† Failure of a stability augments.

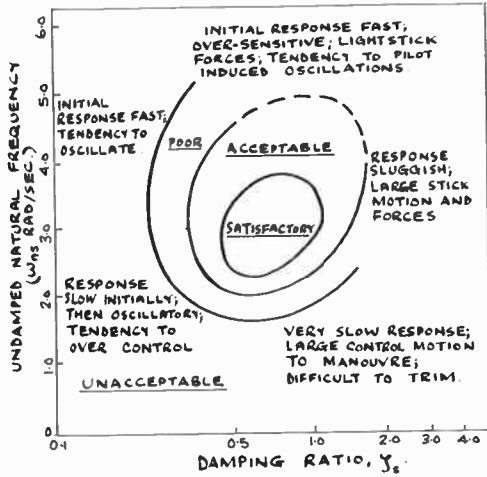


Fig. 5. Desirable quadratic lag parameter values of human operator controlled plant. (After Ref. 21.)

velocity, and then feeding back to a summing junction a 'mixed' signal combining all the information necessary to shape the plant transfer function.²³ This is analogous to the case of a position servomechanism in which artificial damping is provided by tachometer feedback, although for engineering reasons this is usually feedback separately to form a rate loop within the main position loop.

Figure 6 shows the principle applied to an aircraft stability augmentation system. By suitable choice of gains within the forward and return paths of the system, the augmented plant transfer function can be shaped to include a short period quadratic lag with acceptable values of ζ_s and ω_{ns} . This is not to imply that the plant is necessarily second order. For example, fixed wing aircraft exhibit a long period (phugoid) oscillation in the pitch plane. Typically this can have a period of 50 seconds, and can be divergent, with ζ_p negative. However, it is found that pilots can cope with a mildly divergent phugoid mode provided the short period mode has satisfactory characteristics.²¹ So for stability augmentation systems, the designer will usually concentrate on short period mode compensation.

10 Plant Augmentation via State Estimation

Let us now consider how plant augmentation can be achieved when all desirable sensor signals are not available. Modern control theory refers to this problem

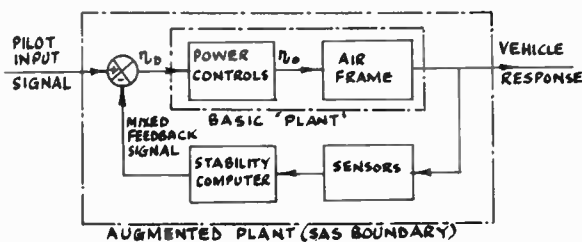


Fig. 6. Multi-sensor plant augmentation. (After Ref. 23.)

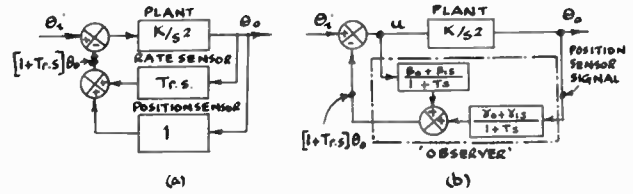


Fig. 7. 'Observer' equivalence to rate feedback plant augmentation. (a) Multi-sensor system. (b) Observer concept.

as 'state estimation', and embraces two very different approaches. It is commonly linked with the Kalman filter,²⁴ but it is also known as the 'observer' problem, associated with Luenberger,²⁵ in which we seek to reconstruct missing signals using only integrators. However, modern control theory simply provides a rational solution to this problem, rather than opening up new possibilities for system design. Thus it is found that for many years 'classical' trained control system designers have been constructing observers to estimate inaccessible signals needed in configuring a satisfactory system, admittedly on an *ad hoc* basis.

In terms of the evolution of system design techniques, the H-equivalent method is a useful classical technique,¹⁶ which integrates well with existing methods, and is worthy of better publicity. However, for the purpose of this paper we shall use a pragmatic approach in which we concentrate on devising integrator-based compensation to yield the desired equivalent signal at a particular point in the loop.²⁶ An algorithm which generalizes this approach is available.²⁷

Figure 7(a) shows a simple second-order system in which the basic plant is a double integrator. Velocity feedback is essential to achieve adequate damping. The augmented plant transfer function is thus

$$\frac{\theta_o}{\theta_i}(s) = \left[\frac{1}{1 + T_r s + s^2/K} \right] \tag{4}$$

If we are prohibited from measuring velocity directly, then we require an 'observer', which supplied with the only available signals, θ_o and u , will generate the desired feedback signal $[1 + T_r \dot{\theta}_o]$, so that equivalence is maintained. Figure 7(b) shows how this will be achieved. Both θ_o and u are passed through filters with the same denominator, which is set by the designer. The filter numerators are different, and must be related to the needs of estimating velocity.

Adding the observer will result in the augmented plant now being of third order, but reducing to second order by choosing the parameters such that pole-zero cancellation is possible. Thus we aim to achieve

$$\left[\frac{\theta_o}{\theta_i}(s) \right] = \left[\frac{1 + Ts}{(1 + Ts)(1 + T_r s + s^2/K)} \right] \tag{5}$$

From Fig. 7(b), the augmented plant transfer function denominator in terms of the observer parameters is

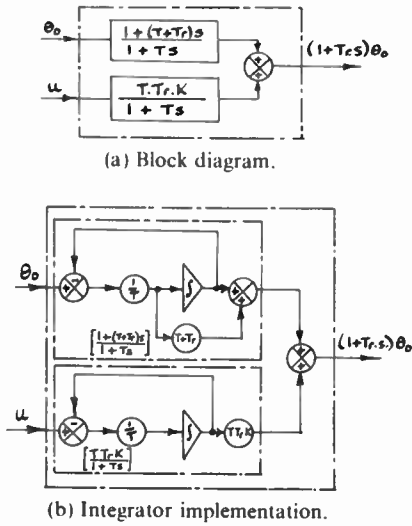


Fig. 8. Rate feedback observer design.

$$D(s) = \left[\gamma_0 + \gamma_1 s + (\beta_0 + 1) \frac{s^2}{K} + \left(\frac{\beta_1 + T}{K} \right) s^3 \right]. \quad (6)$$

Equating coefficients in (5) and (6) yields the solution

$$\begin{aligned} \gamma_0 &= a_0 = 1 \\ \gamma_1 &= a_1 = (T_r + T) \\ \beta_0 &= TT_r K \\ \beta_1 &= 0. \end{aligned}$$

The 'observer' is summarized in block diagram form in Fig. 8(a). To avoid the use of differentiators, standard analogue instrumentation may be used,²⁸ as shown in Fig. 8(b), in which the device is clearly recognized as a 'computer'. The aerospace industry has traditionally referred to such devices as 'computers', thereby highlighting present and future microprocessor applications. For example, this observer could be readily mechanized from a basic low-pass digital filter design based on the Motorola M6800.²⁹

It should be noted that the 'observer' augmented system is only the exact equivalent to the rate-feedback compensated system for the case where all system parameters are at their nominal values. So if sufficient sensor data can be made available of the right quality at the right price, it is preferable to use the instrumentation augmented system. However, an additional useful application of the observer principle is the condition monitoring of sensors in order to increase system integrity.

11 Using an Adaptive Model Display

If the augmented plant transfer function still varies significantly over the flight envelope despite the best use of feedback compensation, microelectronic technology can be used to reduce pilot workload by continuously

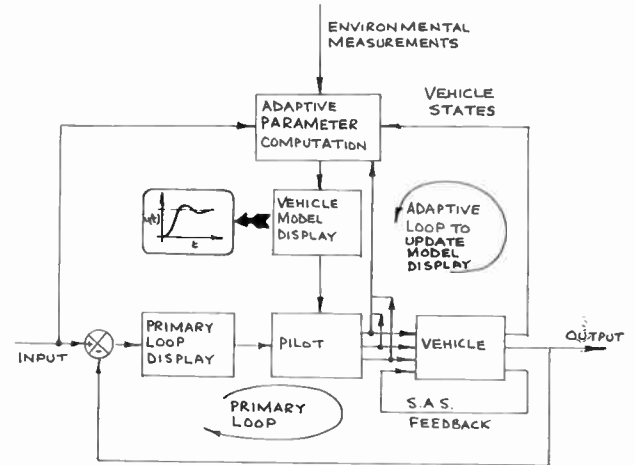


Fig. 9. Adaptive loop used to reduce pilot work-load via display of current vehicle dynamics. (After Ref. 15.)

evaluating and updating the plant dynamics as shown in Fig. 9.¹⁵ Environmental data, and various inputs and outputs are monitored and fed into an on-board mini-computer. Once the transfer function has been evaluated, the characteristics can be displayed using whatever mode is thought to be most appropriate. In Fig. 9, the step response has been estimated, since this gives the pilot immediate visual cues on current vehicle damping ratio and response time, information which can assist him in taking the most effective control actions.

In this instance the mini-computer is performing the task of *identification*. Many techniques exist,^{30,31} the choice resting on the signal-to-noise ratio, non-linearities present, and the speed with which updating is required. It is also helpful, especially during quiescent periods of operation, to inject special command signals into the vehicle so as to provide adequate responses for mathematical analysis by the micro-computer. A short pulse pattern of zero mean may be acceptable, and the dynamics established via the fast Fourier transform. Otherwise a low-level p.n.s. (pseudo-noise sequence) may be generated, and the vehicle cross-correlation function estimated. Under certain circumstances the cross-correlation function approximates to the vehicle impulse response.³² By integration with respect to delay time, the vehicle step response may then be estimated and displayed without the need for violent manoeuvres.³³

It has been suggested that updating the vehicle dynamic model in the manner shown in Fig. 9 can be of considerable assistance to the pilot in detecting, and compensating for, a failure in s.a.s.¹⁵ The extent to which it is of help depends on the rate at which the failure occurs, and the time taken by the adaptive loop to update the display sufficiently for the pilot to identify the cause. Depending on circumstances, the pilot will have somewhere between two and ten seconds to take appropriate action, so that useful information must be provided within this timescale. Once the cause has been

identified by the pilot the action taken is likely to be automatic and in accordance with pre-conditioning attained during training. The adaptive loop will, however, help to reduce the experimentation time with the controls needed by the pilot to identify the cause of failure.

12 Human Operator Quasi-linear Models for Closed-loop Control

In previously referring to the eighth-order system designed by Tipton, mention was made of the approximate transfer function (2.5/s) to describe the human operator behaviour within the closed loop. Much research has been undertaken on the derivation of such models. Figure 10 is a block diagram explanation of how the model is derived from experimental data. The plant is assumed to be a linear transfer function $Y_c(s)$. Using off-line computation, the best-fit linear transfer function is determined which minimizes the mean-square error between actual pilot response and model response. To emphasize the unavoidable curve-fit 'remnant', of Fig. 10, the model is sometimes referred to as a describing function, rather than the normal transfer function.

The generalized human operator transfer function (h.o.t.f.) relevant to one and two-dimensional compensatory control tasks is³⁴

$$Y_{Ho}(s) = \frac{K_{Ho}(1 + T_L s) e^{-\tau s}}{(1 + T_I s)} \quad (7)$$

where τ is the effective time delay including transport lag and high frequency neuromuscular lags, K_{Ho} is the

operator gain, and $(1 + T_L s)/(1 + T_I s)$ is the operator's equalization characteristic. K_{Ho} , T_L , and T_I apparently can be adjusted by the operator, and to some extent the variation can be used to explain differences between conflicting published transfer functions.

Some results are given in Table 3 which relates the h.o.t.f. to the plant dynamics in the region of the loop cross-over frequency.³⁴ The operator appears to select the most suitable form of equation (7) for the task. So lag-lead, pure lead, pure lag, or pure gain may be chosen for the equalization characteristic as needed to achieve good low frequency response and an adequate phase margin (typically between 60° and 110°).

As a consequence, irrespective of the detailed high- and low-frequency dynamics, if the man-machine system is controllable, the compensated loop transfer function can be approximated in the cross-over frequency region by the simple transfer function

$$Y_L(j\omega) = Y_p(j\omega)Y_{Ho}(j\omega)$$

where

$$Y_L(j\omega) \doteq \left[\frac{\omega_c e^{-j\omega\tau_c}}{j\omega} \right] \quad (8)$$

because the human operator makes the necessary adjustment. Typical values for a study in which the plant transfer function is a double integrator and the command signal covers the range 0 to 2.5 rad/s are:

$$\omega_c = 3.6 \text{ rad/s}$$

$$\phi_m = 35^\circ$$

$$\tau_c = 0.267 \text{ s.}$$

Table 3

How the human operator shapes $Y_{Ho}(s)$ to suit the vehicle dynamics in the region of cross-over frequency.³⁴

$$\left(\text{General form of } Y_{Ho}(s) = \frac{K_{Ho} \cdot e^{-\tau s} (1 + T_L s)}{(1 + T_I s)} \right)$$

Approximate vehicle transfer function in region of crossover frequency, ω_c	Equalizer type chosen by pilot from $[(1 + T_L s)/(1 + T_I s)]$	Resulting approximate pilot transfer function	Location of equalizer break frequency
K	Lag-lead	$\frac{K_{Ho} e^{-\tau s}}{1 + T_I s}$	$\frac{1}{T_I} \ll \omega_c$
$\frac{K}{s}$	High-frequency lead	$K_{Ho} e^{-\tau s}$	—
$\frac{K}{s^2}$	Low-frequency lead	$K_{Ho}(1 + T_L s) e^{-\tau s}$	$\frac{1}{T_L} \ll \omega_c$
$\frac{K}{s(1 + Ts)}$	If $T > \tau$, use mid-frequency lead	$K_{Ho}(1 + T_L s) e^{-\tau s}$	$\frac{1}{T_L} \approx \frac{1}{T}$
	If $T < \tau$, use high-frequency lead	$K_{Ho} e^{-\tau s}$	—
$\frac{K}{1 + 2\zeta\left(\frac{s}{\omega_n}\right) + \left(\frac{s}{\omega_n}\right)^2}$	If $(\omega_n \ll 1/\tau)$, use low-frequency lead	$K_{Ho}(1 + T_L s) e^{-\tau s}$	$\frac{1}{T_L} \ll \omega_c$
	If $(\omega_n > 1/\tau)$, use lag-lead	$\frac{K_{Ho} e^{-\tau s}}{1 + T_I s}$	$\frac{1}{T_I} \ll \omega_c$

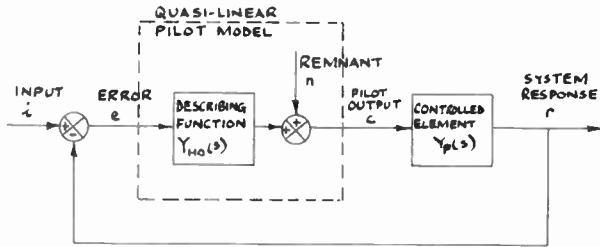


Fig. 10. Definition of 'remnant' in human operator quasi-linear transfer function models. (After Ref. 34.)

Note that τ_c allows for 90° lag from one of the integrators, the neuromuscular and reaction time delays, plus the lead developed from the equalization characteristic, giving 55° total lag at crossover frequency. The relatively low phase margin indicates that this is not an easy task for the operator, who, as shown in Table 3 is expected to provide the limit of his lead capability.

13 The Significance of the 'Remnant'

In Fig. 10 the 'remnant' is conceptually shown as the curve fit error between the output from the best linear transfer function which can be obtained by curve fitting, and the actual output from the human operator, in the mean square sense. The actual transfer function needed to minimize the error is itself a measure of efficiency of design of the man-machine system. In general, the simpler the transfer function needed to yield an adequate curve fit, the more satisfactory will be the design. Thus pilot ratings of the design can be cross-checked via modelling of simulator performance.

Table 4 shows the best curve fit transfer functions determined during the experiments leading to the construction of the ζ_s versus ω_{ns} contours of Fig. 5. The values of ζ_s and ω_{ns} quoted should be regarded as typical, rather than exact, since the original research indicated regions, rather than spot points, for which the transfer functions are appropriate.²⁰ It can be seen that in the region rated by the pilots as satisfactory, the transfer function modelling of human operator response is just a gain plus a pure time delay. This is regarded as a general indication that the man-machine system has been

optimally designed, and provides a standard against which a proposed configuration can be judged.

Thus the transfer function $(2.5/s)$ chosen for the 'quickened' system of Fig. 4 should be seen as a suitable approximation to the desired human operator behaviour in the region of cross-over frequency. Also $Y_{H0}(s) \approx (2.5/s)$ is a more convenient form of model for use with the particular design technique chosen, compared with a pure time delay.

Once the 'best' curve fit transfer function has been determined following simulator experiments and/or trials on a particular man-machine system configuration, the 'remnant' can now be examined. If the remnant is small, then the human operator is performing the task in a linear fashion. On the other hand, if the remnant is large, then the human operator is performing as a non-linear controller, as illustrated in Fig. 11. It is found that the large remnant also correlates with pilots' opinions. They rate systems which require them to work continuously in a non-linear mode as poor, so that the remnant can also be used to monitor the effectiveness of a particular configuration. The use of the word 'continuously' is quite deliberate: in stabilizing a divergent phugoid mode, a pilot will accept the need for occasional pulsed non-linear behaviour to dampen the oscillation.

14 Helicopter Dynamics

The helicopter is a vehicle which, without augmentation, is extremely demanding of the pilot. For example, the relationship between stick position and helicopter lateral position involves four integrations. This is because a stick movement changes the angle of attack of the rotor blades, which in turn results in a movement about the centre of mass of the vehicle, the second integral of which is roll angle. Two further integrations result because the lateral thrust of the helicopter is proportional to the roll angle, and lateral acceleration needs integrating twice to determine lateral position.

Clearly, from the 'plant' alone, 360° phase lag will occur at cross-over frequency, so that observing lateral position alone, the pilot needs to provide at least 180° of

Table 4

Human operator transfer functions associated with typical combinations of short period damping ratio and undamped natural pulsance of Fig. 5²⁰

	0.75	0.60	0.25	0.15
ζ_s	0.75	0.60	0.25	0.15
ω_{ns}	2.5 r/s	3.5 r/s	3.5 r/s	1.5 r/s
Pilot gain	0.16 in/°	0.25 in/°	0.50 in/°	0.0625 in/°
Pilot dynamics	$\frac{(1+0.67s)e^{-0.2s}}{(1+0.2s)}$	$e^{-0.2s}$	$\frac{(1+0.77s)}{(1+2.5s)}$	$\frac{(1+2s)^2}{(1+0.5s)^2}$
Pilot opinion	Acceptable	Satisfactory	Poor	Unacceptable
Remnant	Moderately linear	Highly linear	Non-linearity becoming evident	Much non-linearity

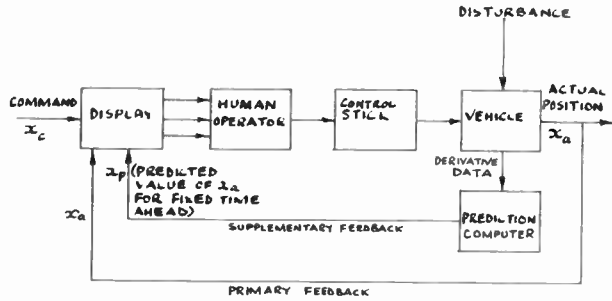


Fig. 14. Assisting the human operator with fixed-time ahead prediction and display. (After Ref. 37.)

pilot in the form of short term prediction ahead for key variables.³⁷ For example, it is suggested that displaying not only the current value of position, but additionally the expected value τ seconds ahead will improve control quality. Figure 14 shows the principle in block diagram form. The future value is predicted using the Taylor series expansion

$$x_p(t) = x_a(t + \tau) \approx \sum_{n=0}^{n=m} \frac{\tau^n}{n!} \left(\frac{d^n x_a(t)}{dt^n} \right). \quad (9)$$

Simulator results with a human operator controlling a v.t.o.l. third-order model (including a double integrator) showed considerable improvement in control, with reasonable values for the expansion being $m = 2$; $\tau = 0.7$ s. For these experiments the disturbances applied to the simulation were in frequency range $0.50 \rightarrow 0.5$ Hz.

This technique is extremely simple, and is very modest in computational needs. Other methods of prediction, such as the Kalman filter, could obviously be used as an alternative to the Taylor series expansion. If the

derivative terms are not available as sensor data, then these alternatives would have to be considered, pushing up the computational requirements. Note that two signals per channel are feedback, whereas in 'quickening' only the optimum mixed signal is displayed.

15 Helicopter Stabilization

Once it is decided to provide helicopter stability augmentation, the various levels of assistance can be readily identified, as shown in Fig. 15.³⁸ For s.a.s., roll velocity is measured, or estimated, and fed back to turn the first integrator into a first-order lag, thereby reducing the phase lag at crossover frequency. An a.f.c.s. measures or estimates roll angle and roll velocity, feeding back to form a second-order lag whose damping ratio and natural frequency could be tuned to suit Fig. 5. Hover augmentation (h.a.s.), which would be extremely useful for air/sea rescue work, additionally feeds back yaw velocity. Finally, the most sophisticated system would feed back yaw position relative to a suitable datum.

The change in aircraft response with successive feedback closures shows that ultimately the pilot task is reduced to providing long-term adjustment of the aircraft position. It is found in practice that it is sufficiently sophisticated to provide h.a.s., thus reducing the pilot's task to a yaw velocity control function. For operation in a hostile environment, some form of inertial velocity sensing is desirable, as an aircraft could easily be detected if it relied on radio or Doppler techniques. One solution involving the further use of microelectronics is to implement a sensor-computer combination which will produce signals proportional to Earth-referenced velocities.³⁸

DEGREE OF AUGMENTATION	BLOCK DIAGRAM	STICK MOVEMENT	VEHICLE ROLL ANGLE	VEHICLE LATERAL DISPLACEMENT
FREE VEHICLE				
STABILITY AUGMENTATION SYSTEM (SAS)				
AUTOMATIC FLIGHT CONTROL SYSTEM (AFCS)				
HOVER AUGMENTATION SYSTEM (HAS)				
HAS PLUS POSITION FEEDBACK				

Fig. 15. Various stages in improving helicopter flying controls. (After Ref. 38.)

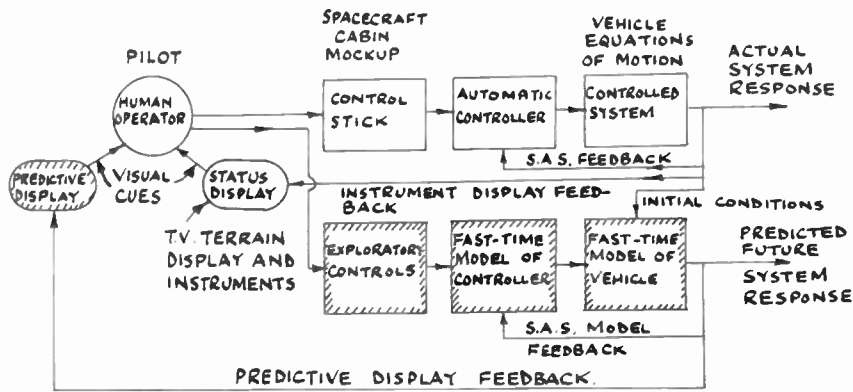


Fig. 16. 'Fast-model' predictor for spacecraft landing trajectory optimization. (After Ref. 39.)

16 Terminal Phase Control

As our final example on the use of microelectronics to improve man-machine system performance we consider the case shown in Fig. 16 where a 'fast model' of the vehicle dynamics provides long-term predictions of future behaviour.^{9,39} This is an important application for docking situations, especially in systems with large response times, since early action must be taken to achieve the desired goal. The 'fast model' is subject to inputs from the exploratory controls and the equations of motion, scaled faster by a factor of 100:1, or even 1000:1, are then solved to provide predictions of the future behaviour of the vehicle as a result of the present control action. The display can be quite sophisticated, as shown in Fig. 17, which gives the expected orientation and trajectory for a spacecraft.

17 Conclusions

Man-machine systems can be described in part using conventional control engineering terminology. By representing both human operator performance and desired plant dynamics in transfer function form, the author hopes to have drawn attention to guidelines which considerably assist in the design and understanding of complex systems. Recent advances in microelectronics offer immense opportunities to reduce pilot workload through a variety of techniques including the use of 'observers', 'quickened displays', 'prediction displays', 'plant dynamic models', and 'fast models'. Originally implemented with analogue devices, many of these techniques would prove fruitful for microprocessor application once the reliability (including software reliability) has been proved.

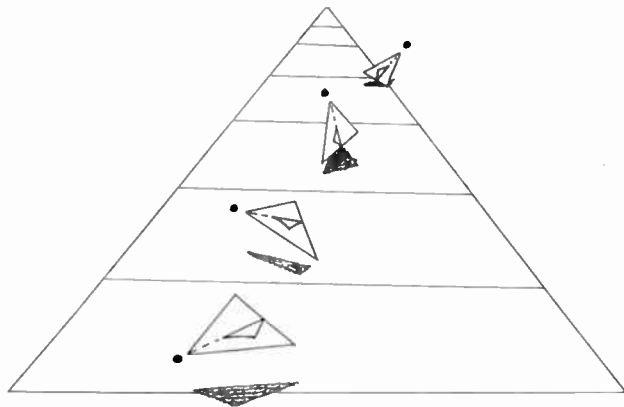


Fig. 17. Spacecraft predictor display shows position and attitude of a tumbling vehicle with respect to a desired command path. (After Ref. 39.)

It is possible to engineer the control stick and exploratory controls so that the pilot can 'freeze' his control action once he is satisfied with the outcome. This can be done by providing a freeze button on the stick, which he does not press until ready. Simulator studies show that using the 'fast-model' technique permits spacecraft pilots to correct rapidly changing thrust disturbances, not only more precisely, but with substantially less fuel consumption compared to results obtained with alternative displays.

18 References

- 1 Reifer, D. J., 'Software failure modes and effects analysis', *IEEE Trans on Reliability*, R-28, no. 3, pp. 247-249, August 1979.
- 2 Osder, S. S., 'Chronological overview of past flight control system reliability in military and commercial operations', Paper 2, AGARDograph no. 224, 1977.
- 3 Krendel, E. S. and McRuer, D. T., 'A servomechanisms approach to skill development', *J. Franklin Inst.*, 269, no. 1, pp. 24-41, 1960.
- 4 Veldhuyzen, V. and Stassen, H. G., 'Simulation of ship manoeuvring under human control', Proc. 4th Ship Control System Conference, The Hague, 1975, pp. 6.148-6.163.
- 5 Stuurman, A. M., 'Human transfer function in ship steering: effect of feel in the wheel', Proc. 4th Ship Control System Conference, The Hague, 1975, pp. 6.112-6.130.
- 6 Whalen, A. C. and Khan, L., 'Digital simulation for advanced naval vehicle dynamics', ORINC Report, Silver Spring, Maryland, U.S.A.
- 7 Schladover, S. E., Wormby, D. N., Richardson, H. E. and Fish, R., 'Steering controller design for automated guideway transit vehicles', *ASME J. Dynamic Systems*, March 1978, pp. 1-8.
- 8 McRuer, D. and Weir, D. H., 'Theory of manual vehicular control', *Ergonomics*, 12, pp. 599-633, 1969.
- 9 Fargel, L. C. and Ulbrich, E. A., 'Predictor displays extend manual operation', *Control Engineering*, August 1963, pp. 57-60.
- 10 Tustin, A., 'The nature of the operator's response in manual control and its implications for controller design', *J. Instn Elect. Engrs*, 94, pp. 190-202, 1947.
- 11 Craik, K. J. W., 'Theory of the human operator in control systems', *Brit. J. Psychol.*, 38, pp. 56-61 and pp. 142-8, 1947.
- 12 North, J. D., 'The human transfer functions in servo systems', in 'Automatic and Manual Control', ed. A. Tustin (Academic Press, New York, 1952).

13 Bates, J. A. V., 'Some characteristics of the human operator', *J. Instn Elect. Engrs*, **94**, pp. 298-304, 1947.

14 Elkind, J. I., 'Characteristics of simple manual control systems', Lincoln Lab MIT Report III, April 1956.

15 Li, Y. T., Young, L. R. and Meiry, J. L., 'Adaptive functions of man in vehicle control systems', in 'Theory of Self-Adaptive Control Systems', pp. 43-56 (Plenum Press, London, 1966).

16 Tipton, C. L., 'Man-machine system equilization and its implementation', Paper presented at NASA Conference on Manual Control, University of South California, March 1967.

17 Birmingham, H. P., Kahn, A. and Taylor, F. W., 'A demonstration of the effects of quickening in multiple co-ordinate control tasks', NRL Report no. 4380, 1954.

18 Schultz, D. G. and Melsa, J. L., 'State Functions and Linear Control Systems', Chap. 9 (McGraw-Hill, New York, 1967).

19 Towill, D. R. and Mehdi, Z., 'A new approach to system transient response sensitivity', *Int. J. Control*, **15**, no. 2, pp. 319-31, 1972.

20 Hall, I. A. M., 'Study of the human pilot as a servo element', *J. R. Aeronaut. Soc.*, **67**, pp. 351-60, June 1963.

21 O'Hara, F., 'Handling criteria', *J. R. Aeronaut. Soc.*, **71**, no. 676, pp. 271-91, April 1967.

22 Blakelock, J. H., 'Automatic Control of Aircraft and Missiles', Chap. 1 (Wiley, New York, 1965).

23 Muzzey, C. L., 'Improving airplane handling characteristics with automatic controls', *Am. Soc. Mech. Engrs Trans.* **78**, pp. 144-52, 1956.

24 Kalman, R. E. and Bucy, R. S., 'New results in linear filtering and prediction theory', *ASME J. Basic Engng*, **8**, pp. 95-108, March 1961.

25 Luenburger, D. G., 'An introduction to observers', *IEEE Trans. on Automatic Control*, AC-16, pp. 596-602, 1971.

26 Towill, D. R., 'Coefficient plane models for control system analysis and design', Research Studies Press Monograph, 1980 (to be published).

27 Chen, C. T., 'Analysis and Synthesis of Linear Control Systems', pp. 202-8. (Holt, Rinehart and Winston, New York, 1975).

28 Kirby, J. E. D., Towill, D. R. and Baker, K. J., 'Transfer function measurement using analog modelling techniques', *IEEE Trans. on Instrumentation and Measurement*, IM-22, no. 1, pp. 52-61, March 1973.

29 Allen, P. J. and Holt, A. G. J., 'Microprocessor implementation of a simple low-pass filter', in 'The Challenge of Microprocessors', M. G. Hartley and A. Buckley (eds), pp. 121-39 (Manchester University Press, 1979).

30 Astrom, K. J. and Eykhoff, P., 'System identification—a survey', *Automatica*, **7**, pp. 123-62, 1971.

31 Graupe, D., 'Identification of Systems' (Van Nostrand Reinhold, New York, 1972).

32 Fry, D. E., 'Use of cross-correlation and power spectral techniques for the identification of Hunter Mark II dynamic response', RAE Technical Report, no. 69156, July 1969.

33 Towill, D. R., 'Dynamic testing of control systems', *The Radio and Electronic Engineer*, **47**, no. 11, pp. 505-21, November 1977.

34 McRuer, D. J. and Jex, H. R., 'A review of quasi-linear pilot models', *IEEE Trans. on Human Factors in Electronics*, HFE-8, no. 3, pp. 231-49, September 1967.

35 Meadows, J., paper presented at IERE Colloquium on 'Design of Control Systems for Advanced Aircraft having Relaxed or Negative Stability', London, October 1979.

36 Benjamin, P., 'A hierarchical model of a helicopter pilot', *Human Factors*, pp. 361-74, August 1970.

37 Dey, D., 'Prediction displays: a simple way of modelling', *Control Engineering*, pp. 82-5, July 1969.

38 Buffum, R. S. and Tribken, E. R., 'Strapdown-inertial techniques broaden vtol horizons', *Control Engineering*, pp. 95-9, April 1968.

39 Kelley, C. R., 'Predictor displays—better control for complex manual systems', *Control Engineering*, pp. 86-90, August 1967.

Manuscript first received by the Institution on 30th January 1980 and in final form on 28th April 1980 (Paper No. 1953/ACS 80)

Standard Frequency Transmissions

Communication from the National Physical Laboratory

Relative Phase Readings in Microseconds NPL—Station
(Readings at 1500 UTC)

JUNE 1980	MSF 60 kHz	GBR 16 kHz	Droitwich 200 kHz	JUNE 1980	MSF 60 kHz	GBR 16 kHz	Droitwich 200 kHz
1	1.8	21.0	16.8	16	1.7	20.2	17.0
2	1.8	21.5	16.9	17	1.7	20.4	17.1
3	1.6	20.7	17.0	18	1.9	20.6	17.2
4	1.1	20.0	17.0	19	1.9	20.7	17.2
5	1.3	20.6	16.9	20	1.9	20.5	17.3
6	1.5	21.5	16.7	21	1.7	20.6	17.4
7	1.5	19.6	16.7	22	1.7	20.8	17.5
8	1.5	19.5	16.7	23	1.7	21.0	17.7
9	1.5	19.4	16.8	24	1.8	21.0	17.8
10	1.6	19.9	16.9	25	1.7	20.5	17.8
11	1.9	19.6	16.9	26	1.7	20.7	17.9
12	1.8	19.6	16.9	27	1.6	20.5	17.9
13	1.5	20.3	16.9	28	1.6	20.0	18.0
14	1.6	21.0	17.0	29	1.6	19.8	18.0
15	1.7	19.9	17.0	30	1.6	21.2	18.1

Notes: (a) Relative to UTC scale (UTC_{NPL}—Station) = +10 at 1500 UTC, 1st January 1977.
 (b) The convention followed is that a decrease in phase reading represents an increase in frequency.
 (c) 1 μs represents a frequency change of 1 part in 10¹¹ per day.

An overview of contemporary 'portable' digital a.t.e. system architectures

MICHAEL N. GRANIERI, B.S.E.E.*

and

WILLIAM J. SCHMITT, B.S.E.E., M.S.E.E.*

Based on a paper presented at the Network/IERE Conference, 'Automatic Testing 79' at Brighton in December 1979.

SUMMARY

The evolution of the 'portable' or 'benchtop' digital tester is briefly discussed in this paper in terms of the primary 'drivers' which lead to its development. The analysis of three current 'representative' portable digital a.t.e. system architectures is then provided and the impact each has on the six major functions common to any a.t.e. system design is briefly discussed. The paper also addresses the impact of the various architectures as they relate to the test program generation process. The paper then briefly deals with the issue as to where digital benchtop/portable architectures appear to be headed and architectural improvements needed if the benchtop tester market is to realize its potential.

* ManTech International Corporation, 2341 Jefferson Building, Arlington, Virginia 22202, U.S.A.

1 Background

Over the past four to five years, strides have been made in the software and hardware technology that have given the system designers new tools to design highly integrated and compact automatic test systems. These systems are commonly referred to as 'portable' or 'benchtop' testers in both the commercial and military marketplace. The capabilities of this category of tester typically lie between that of the minicomputer 'rack and stack' tester and manually-operated logic analysers and oscilloscopes. This category of tester is usually designed around a microcomputer controller and is typically digital in nature in that it has little or no analogue or switching capability in its design. Although functional capabilities and architectural implementation of this category of testers may vary from tester to tester—they all possess the following common characteristics:

Low weight (less than 30 kg)

Highly integrated

Highly interactive

Ability to store test intelligence

Low cost (typically less than \$30,000)

Modular functional block orientation/architecture

Require little or no interpretation of measurement results

Predominantly self-sufficient in performing the testing function

Do not require extensive documentation or special features designed into the unit under test to perform the testing function.

The requirement for this particular category of tester was primarily initiated by the penetration of digital technology into former analogue or electromechanical product areas, the increasing size and complexity of printed circuit boards, the trend toward shorter product life-cycles, and the scarcity of and expense associated with providing trained product support specialists at forward field locations to support a growing multitude of products containing advanced digital semiconductor circuitry. These factors have led to a rapid increase in field service cost over a relatively short period of time. The future, with respect to field service maintenance, does not appear too promising either. Current industry reports¹ estimate that annual field service maintenance costs are expected to double in relation to product hardware costs in five years. Both Government and Industry managers, concerned about these rising costs, are putting pressure on their service organizations to bring field service cost under control.

There are today two basic philosophies which may be adopted by a field service organization—on-site component level repairs, or on-site replacement of a faulty board or module with a working spare. This latter approach, commonly referred to as 'board swapping', is the most widely used of the two philosophies, especially where the products involved are technically complex.

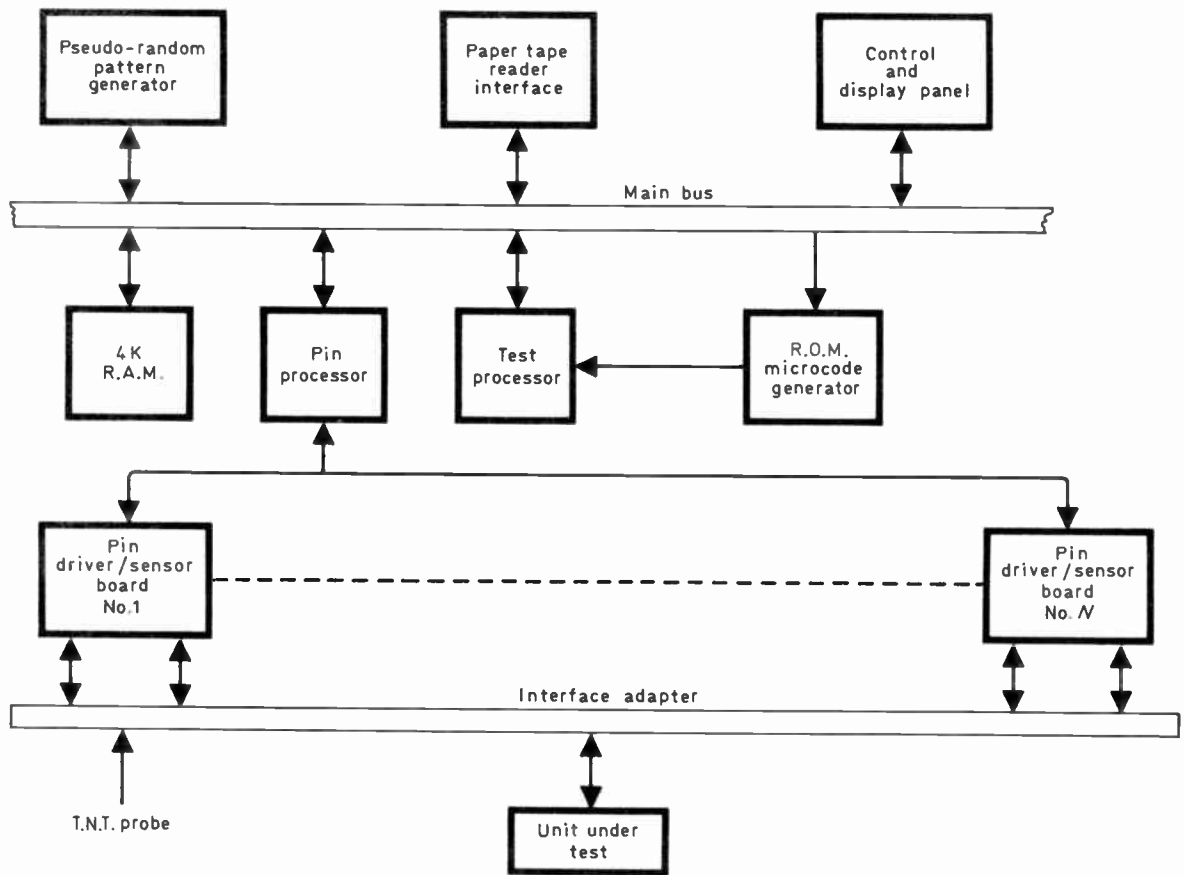


Fig. 1. Representative first-generation portable/benchtop a.t.e. system architecture.

The on-site component-level repair approach has one distinct advantage over board swapping. The dollar value of spare part inventories required for component level is relatively low. However, this single advantage is offset by two primary disadvantages:

Very few commercial and military system level equipments lend themselves to built-in test diagnostics capable of localizing a fault to the component level.

Because trouble shooting is more difficult and because it takes longer, it is necessary to maintain a larger staff of more highly skilled technicians.

Alternatively, the board swapping approach requires less skill on the part of the service engineer, which makes it easier to recruit and to train people, and minimizes customer downtime. However, for a board swapping program to be effective there must be adequate level of spare boards stocked at field locations so that customers can continue to be supported even when bad boards are being repaired. Since the board-repair pipeline is typically three to six months long with a considerable number of good and bad boards floating along in all directions, the level of total inventories (stock at each location plus the 'float') can be enormous.

The introduction of portable or benchtop a.t.e. in the mid-1970s provided a support alternative which combined the best features of the two diverse service philosophies. The ability of portable testers to screen good boards from bad boards and provide diagnostic fault isolation to the chip enables field organizations to minimize their inventory and investment in printed circuit boards in the spares pipeline and at the same time satisfy customer mean-time-to-repair (m.t.t.r.) requirements.

2 'Portable/Benchtop' Digital A.T.E. System Architecture

Understanding the basic concepts of a.t.e. system architecture and design is fundamental to the planning and utilization of not only large-scale a.t.e. systems but small-scale or portable a.t.e. systems as well. A.t.e. system architecture has been previously defined³ as 'the conceptual framework governing the design of an a.t.e. system as it pertains to inter-element relationships, input/output functional capabilities, and system throughput'. The choices implicit to the development and/or selection of a portable a.t.e. system architecture are the assignments or subdivisions of responsibility for

performing each of the following functions common to any a.t.e. system design:

- Operator control function
- Display function
- Stimulus generation function
- Response monitoring function
- Switching function
- System control/computation/editing/compilation function.

The definition of a.t.e. architecture utilized precludes manufacturers and users from considering development changes as architectural ones; thus this definition limits the range of a.t.e. system architectural considerations, but allows varied implementations for each architectural type. The definition does not consider aspects of 'reduction to practice' or component selection. However, it does consider the aspect of design as it relates to system modularity, maintenance, and system methods of doing work.

The concept of modularity is common to most current portable a.t.e. system architectures. This approach to test system design is one solution⁴ to the problem of controlling costs in the acquisition, maintenance, and logical upgrading of portable automatic test equipment. The term 'modular' as used here pertains to the partitioning of a.t.e. system functions (i.e. switching, control) into logical sub-systems (modules), typically on printed circuit boards.

In designing a test system, the modular structure is the architecture, and must be defined first, with system functions designed around that structure. Obviously, non-modular systems cannot be retrofitted to modularity—the architecture must exist from the ground up. Modular system characteristics common to most portable a.t.e. system architectures can be summarized as follows:

Functional-block orientation

Major system functions or sub-functions are contained on single boards (i.e. functions not subdivided). This approach simplifies service and upgrades.

Bus-oriented/software controlled

The only effective method of interfacing to widely variant modules, but self-invariant once bus structure is established.

Back plane interconnects

Minimizes propagation delays, lowers cost by eliminating excessive cabling. Improves reliability and system upgrading capability. All boards plug-connected for easy interchange.

Common board size

Simplifies original design layouts, establishes common

power and signal pins, maximizes p.c.b. component volumes for lowest cost.

The advantages of a modular approach to test system architecture is applicable to all levels of test equipment, large or small. However, the ability to reduce original and on-going test costs, while still allowing regular upgrading (also at low cost), makes a modular system particularly attractive to the portable a.t.e. system user who must maintain a moderate testing budget while still utilizing the latest test technology.

3 Representative Contemporary Portable Digital A.T.E. System Architectures

Over the past four to five years, a number of portable/benchtop systems have entered the a.t.e. marketplace. A brief analysis of what the authors consider as 'representative' modular architectures, currently available in 'fielded' systems, follows to give the reader a feel for the design philosophies undertaken and the functional test capabilities available in the current portable a.t.e. marketplace. Table 1 summarizes typical capabilities which can be derived from these architectures.

4 First-generation Portable/Benchtop Digital A.T.E. System Architecture

Figure 2 depicts what the authors consider to be a representation of a typical first-generation micro-programmable portable/benchtop test system architecture. This architecture is capable of performing functional tests of digital circuits by applying input patterns at standard logic levels (i.e. TTL) and verifying that the circuit response is correct. The inputs can be either specifically programmed stimuli or pseudo-random patterns. The response verification consists of either output pattern recognition, transition count comparisons, or a combination of the two.

A 'known good board' is usually required in program development, but it is not required to test other boards. Trouble shooting and/or diagnostics are typically performed using a transition counting probe, a logic probe, or a fault dictionary as follows:

Fault dictionary

After a test program indicates that a board has failed (typically indicated by blinking red indicators for the failed u.u.t. output pins), the operator is prompted to check the failed test number in the character display. The operator then looks up the failed test in the fault dictionary and matches the failed (blinking) pin to the corresponding pin in the fault dictionary which lists probable cause of failure. In most cases the fault dictionary isolates trouble to one or two bad i.c.s.

Logic probe

In conjunction with a fault dictionary and simulator data, provides greater fault isolation resolution. The

Table 1
Typical portable/benchtop digital a.t.e. system architecture capabilities

Capability	Architecture		
	First-generation (micro- programmable)	Second-generation (uni-processor)	Third-generation (multi-processor)
STIMULUS GENERATION:			
clock pulse width/frequency c.t.l.	—	—	x
multi-level stimulus generation capability	—	—	x
skew mode programming	x	x	x
broadside mode programming	—	x	x
pseudo-random stimulus generation	x	—	x
tri-state	—	x	—
SWITCHING AND LOADS:			
bidirectional pin interface	x	x	x
programmable pull-up/pull-down pin current control	—	—	x
switching	—	—	—
RESPONSE MONITORING:			
multi-level response monitoring capability	—	—	x
strobe capability	x	x	x
programmable response monitoring delay time	x	x	x
scope probe	x	—	—
transition c.t. probe	x	—	x
d.v.m. counter, AND/OR function generator capability	—	x	x
SYSTEM CONTROL:			
microprogram	x	—	x
microprocessor	—	x	x
IEEE 488 interface capability	—	x	x
RS 232 interface capability	x	x	x
PRIMARY INPUT MEDIA:			
paper tape	x	—	—
magnetic tape cassette	—	x	x
p.r.o.m.	x	x	—
diskette	—	—	—
TEST PROGRAM GENERATION:			
fault dictionary	x	x	x
scope trace probing	x	—	—
transition counting	x	—	—
enhanced transition counting technique—insensitive to anomalies introduced via complex feedback lapses	—	—	x
SOFTWARE:			
English-'like' test language	x	x	x
conditional jump	x	x	x
assembly language	—	—	—
on-line editor	x	x	x
on-line program preparation	—	x	x
off-line program preparation	x	x	x
verify/learn software	x	x	x
guided probe software	—	—	x
system self-test program (externally loaded)	x	—	—
system built-in-test (internal)	—	x	x
PRIMARY OPERATOR CONTROL:			
keyboard	—	—	x
discrete switches	x	—	—
display/touch switch response	—	x	—
'command key' capability	—	—	x
PRIMARY SYSTEM DISPLAY:			
discrete l.e.d. display	x	—	—
alphanumeric display	—	x	x
peripheral output device interface capability	—	x	x

x—, distinct advantage over previous generations.

operator probes the fault locations indicated by the dictionary entry and compares logic levels with the correct levels supplied via a test simulator.

Time nodal (t.n.t.) signatures

Provides another technique for tracing 'upstream' from a failed output pin or an internal node. This capability does not utilize software simulation but relies upon a 'known-good' board for initial set-up. During board testing and trouble shooting, t.n.t. signatures (numbers) displayed on the tester are compared to t.n.t. signatures which have previously been marked on a schematic. The t.n.t. signatures on the schematic are known to be good and when there is a mismatch between signatures, the operator can quickly check back through the circuit with the t.n.t. probe to locate the source of the trouble.

A brief discussion of the primary elements of which this architecture is typically composed is presented below:

Test processor and r.o.m. microcode generator

Typical first-generation portable test system architectures contained microprogrammed test processors to execute stored test programs and act upon test results. Utilizing this approach, the instructions of the processor are determined by a combination of hardware and microcode. This approach affords the tester faster execution speed than is possible in a minicomputer controlled system and greater flexibility than hardwired processors.

Pin processor and pin driver sensor electronics

These elements provide test stimuli and verify results as specified by the test program. Inputs are typically applied sequentially in the order specified in the test program, or in a pseudo-random sequence with the relative frequency of pin changes specified in the test program. Outputs are typically strobed simultaneously after a programmable delay time.

Paper tape reader interface and random access memory

These elements provide the inputting and storage of test program data.

Pseudo-random pattern generator

Large numbers of patterns can be generated and applied to u.u.t. inputs utilizing pseudo-random pattern generation. This technique assumes that application of a large enough number of patterns eventually will exercise the u.u.t. thoroughly and propagate the effects of all faults to u.u.t. output pins. A variety of pattern generators have been used in first-generation portable a.t.e. system architectures, including both fixed patterns (such as binary-count and Gray code) and pseudo-random patterns. Pseudo-random patterns are those which have random statistical properties for the duration of the test but are repeatable each time that the test is executed.

5 Operator Control and Display Panel

System control and display functions for first-generation portable a.t.e. system architectures were usually implemented via a series of discrete switches and l.e.d.

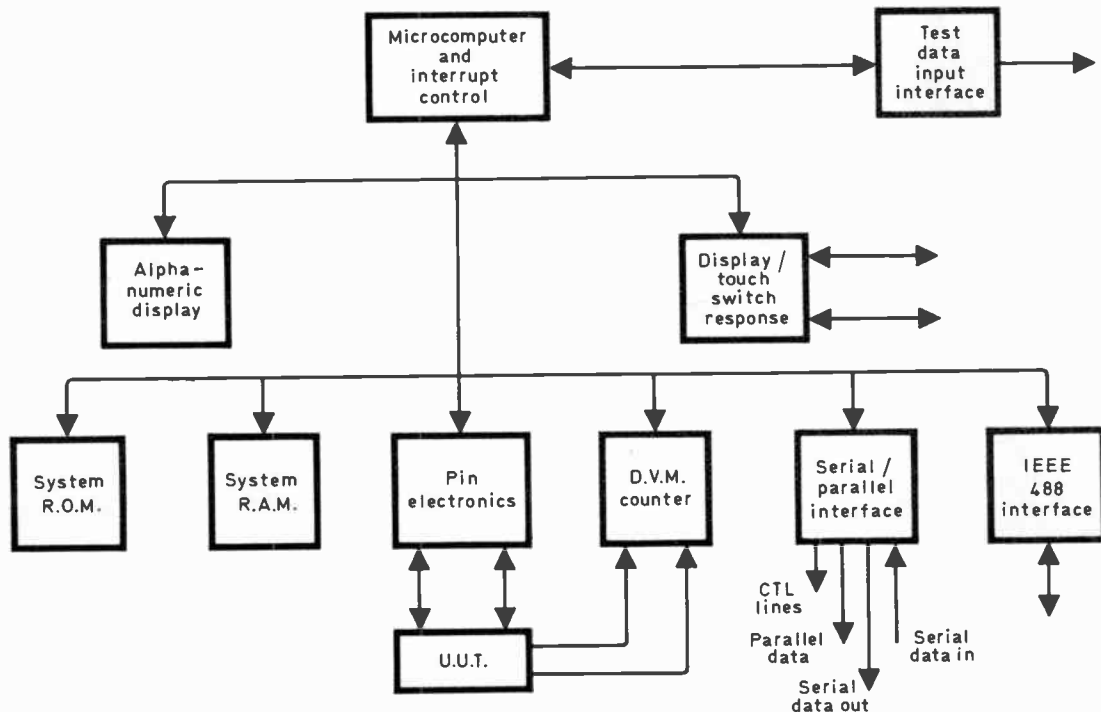


Fig. 2. Representative second-generation portable/benchtop a.t.e. system architecture.

devices located on the top or front panel of the test systems. The controls and displays provided usually fell into the following categories:

- Power controls
- Display of tester operating modes
- Display of test results and tester status
- Operator program load and test execution control
- U.u.t. pin status/failure indicators.

First-generation portable a.t.e. system architectures, although powerful machines in their own right, typically lacked the following primary capabilities:

- Alpha-numerical man-machine communication
- On-line program preparation capability
- Guided probe software
- Peripheral output device interface capability
- Multi-level stimulus generation capability
- Multi-level response monitoring capability
- Limited clock rate capability, no control over clock pulse width or duty cycle
- Programmable pull-up/pull-down current control capability
- Little or no switching or analogue stimulus/response capability
- Ability to interface with other instruments (i.e. IEEE 488 capability).

6 Second-generation Portable A.T.E. System Architecture

A simplified diagram representative of second-generation uniprocessor portable/benchtop a.t.e. system architecture is shown in Fig. 2.

The major elements of this typical system consist of:

Microcomputer and interrupt control

The test system microcomputer and interrupt control circuitry are typically on the same printed circuit board. This system element usually consists of, besides the primary microcomputer and interrupt control elements, a master oscillator and power on reset circuitry. The microcomputer controls the operation of the tester via a tri-state I/O bus which typically consists of a 16-bit address bus, 8-bit data bus, and various control signals. As each instruction is fetched from the system r.a.m., it is placed in the microcomputer's instruction register and decoded and subsequently executed.

System r.a.m.

The system r.a.m.'s function is to store u.u.t. test data (i.e., test program) for execution by the tester.

System r.o.m.

The system r.o.m. contains the test system executive control program which provides the operational software required to test a u.u.t. The system r.o.m. may also provide on-line compiler/interpreter capability for on-line program preparation.

Test data input interface

Provides a buffered extension of the test system memory for test data to be synchronously entered into the tester.

Alpha-numeric display

Typically provides system and user programmed messages or instructions to the operator.

Display/touch switch response

Allows a highly interactive man/machine interface via a display to touch switch response control system.

Pin electronics

Pin electronics provide the stimulus and response interface to the u.u.t. Typically, any pin can be defined as a stimulus, output response or tri-state (high impedance).

Digital voltmeter/counter

Typically, second-generation portable/benchtop system architectures provide digital voltmeter and/or frequency measurement/counter capability via functional printed circuit boards. However, these instrument cards are usually provided with little or no switching capability and the operator must utilize them in a similar manner as he would a probe.

Serial/parallel interface

Serial/parallel interface provides the capability for using a teleprinter or c.r.t. to enhance the tester's man/machine interface capability.

Second-generation portable test system architecture possesses basically the same testing capability of first-generation portable/benchtop system architecture. However, analysis of Fig. 1 indicates that this architecture has led to significant enhancements over its first-generation cousins as summarized below:

- On-line program preparation capability
- Internal system built-in-test capability obviates the need for system self-test program
- Enhanced man/machine interface via display/touch switch response operator controls and alpha-numeric displays and ability to interface with external peripherals (e.g. c.r.t., teleprinter)
- Highly integrated pin electronics architecture with tri-state capability
- Analogue d.v.m., counter, function generator test capability
- Flexible microcomputer control
- Ability to enhance test system capability by controlling other test resources or be controlled via IEEE 488 bus.

However, as Fig. 1 also indicates, this architecture still leaves something to be desired in the following areas:

- Lack of guided probe software
- Operator control via test system keyboard control
- Lack of clock pulse width/frequency control

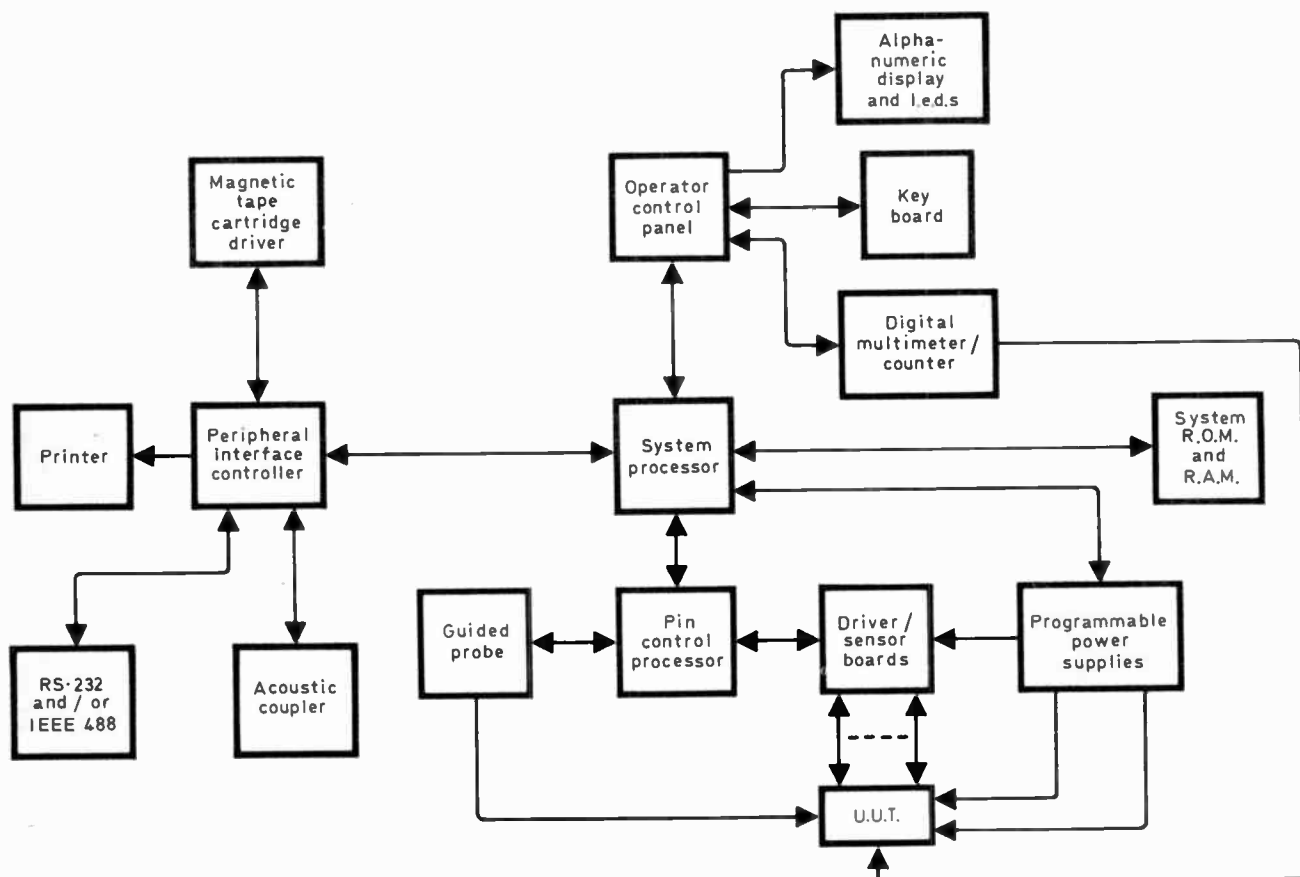


Fig. 3. Representative third-generation portable a.t.e. system architecture.

Lack of multi-level stimulus generation/response monitoring capability
 Lack of switching and programmable load capability.

7 Third-generation Portable A.T.E. System Architecture

Figure 3 depicts what the authors consider to be a representation of a typical third-generation portable multiprocessor a.t.e. system architecture.

This system architecture typically combines hardware and software features in a compact package and uses the latest device l.s.i. technology for many circuit functions. The system processor is typically a general-purpose, high-performance metal-oxide device with a data field of 8 or 16 bits and a 16-bit address field with byte addressing. The test system interprets test instructions directly using microcode stored in r.o.m.s. A hardware microprogram interprets the high-level test statements much more rapidly than would be possible with a software interpreter.

The system r.a.m., as in previous generations, is utilized to store user test programs and the system r.o.m., besides providing microcode capability, typically contains a system self-test program which is executed upon application of power to the tester.

Third generation portable a.t.e. system architectures

typically possess multiple means of loading test programs into the tester such as:

- Magnetic tape cartridge
- Communications interface via acoustic coupler
- RS232
- IEEE 488.

Most of the instrument-to-operator interface in this architecture category is achieved via a keyboard and alpha-numeric display. The operator may enter test program statements and system commands with a full alpha-numeric keyboard or with a 'command' key to enter, with a single keystroke, certain common system command and programming statements which are written on the keys.

The most dramatic increase in capability of third-generation over previous generations of architectures is in the testing subsystem. Pin electronics typically possess multi-level stimulus generation and response monitoring capability in conjunction with programmable pull-up and pull-down current control capability. These capabilities minimize interface adapter requirements and enable third-generation architectures to be compatible with a wide cross-section of units under test.

Another dramatic increase in capability, over previous architectures, is the ability to provide complex clock

signals of various repetition rates and pulse widths at any test system I/O pin. This capability approaches that provided via digital word generators in second-generation a.t.e. rack and stack systems.

This capability is typically provided for via a pin control processor. This architecture element can be programmed separately from the system processor. Typically the pin control processor in third-generation a.t.e. system architectures can be used in three different modes:

Normal mode

In which pin change instructions are executed by the system processor and passed directly to the testing system.

Subprogram mode

In which the system processor loads a program segment into the pin control processor r.a.m. and waits while it is executed at high speed.

Multiprocessing mode

Whereby both the system and pin control processor operate simultaneously. The main processor loads a program into the high-speed processing r.a.m. and starts its execution while continuing execution of the main program.

Another significant architecture innovation enjoyed by third-generation users is 'guided probe' fault isolation capability. This capability is achieved by prompting the user, via a series of probing instructions, from a failing output pin to a faulty node and/or i.c. In addition to the basic test program, two additional types of information are required to implement this capability:

A 'circuit image' or wire list description of the interconnection of the components on the board under test.

A table of expected responses at each node.

Since a large board can have 1000 or more nodes, a means of compacting response nodal data is desirable.

Techniques for reducing bit streams of 1's and 0's have been used in board testers for years. Our previous discussion of first-generation testers described briefly one such method—the time-weighted transitions count method. However, all of these techniques have a common disadvantage when used on complex boards containing feedback loops. The effect of the fault propagates around such loops so that all of the nodes in the loop appear faulty, and fault isolation to a single component is virtually impossible. Some modern third-generation testers possess proprietary data computing techniques able to isolate faults to a single component even in complex feedback loop environments.

8 Conclusion

Three contemporary representative portable a.t.e. system architectures have been discussed and typical

capabilities identified. The transition from micro-programmable to uniprocessor to multiprocessor control in benchtop a.t.e. architectures, as pointed out in the text, is also accompanied with dramatic advances primarily in pin electronics, a.t.e. operator control and display capabilities, and portable a.t.e. guided probe software. Advancements, primarily in the latter two areas have had a significant architectural impact in portable a.t.e. system design in that they have affected in a positive manner the way these systems do work and as a result have enhanced the operational throughput of these systems.

However, upon analysis of the present architectures and capabilities available in the current marketplace, the authors project that the next or subsequent generations of a.t.e. system architecture will in most likelihood possess one or more of the following capabilities:

Non-return-to-zero stimulus/response handling capability

Enhanced pin electronics capability utilizing high speed/high performance digital to analogue converter technology

Mini-floppy disk storage capability

Flexible 'hard contact' switching and analogue stimulus/response monitoring capability

Response sampling capability at each pin to enable multiple parametric measurements to be made (i.e., rise-time, fall-time, pulse width) in support of future high speed digital integrated circuits.

Whether existing portable test system architectures will be allowed to mature or new ones developed is largely dependent on the perception and needs of its current and future users and as to how they answer the following philosophical question: 'How much testing should be done by a portable field service tester?'

9 References and Bibliography

- 1 Richman, T., 'Smart test equipment for the field', *Electronics Test*, 2, No. 4, pp. 24-9, April 1979.
- 2 'The 2225 portable service tester', General Radio Co.
- 3 Durgavich, J. J., Granieri, M. N. and Woodfine, J. J., 'ATE system architecture alternatives', Autotestcon '78 Conference Record, November 1978.
- 4 Illes, G., 'Modularity in test system architecture', 1978 Semiconductor Test Conference Record, November 1978.
- 5 '500 Series Logic Circuit Tester Operator/Programmers Manual', Three Phoenix Test Inc.
- 6 Anderson, R. E., 'Portable program—controlled digital test system', '74 ASSC Conference Record, November 1974.
- 7 Young, W., 'On-site microprocessor controlled portable module testers', *IEEE Trans on Instrumentation and Measurement*, IM-27, no. 2, pp. 147-51, June 1978.
- 8 Anderson, R. E. and Fulkis, R. G., 'Processor-based tester goes on-site to isolate board faults automatically', *Electronics*, 51, no. 10, pp. 111-17, May 1978.
- 9 Parker, I. N., Brown, R. F., Bond, D. F. and Cooke, P., 'A versatile and modular architecture for micro-processor based ATE', Automatic Testing Deutschland Test and Measurement Exhibition '79 Conference Record, March 1979.

*Manuscript received by the Institution on 11th December 1979
(Paper No. 1954/M1 14)*

Recording tape properties and digital recording system performance

B. K. MIDDLETON, B.Sc., Ph.D.,
M.Inst.P., C.Eng., M.I.E.E.*

and

T. BROWN, B.Sc.†

Based on a paper presented at the IERE Conference on Video and Data Recording at Southampton in July 1979.

1 Introduction

When considering which recording tapes to use for a particular high-density digital application it is difficult to assess the likely suitability of tapes prior to having carried out actual measurements on them. Whilst measurements are always necessary it would be advantageous to know some properties of tape performance which could be quoted thereby implying specific recording properties. Some progress in this direction has been made by virtue of the fact that parameters have already been identified which specify the outputs from tapes at short wavelengths¹⁻⁴.

The purpose of this paper is to show that these parameters do give an indication of the contribution of the tape properties to the behaviour of a recording system. Measurements on a recording system, shown schematically in Fig. 1, operating at around 13 330 flux reversals per inch and using a phase modulation system of encoding the digital data (see Fig. 2), are described to consolidate the propositions put forward in this paper.

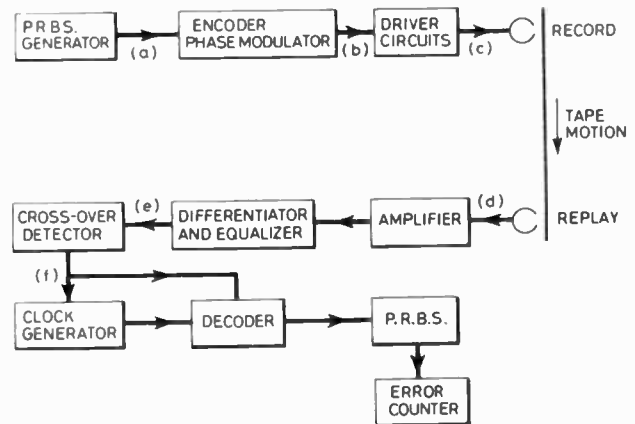


Fig. 1. Block diagram of the recording system.

SUMMARY

The output voltage obtained from a recording tape used in a high density digital application has been shown to be characterized by simple parameters. These parameters have been investigated and predicted to contribute to the signal-to-noise ratio expected from the tape and consequently the error rate obtained from a recording system using it. Measurements on a recording system gave confirmation of the basic ideas behind these predictions.

It is shown that many facets of a recording system conspire to limit its performance and so a generalized formula for specifying system operation cannot yet be produced but the role of tape and system parameters can be considerably elucidated.

2 Theory

The purpose of this Section is to discuss the recording properties of magnetic tapes and how these affect the overall design and performance of a recording system. Expressions are obtained for the outputs derived from a recording tape and the processing of these signals by the replay electronics is discussed. The signal-to-noise ratios produced by the electronic circuitry is then shown to control the error rates expected from the system. With this step an overall view of recording system performance is obtained.

* Department of Electrical and Electronic Engineering, Manchester Polytechnic, Chester Street, Manchester M1 5GD, England.

† Formerly with Manchester Polytechnic; now at University Medical School, University of Manchester, Oxford Road, Manchester 13.

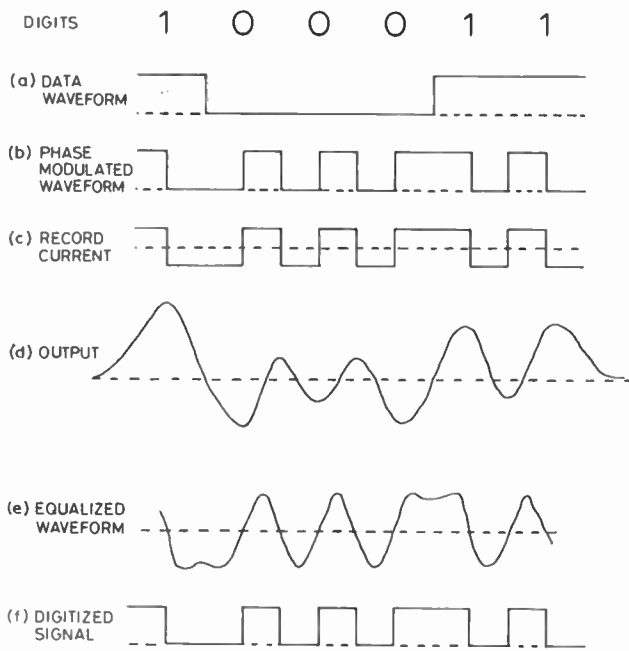


Fig. 2. Waveforms occurring at various stages of the system represented in Fig. 1. The waveforms are labelled with letters which are also used to indicate the parts of Fig. 1 to which they apply.

2.1 Record and Replay Processes

Corresponding to a step change in record current there would ideally be a step change of magnetization recorded in the tape. However, recorded magnetization transitions are never abrupt but have a definite width. In this work the usual assumption is made^{2,4} whereby the magnetization component M along the x direction, parallel to a recorded track, at a transition is given by the well-known formula

$$M = \frac{2}{\pi} M_0 \arctan \frac{x}{a} \tag{1}$$

where M_0 is the peak magnetization of the medium and the transition width is proportional to the parameter a , as shown in Fig. 3 (a). The latter parameter is assumed to be smallest at the top surface of the tape, where it takes a value a_t , and to vary linearly through the depth of the tape to take a larger value a_b at the bottom surface (see Fig. 3(b)). It is then possible to estimate the output voltage e expected^{2,4} when the transition moves past a narrow gap head, with velocity v , to be

$$e = K \frac{M_0}{1+\alpha} \ln \left[\frac{(a_t + d + D(1+\alpha))^2 + \bar{x}^2}{(a_t + d)^2 + \bar{x}^2} \right] \tag{2a}$$

where

$$\alpha = \frac{a_b - a_t}{D} \quad \text{and} \quad \bar{x} = vt \tag{2b}$$

D is the greater of tape thickness or depth of recording, d

the head to tape separation on replay, and K a constant of proportionality.

In digital recording it may be assumed that the output voltage arises from the superposition of a sequence of pulses of the type given by equation (2a). In the particular case of a series of transitions of alternating polarity separated by a distance $\lambda/2$ the total output voltage amplitude can be shown to be⁴

$$e = K \frac{2M_0}{1+\alpha} \ln \left[\frac{\tanh \{(a_t + d + D(1+\alpha))/\lambda\}}{\tanh \{(a_t + d)/\lambda\}} \right] \tag{3a}$$

The above reduces at short wavelengths to⁴

$$e \simeq K \frac{4M_0}{1+\alpha} \exp [-2\pi(a_t + d)/\lambda] \tag{3b}$$

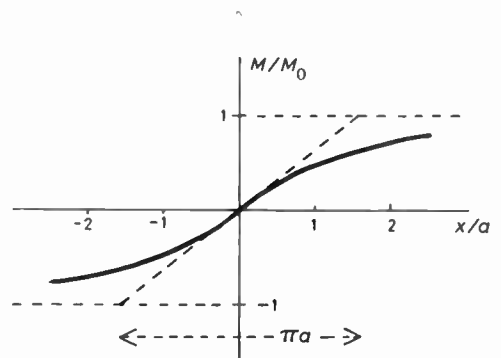
This formula will be used later.

Returning to consider isolated pulses it is possible, knowing the output voltage resulting from a step change of input current, to determine the transfer function of the tape channel. Using the Fourier transform pair

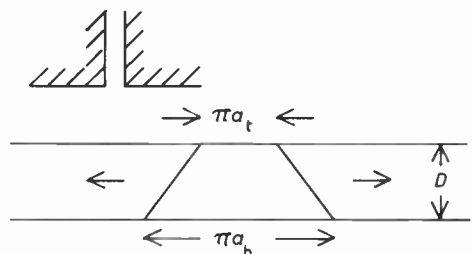
$$v(t) = \int_{-\infty}^{+\infty} V(f) \exp [2\pi jft] df \tag{4a}$$

$$V(f) = \int_{-\infty}^{+\infty} v(t) \exp [-2\pi jft] dt \tag{4b}$$

the transforms of the input, a step change in current from $+I$ to $-I$, and the output, given by eqn. (2a), are expressed respectively in terms of the wavenumber k as



(a) The assumed variation of magnetization at a transition according to eqn. (1).



(b) The variation of transition width through the depth of the tape.

Fig. 3.

$$I(k) = \frac{2I}{jkv} \tag{5a}$$

$$E(k) = K \frac{M_0}{1+\alpha} \frac{1}{\pi k} \times (1 - \exp[-kD(1+\alpha)]) \exp[-k(a_1+d)] \tag{5b}$$

where $k = 2\pi/\lambda$, $f\lambda = v$ and $j^2 = -1$. Therefore the transfer function of the record-replay channel $H(k) = E(k)/I(k)$ is

$$H(k) = j \frac{v}{2\pi l} K \frac{M_0}{1+\alpha} \times (1 - \exp[-kD(1+\alpha)]) \exp[-k(a_1+d)] \tag{6}$$

The presence of the j describes the differentiating action of the replay process in that it produces a 90° phase shift in all the Fourier components passing through the system. Equation (6) will be used in the next Section.

2.2 Replay Electronics

The output voltage from the recording channel consists of a sequence of pulses created as a result of step changes of record current, the latter representing the data stored (see Fig. 2). To recover the data the use of a set of replay electronics with transfer function given by the reciprocal of that of the tape channel, namely

$$H'(k) = - \frac{j}{\frac{v}{2\pi l} \cdot \frac{KM_0}{1+\alpha}} \cdot \frac{\exp[k(a_1+d)]}{(1 - \exp[-kD(1+\alpha)])} \tag{7a}$$

$$\simeq - \frac{j}{\frac{v}{2\pi l} \cdot \frac{KM_0}{1+\alpha}} \cdot \exp[k(a_1+d)] \tag{7b}$$

$\pi D(1+\alpha) > \lambda$

would lead to an overall channel response of unity and therefore a reproduction of the original data. In this respect the channel is referred to as being 'equalized flat' and the equalization would have been achieved by amplitude and phase correction to the replayed signal. The phase correction, indicated by the presence of j in eqn. (7), is a 90° shift to compensate for that introduced by the replay process. Equalization of the type predicted by eqn. (7) was used in the experiments to be described later.

In high-density recording pulses overlap with consequences in terms of the reduction of pulse amplitudes and peak shifts as shown in Fig. 2. These effects would be eliminated by a transfer function of the type given by eqn. (7) if the bandwidth of the system were infinite. However, in order to keep noise down to a manageable level, and for obvious practical reasons, bandwidths are finite. This results in some components of the signal not emerging from the equalization circuit.

The corresponding waveform is then not a sequence of step transitions but of transitions of finite switching times which interfere or overlap one another, as shown in Fig. 2. This is intersymbol interference which may cause the cross-over positions to be shifted with respect to the original transitions with consequential timing errors and possible loss of data during data recovery. Timing shifts will be discussed later.

In many systems phase and amplitude correction is produced by differentiation of the replayed pulses with respect to time. This produces the required 90° phase shift and some amplitude correction. However, the zero-crossings of the resultant signal represent the locations of the pulse peaks, the latter being shifted with respect to the positions of the transitions originally recorded only by the amount of peak shift in the replay pulse pattern.

2.3 Timing Margins, Noise, Peak Shifts, and Error Rates

In an ideal recording system voltage cross-overs appearing at the input of the cross-over detector occur exactly at the time locations required to represent the data. However, timing shifts caused by noise, replayed pulse peak shifts, and other factors already discussed result in variations of timing of the cross-overs. If these shifts are greater than some value T_w , the timing margin for which the electronics can successfully operate, the information will not be decoded.

In the particular case where only random noise is present (no peak shift etc.) and the r.m.s. to r.m.s. signal to noise ratio is SNR at the input to the cross-over detector the probability of error P in the decoding system is⁵

$$P = \text{erfc}(SNR \sin \omega_s T_w) \tag{8}$$

where ω_s is the highest angular signal frequency replayed.

The effects of displaced cross-overs in the equalized flat system, used here, and the effect of peak shift in a differentiating channel⁶ are to reduce the margins within the window, $2T_w$, available for tolerating noise and, therefore, to increase error rate. The probability of error is consequently modified from that predicted by eqn. (8) but still retains a similar dependence on the signal-to-noise ratio⁶.

2.4 Signal-to-Noise Ratios

Power signal-to-noise ratios in tape noise limited systems have been predicted by Mallinson^{7, 8} for the particular case $a_1 = 0$. These calculations have been repeated, assuming that $a_1 \neq 0$ and that the system is equalized flat up to an upper cut-off frequency f_m for which the corresponding wavelength on the tape is $\lambda_{\min} = v/f_m$. Taking the square root of the resulting power signal to noise ratio gives the voltage SNR as

$$SNR \propto (a_1 \lambda_{\min})^{\frac{1}{2}} K \frac{4M_0}{1+\alpha} \exp[-2\pi a_1/\lambda_{\min}] \tag{9}$$

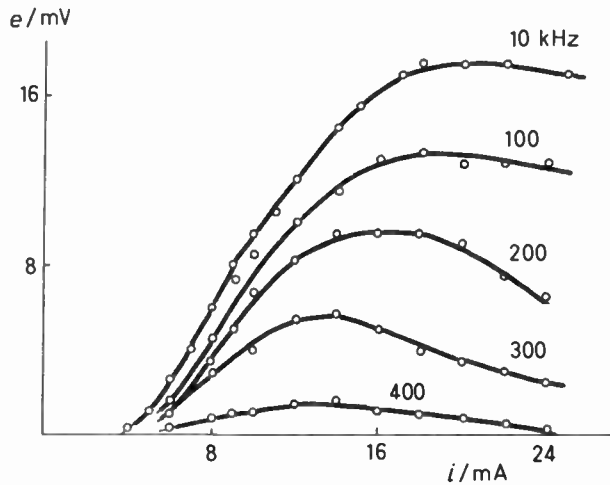


Fig. 4. Measurements of output voltage as a function of square wave record current amplitude for differing frequencies.

This expression differs in detail only from that given by Mallinson⁹ but has in common with it the exponential involving the transition width parameter a_t .

When the system is limited by white noise produced by the electronics at the pre-equalization stage the corresponding SNR can easily be shown to be given by

$$SNR \propto (a_t + d)^{\frac{1}{2}} K \frac{4M_0}{1 + \alpha} \exp [-2\pi(a_t + d)/\lambda_{min}] \quad (10)$$

This equation differs from eqn. (9) largely in that $(a_t + d)$ occurs rather than a_t . If d is smaller than a_t , which is thought to be the case here, then there is little difference between the predictions.

It can be seen that the SNR of an equalized system strongly reflects the output directly from the tape. Since the probability of error is a function of SNR it is to be expected that the observed error rate in a system should be related to output voltage and in particular to the way it is characterized by a_t or $(a_t + d)$ or both.

3 Measurements on Recording Tape

All the measurements were taken on an instrumentation tape deck operating at a tape speed of 60 inches per second. The tape used was 1 inch wide 3M 951 Instrumentation Tape and the heads were SE Labs 7 track 600kHz Type M with replay gaps of $2 \mu\text{m}$.

Figure 4 shows graphs of the output voltage as a function of the amplitude i of square wave record current of differing frequencies. These curves are of the expected form whereby increasing frequency is shown to decrease signal output. The latter effect is shown also by plotting output voltage as a function of frequency f , for a fixed value of record current amplitude, in Fig. 5. The curve is plotted on a log-linear scale and at higher frequencies the straight line relationship confirms the exponential law predicted by eqn. (3b). From the slopes of this and other

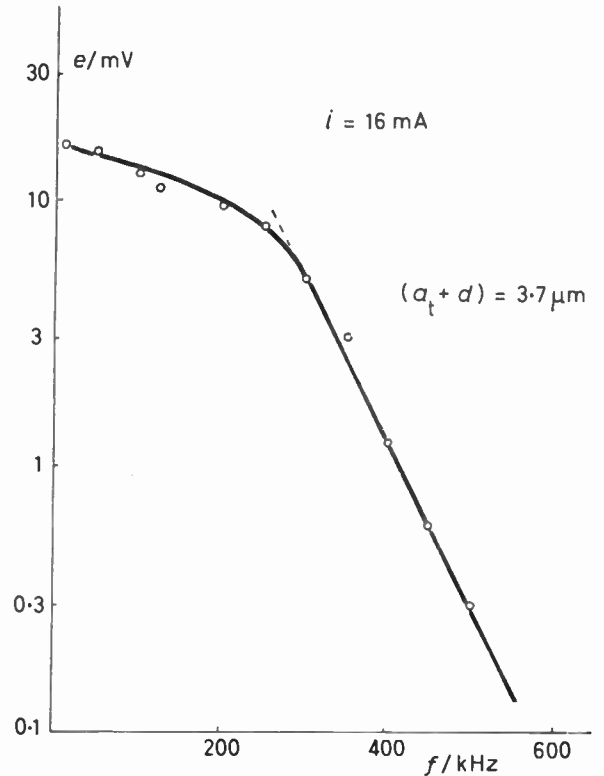


Fig. 5. Output voltage as a function of the record frequency for fixed current amplitude.

similar lines values of $(a_t + d)$ have been obtained using eqn. (3b). The quantity $(a_t + d)$ is plotted as a function of record current in Fig. 6. Also using eqn. (3b) values of $K4M_0/(1 + \alpha)$ have been determined and are plotted in Fig. 7.

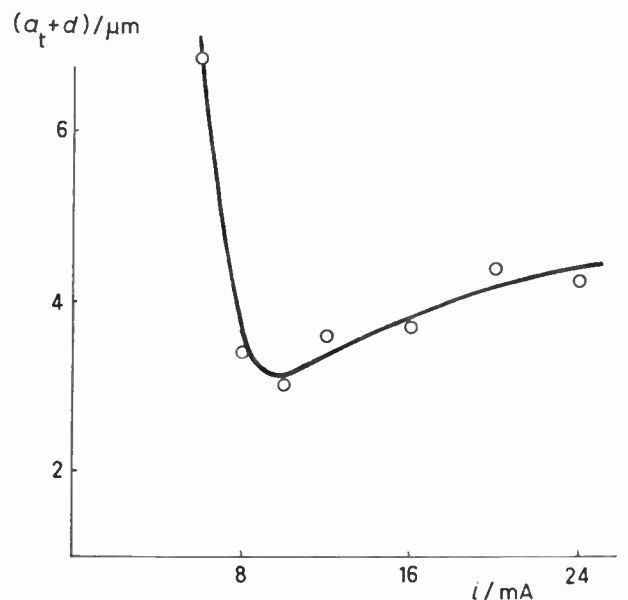


Fig. 6. The parameter $(a_t + d)$ as a function of record current amplitude.

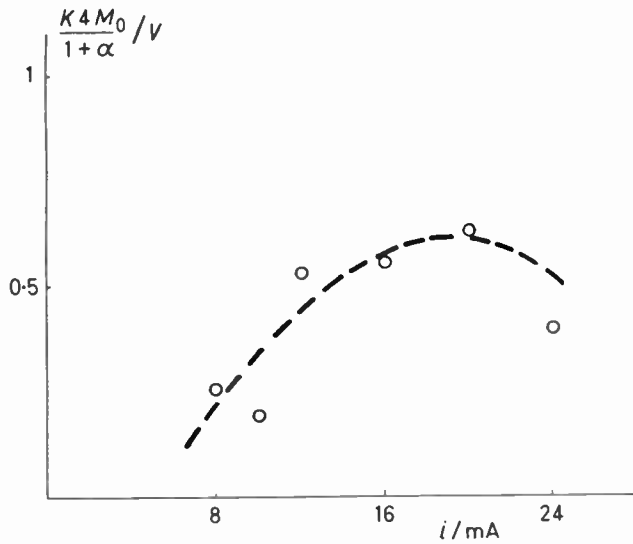


Fig. 7. $K4M_0/(1+\alpha)$ as a function of record current amplitude.

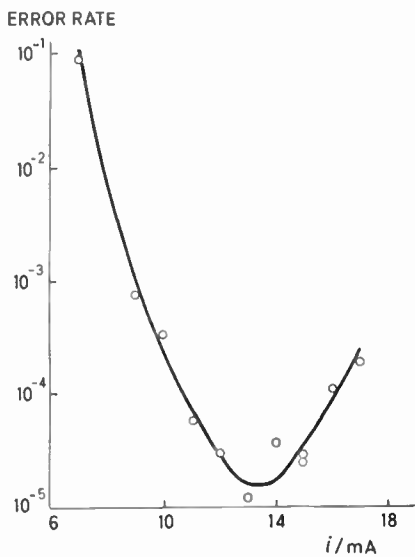
The linear relationship demonstrated in Fig. 5 has been observed on a wide range of tapes¹⁻⁴ and has gained wide acceptance. In this case the derived values of (a_i+d) plotted in Fig. 6 show a minimum near to a record current of 10 mA. The values of $K4M_0/(1+\alpha)$ show a different relationship to record current in Fig. 7 where a maximum is reached near to 20 mA. Both of these variations combine, as indicated by eqn. (3b), to determine the output voltage. The maximum of output voltage shown in Fig. 4 occurs at around 13 to 14 mA, nearer to the minimum in (a_i+d) than the maximum in

$K4M_0/(1+\alpha)$. Therefore (a_i+d) plays the most significant role in determining output voltage particularly since it occurs in the exponential part of eqn. (3b). Consequently (a_i+d) and $K4M_0/(1+\alpha)$ are proposed as significant parameters of tape performance although the former is put forward as being of most importance.

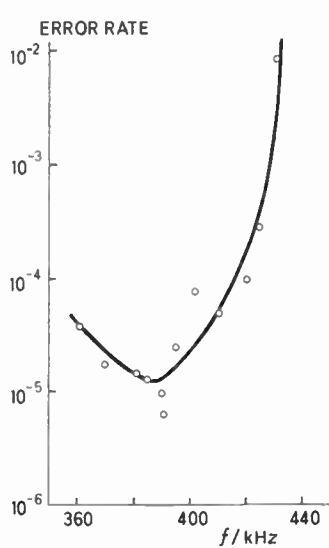
The general variation of (a_i+d) with record current is what is expected from theory², while the variation of $K4M_0/(1+\alpha)$ is anticipated since the peak magnetization in the tape should increase with record head field amplitude and therefore record current amplitude.

4 Measurements on a Recording System

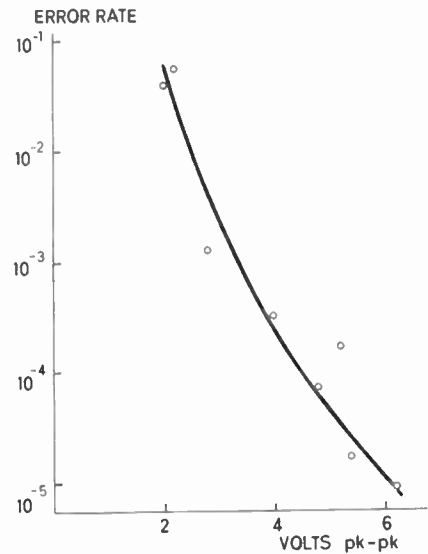
A recording system was designed and built and used to record information in phase-modulated form. Recording with a top square-wave frequency of 400 kHz was used corresponding to 13 330 flux reversals per inch or 6665 bits per inch. The system is shown in block form in Fig. 1 and consisted, on the record side, of a pseudo-random sequence generator (p.r.b.s.), an encoder (phase modulation), and head driver circuits. On the replay side are an amplifier, an equalizing circuit employing a parallel L-C tuned circuit, a differentiating circuit, a cross-over detector, a digital clock regenerating circuit, a decoder, a p.r.b.s. for comparing the regenerated and recorded information, and an error counter. A schematic representation of the waveforms occurring at various parts of the circuit is shown in Fig. 2. Sequences of 1024 bits were recorded over 2400 feet of tape and the number of errors counted on replay. Many parameters were varied and their consequences on error rate determined.



(a) as a function of record current amplitude.



(b) as a function of the 'free running' frequency of the replay clock.



(c) as a function of amplitude of the voltage presented to the input of the cross-over detector.

Fig. 8. Error rates obtained, using the recording system shown in Fig. 1.

A series of measurements were made in which the record current level was varied. The gain of the amplifier was adjusted for each value of record current to keep the voltage level into the cross-over detector constant and the equalization was maintained 'flat' in all cases. The latter was achieved by giving the channel the transfer characteristics indicated by eqn. (7b) over a frequency band from approximately 100 kHz to 600 kHz. With the replay clock having a 'free running' frequency of 400 kHz, error rates were measured as a function of record current amplitude and the results are shown in Fig. 8(a). Clearly there is a minimum in error rate at around 13 mA record current. This is the most important result as far as this work is concerned but other factors do affect the error rate. Figure 8(b), for example, shows the effect on error rate of varying the 'free running' frequency of the replay clock, when record current was fixed at 13 mA. Also Fig. 8(c) shows the effect of varying signal level into the cross-over detector indicating why it was important to keep signal level constant at its input. Clearly large signals are needed for lowest error rates.

5 Discussion

Measurements of error rate as a function of record current reveal a minimum at a current of around 13 mA, which coincides with the value for maximum output voltage. Theory indicates that error rate should be related to the parameters a_i or $(a_i + d)$, and $K4M_0/(1 + \alpha)$ in a way that largely reflects the form of the output voltage. Therefore the coincidence of minimum error rate and maximum output is not particularly surprising. However, it has been argued that the output signal variation with record current is determined primarily by the parameter $(a_i + d)$ and to a lesser extent by the parameter $K4M_0/(1 + \alpha)$. The minimum of error rate occurs at a record current near to that needed to minimize $(a_i + d)$. Therefore the latter is put forward as a significant parameter of tape recording performance. These results are summarized in Fig. 9.

As a development of the last proposition consider the following argument. If it is accepted that $(a_i + d)$ is a dominant factor in controlling the output voltage because it occurs in the exponential part of eqn. 3(b) then it will be that either a_i or $(a_i + d)$, depending on the source of noise, will dominantly control the SNR of eqns. (9) and (10). Therefore for a constant SNR, which ensures a constant error rate in a system, either the ratio a_i/λ or $(a_i + d)/\lambda$ will be constant (λ_{min} will be related to λ). Since packing density is proportional to λ^{-1} it is to be expected that packing density will be proportional to a_i^{-1} or $(a_i + d)^{-1}$. While this last statement is not put forward as a law, because of the approximate nature of the argument, it is indicative of the way that tape

properties contribute via a_i to recording system performance. For example, it was found that, in these experiments, $(a_i + d)$ values of around $3 \mu\text{m}$ were associated with system operation at around 13 000 flux reversals per inch while similar experiments with a high energy tape for which $(a_i + d)$ was measured to be approximately $0.75 \mu\text{m}$ system operation at around 30 000 flux reversals per inch was achieved under broadly similar conditions.

While theory indicates that either a_i or $(a_i + d)$, depending on the source of noise, controls system performance, it is thought that, in this case and in many others, $a_i > d$ and so $(a_i + d)$ may be quoted anyway. Divergences from this situation could be anticipated only in systems which are definitely tape-noise-limited and where $a_i \nlessgtr d$.

Attempts have already been made in the literature to calculate values of $a_i^{2,3}$ and while the theory is still in its early stages of development it is interesting to note its predictions. Using the work of Middleton and Wisely² (in particular eqn. (13) and supporting equations with $H_g/H_1 = 2$), values of a_{21} , the transition width parameter after recording and demagnetization, have been evaluated. The results given in Fig. 10 show that transition width decreases with decreasing remanence to coercivity ratio (M_R/H_c), decreasing thickness D , and decreasing head-to-tape separation on record d .

6 Conclusions

An overall view of a digital magnetic tape recording system has been presented. The relevance of tape

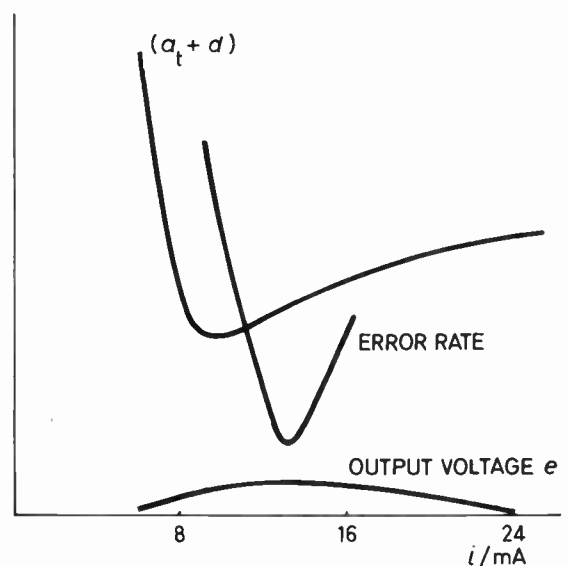


Fig. 9. Summary of observations obtained. $(a_i + d)$, error rate and output voltage as a function of record current amplitude.

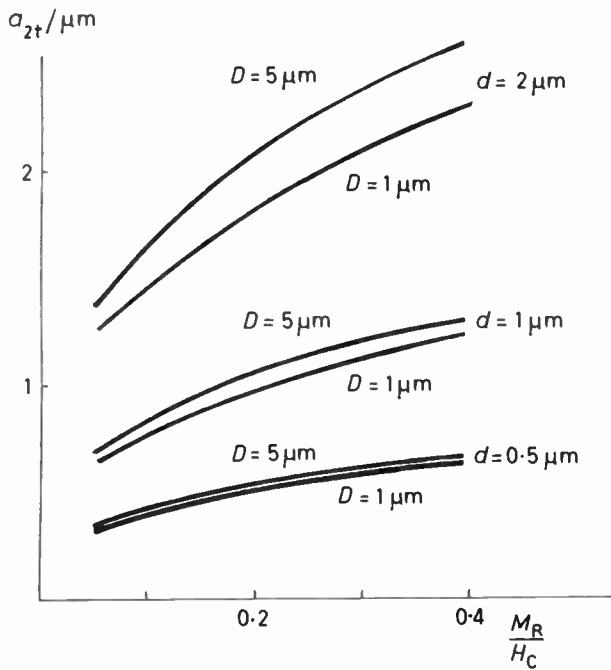


Fig. 10. Predicted variation of the parameter a_{2t} as a function of M_R/H_c for different values of tape thickness D and head-to-tape separation on record d .

properties and the specifications of the replay electronics have been studied. In particular the importance of certain tape parameters has been revealed.

7 Acknowledgment

This work was supported by the Science Research Council under Contract B/RG 67404.

8 References

- 1 Mallinson, J. C., 'A unified view of high density digital recording', *IEEE Trans. on Magnetics*, MAG-11, pp. 1166-9, September 1975.
- 2 Middleton, B. K. and Wisely, P. L., 'The development and application of a simple model of digital magnetic recording to thick oxide media', Conference on Video and Data Recording, IERE Conf. Proc. No. 35, pp. 33-42, July 1976.
- 3 Bertram, N. and Niedermeyer, R., 'The effect of demagnetization fields on recording spectra', *IEEE Trans.*, MAG-14, pp. 743-5, September 1978.
- 4 Middleton, B. K. and Wisely, P. L., 'Pulse superposition and high density recording', *IEEE Trans.*, MAG-14, pp. 1043-50, September 1978.
- 5 Hughes, G. F. and Schmidt, R. K., 'On noise in digital recording', *IEEE Trans.*, MAG-12, pp. 752-4, November 1976.
- 6 Katz, E. R. and Campbell, T. G., 'Effect of bitshift distribution on error rate in magnetic recording', *IEEE Trans.*, MAG-15, pp. 1050-3, May 1979.
- 7 Mallinson, J. C., 'Maximum signal-to-noise ratio of a tape recorder', *IEEE Trans.*, MAG-5, pp. 182-6, September 1969.
- 8 Mallinson, J. C., 'On extremely high density digital recording', *IEEE Trans.*, MAG-10, pp. 368-73, June 1974.
- 9 Mallinson, J. C., 'Design philosophy and feasibility of a 750 mega-bit per second magnetic recorder', *IEEE Trans.*, MAG-14, pp. 638-42, September 1978.

Manuscript first received by the Institution in February 1979 and in final form on 4th June 1980
(Paper No. 1955/CC 32)

Some characteristics of a leaky feeder in a tunnel

B. L. CRITCHLEY, M.Phil.*

and

Q. V. DAVIS, B.Sc., C.Eng., F.I.E.E.†

Based on a paper presented at the IERE Conference on Land Mobile Radio held at Lancaster in September 1979

SUMMARY

Details are given of how magnetic field strength varies throughout a short section of a 1500 m long tunnel fed by a leaky feeder. Both phase and amplitude are examined.

A second series of measurements examines in detail the phase variation along a single line down the tunnel over a distance of 500 m. The results enable judgments to be made about the potentiality for position fixing in a tunnel using phase information.

* Standard Telecommunication Laboratories, London Road, Harlow, Essex.

† Department of Electronic and Electrical Engineering, University of Surrey, Guildford, Surrey GU2 5XH.

1 Introduction

Mobile radio systems in mines and tunnels are now becoming increasingly common by means of the use of leaky feeders. Examples in Britain include many installations by the National Coal Board in the low v.h.f. band¹ and a system at present being installed in the London Underground² which operates at 170 MHz. Abroad there are various installations either in being or planned, including the provision of coverage throughout the tunnels of the whole Swiss motorway system—about 100 km of tunnels in all.³

Up to now most of the work on leaky feeders in tunnels has been concerned with establishing average signal levels, feeder attenuation as influenced by the tunnel environment, and the scale and extent of the variations in the mean signal level. Thus sufficient data now exist to design with confidence a communication system in a tunnel. However, detailed knowledge of the structure and variation of the fields associated with a leaky feeder is still limited, and this paper describes some work to extend that knowledge.⁴ In particular a study has been made of the variations of phase in the tunnel. The tunnel used was a disused railway tunnel 1500 m long and approximately 3 m wide by 4 m high with a flat floor and a curved roof. It had brick walls and the rails had been removed.

2 Volumetric Field Investigation

2.1 Experimental Arrangement

All experiments were performed at about 72.5 MHz. The feeder mounted at a height of 1.5 m was fed by a 1 W transmitter and measurements made about 120 m along the tunnel, sufficiently far for end-effects to be negligible. The coaxial cable employed was BICC Type 3515, a braided, semi-airspaced feeder with velocity ratio 0.87.

The volumetric investigation examined in detail the field variation in three-dimensional space along a section of the tunnel. A position was chosen in the tunnel where there were indications of the existence of a sizable standing wave. An electrically small pick-up aerial was required and for this reason a loop was chosen, the magnetic component of the field thus being measured. It is hoped later to repeat the measurements with an electric field probe.

The probe was attached to a long pole by which it could be held in position at various points spaced out on a rectangular grid of wood which extended over the cross-section of the tunnel. The pole was sufficiently long to isolate the operator and with care the results were thus made repeatable. Measurements were made of field strength and phase, using a vector voltmeter at base. The received signal was connected to the instrument by means of a well-shielded cable. By variously moving and rearranging this cable it was established that its presence did not affect the field and that repeatable results could be obtained.

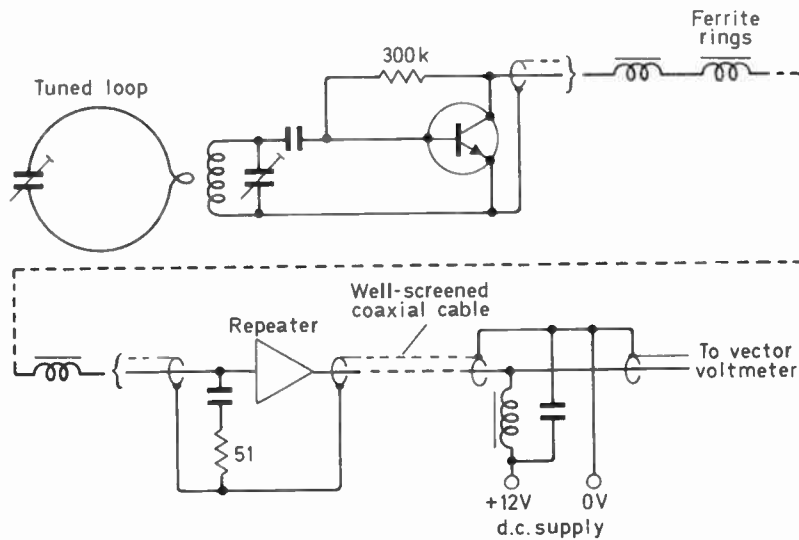


Fig. 1. Circuit diagram of loop antenna system.

Since it is difficult to match a small aerial of low resistance and high reactance to a 50 Ω coaxial cable, the aerial was designed to give a deliberate mismatch into a high impedance. The circuit diagram is shown in Fig. 1. The tuned loop was transformer coupled, with tuned secondary to a transistor having a 50 Ω coaxial cable as its collector load. Further amplification was provided a short distance further down the cable, d.c. being supplied along the cable conductors. Ferrite rings on the thin coaxial line were used to attenuate current flow in the braid to prevent this acting as an aerial and thus distorting the measurements.

Figure 2 shows the frame in one position in the tunnel. Notches can be seen for positioning the aerial accurately at various points on the grid. The feeder is also visible.

2.2 Measured Field Variation

Since space precludes giving much detail, only a representative selection of measurements are given here, all referred to the co-ordinate system shown in Fig. 3.

The three components H_x , H_y and H_z were measured and H_ϕ , the tangential component, derived from them by calculation (due regard being taken to phase).

2.2.1 Radial variation

The most consistent of the various field components is the tangential component, H_ϕ . Its variation against radius is shown in Fig. 4. The solid line shows the variation at $\phi = 0^\circ$. The vertical bars indicate the extent of the spread in both H_ϕ and H_z along a large number of radial lines through the feeder, when for each such line the absolute levels have been shifted up or down to give the best fit to the solid line shown.

The variation follows quite closely the law

$$H \propto x^{-\frac{1}{2}}$$

with extreme values for the index of -1 and -2 .

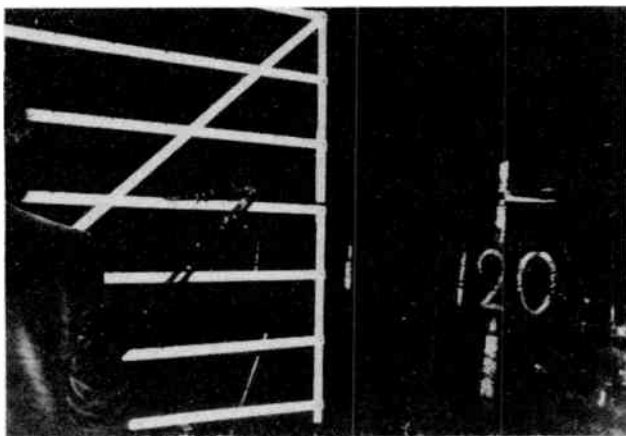


Fig. 2. Measurement frame position in tunnel.

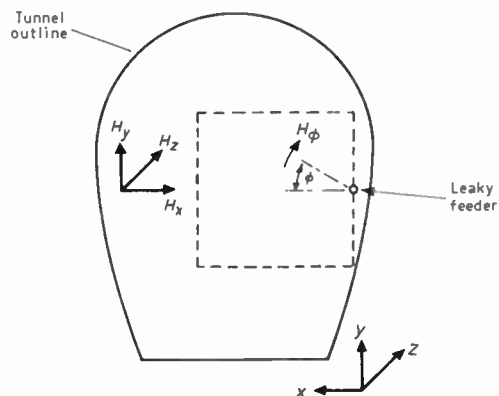


Fig. 3. Tunnel geometry showing position of measurement region.

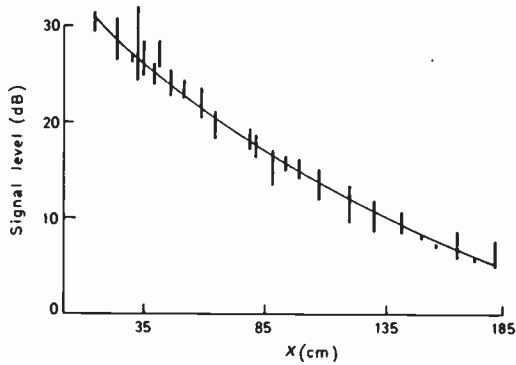


Fig. 4. Signal level variation across the tunnel.

2.2.2 Axial variation

The variation in the three components along a line down the tunnel at 160 cm from the feeder is shown in Fig. 5. This is a fairly representative example which illustrates clearly that the radial component suffers a large standing wave, the longitudinal a much smaller one and the tangential almost none at all.

2.2.3 Phase variations

Phase measurements were made with an uncertainty of less than 8°, and were generally repeatable, the exceptions being in positions of small signal and large standing wave, which is the case with H_x .

Figure 6 shows the phase fronts in the tunnel for all three components in a horizontal plane at the height of the feeder. It is evident that the horizontal field changes quite dramatically in this region of the tunnel with erratic

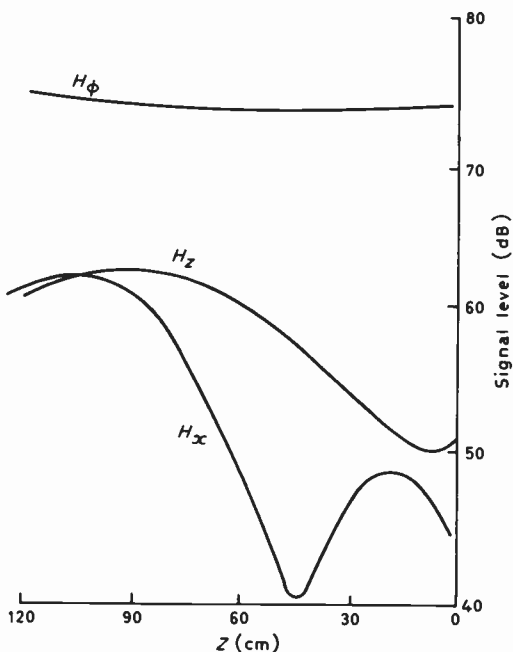


Fig. 5. Signal level variation along tunnel for three components.

but nevertheless consistent phase fronts. In sharp contrast the tangential component is fairly uniform and free of standing waves.

Figure 7 is a plot of the phase fronts in a short length of tunnel for the component H_ϕ , showing clearly how they bend toward the walls. Figure 8 shows variation across the tunnel for the same field component.

3 Linear Field Investigation

3.1 Phase Variation

As the previous measurements have indicated, not surprisingly, the phase variation along a line down the tunnel is not a simple linear progression. It is of interest to characterize this variation over longer distances in order to make judgments about the possibility of distance measurement, or position fixing using phase information, and of phase noise in a phase- or frequency-modulation communication system associated with a high speed vehicle. A very careful set of measurements was therefore carried out over distances up to 500 m.

For these measurements a conventional vertical whip aerial was used and the frequency was 72.375 MHz. The receiver was kept a constant 1 m from the feeder. As in the previous set of tests care was taken to establish that measurements were not affected by the reference cable or by free radiation from the transmitter, and that results were repeatable.

Both amplitude and phase were recorded. Figure 9 shows a typical result. The phase variation has been plotted in terms of deviation from the best fit straight line and the amplitude results are corrected for the attenuation of the feeder itself.

Interestingly, over many series of measurements the phase curve remained remarkably unchanged although quite large changes occur from test to test in the curves for amplitude. It is noteworthy that in the phase plots there is no significant evidence visible of 'drop-outs' in the signal strength. In the tests of which Fig. 9 is an example, the mean phase gradient was 1.85 rad/m representing a velocity ratio of 0.816.

A frequency analysis was performed on the spatial frequency distribution of the phase and amplitude variations and evidence was found of a feature at a spatial frequency of period 2.02 m. This can be attributed to a 'beat' between the leaky feeder mode and the TE_0 waveguide mode whose wavelength in the tunnel is 2.53 m.

4 Conclusions and Discussion

It seems reasonable to conclude that standing waves are not caused by reflections as is sometimes thought but by mode conversion due to the interaction of modes having common polarizations. For instance, the strange behaviour of the transverse magnetic field vector indicates that this is probably the polarization where the majority of mode conversion exists. No evidence of feeder damage or termination was discovered to account

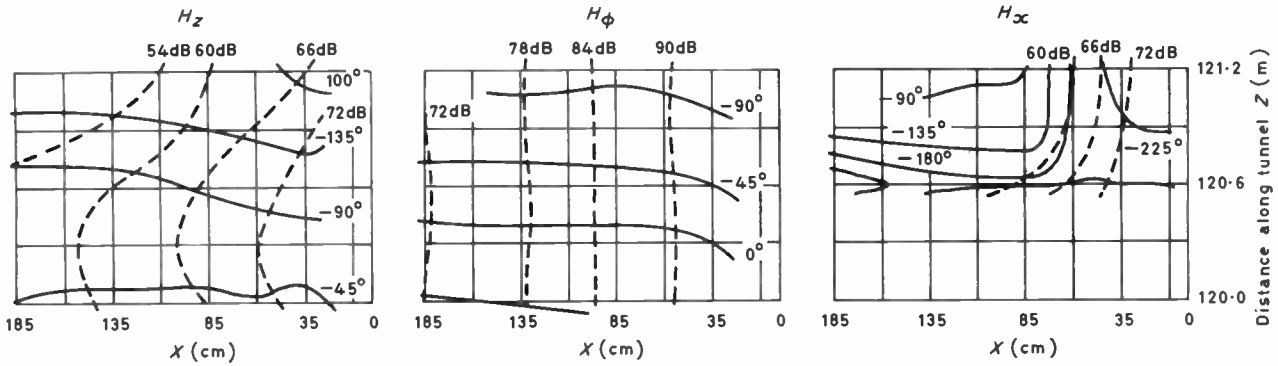


Fig. 6. Phase fronts and amplitude contours in the tunnel, at the height of the feeder.

otherwise for this phenomenon; in any event a reflection within the leaky feeder would have disturbed the field in all polarizations.

A point arising from the foregoing suggests that there is an optimum orientation for the aerial of a receiver coupling into the magnetic field which would appear to give a substantially lower drop-out occurrence, hence, improved reception.

The tangential H vector consistently shows a curvature in the phase fronts synonymous with power

flow into the lossy tunnel walls. A similar curvature in this and other polarizations close to the feeder indicates propagation towards the feeder (at this particular point). The conclusions from this point to three possibilities; it is either a tunnel wall effect (as mentioned previously), or a concentration of power close to the feeder, or a flow of power back into the feeder. The third possibility seems unlikely but it was not feasible at the time to make further relevant phase measurements without seriously disturbing the field and the feeder.

The linear phase change with distance could be employed advantageously to determine the position of a remote transmitter. By transmitting successively higher frequencies, or by modulating the carrier, the receiving station can eliminate ambiguities in the measurement. The eventual positional accuracy would depend upon the phase deviation from the linear gradient but with careful feeder positioning this could be minimized to the randomness in the system.

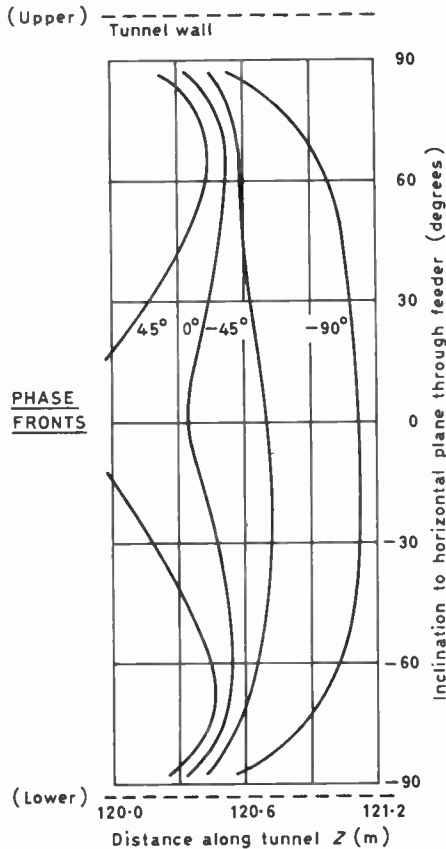


Fig. 7. Tangential H vector variation in semi-cylindrical plane 1.00 m radius from leaky feeder.

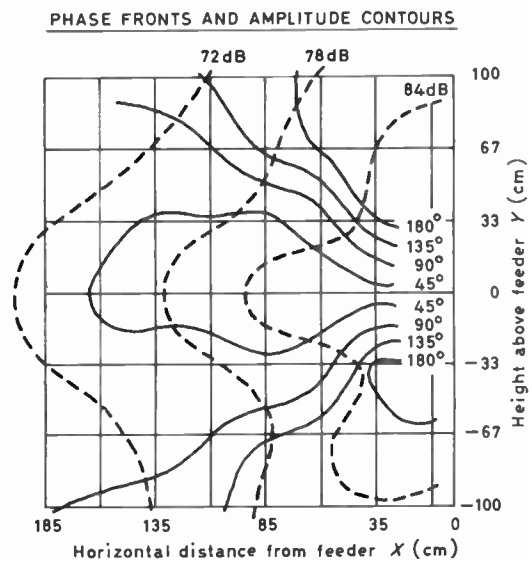


Fig. 8. Variation of tangential component across tunnel.

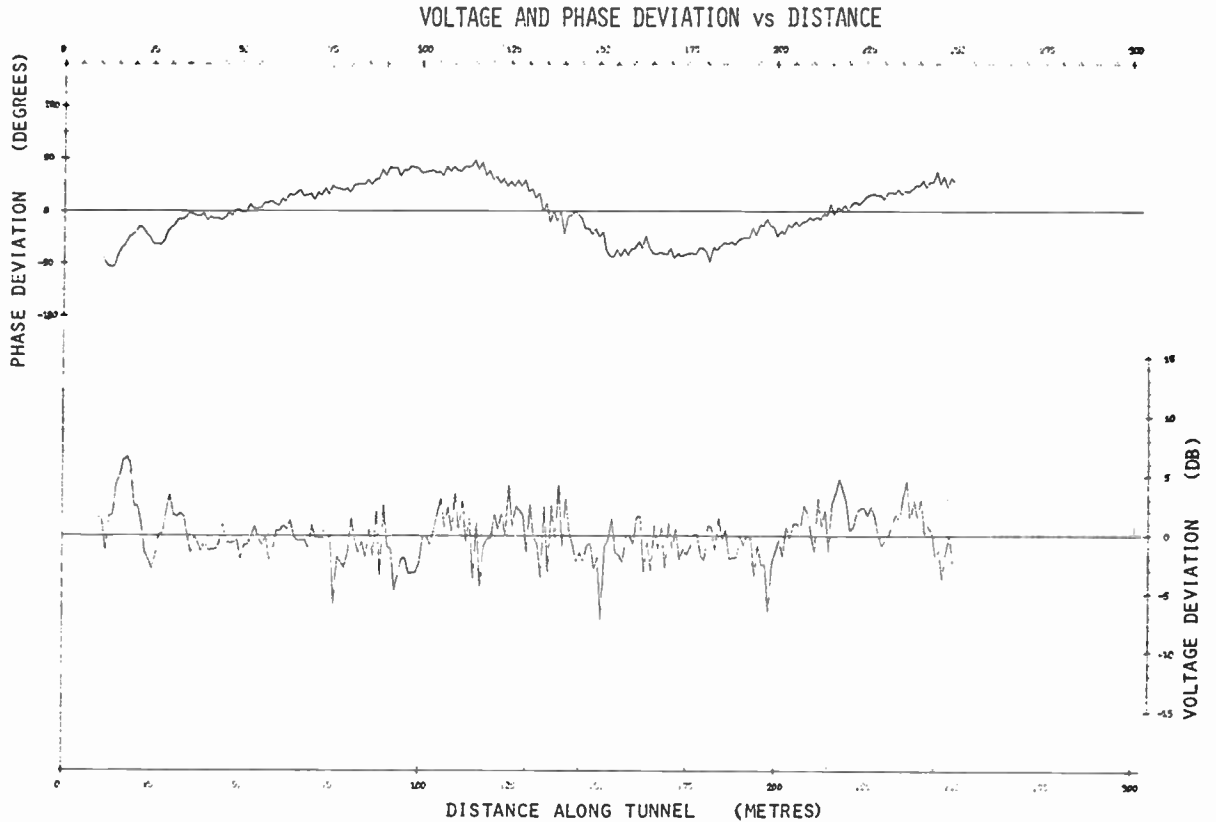


Fig. 9. Amplitude and phase deviations along tunnel.

A particular source of error shows up very well in Fig. 9 as a periodic variation from the mean phase gradient. It correlates closely with the variation in the depth of feeder sag between supports. Thus cable hanging is critical.

The Doppler shift due to velocity u is fairly close to that in free space, and is given by

$$f_D = \frac{\beta u}{2\pi} \text{ Hz,}$$

which is only a few hertz at v.h.f. for normal vehicular motion. The fluctuations in the phase give rise to noise in an f.m. system

$$\begin{aligned} \Delta\omega_n &= \frac{d\phi}{dt} \\ &= u \frac{d\phi}{dx}. \end{aligned}$$

This again has a maximum value of only a few hertz and thus should contribute negligible f.m. noise.

5 Acknowledgments

B. L. Critchley acknowledges the receipt of a maintenance grant from S.R.C. during the performance of this work. Support was also provided by the Mining Research and Development Establishment, N.C.B.

The authors are grateful to Dr D. J. R. Martin of N.C.B. and Mr D. Cree of British Rail, and Mr R. W. Haining of the University of Surrey, for helpful discussions.

6 References

- 1 Davis, Q. V. and Martin, D. J. R., 'Radio communication by leaky feeder', *Electronics and Power*, **20**, no. 17, pp. 753-5, 3rd October 1974.
- 2 Isberg, R. A., 'Radio communication in subways and mines through repeater amplifiers and leaky transmission lines', Proc. IEEE Conf. on Vehicular Technology, Denver, 1978.
- 3 Grussi, O. and König, P., 'Funkversorgung in Strassentunnels', *Technische Mitteilungen PTT, Bern*, no. 10, 1977.
- 4 Critchley, B., 'An investigation of the electromagnetic field surrounding a leaky feeder in a tunnel', Thesis, University of Surrey, 1977.

Manuscript first received by the Institution in June 1979 and in final form on 19th February 1980. (Paper No. 1956/Comm 205)